Night Vision Thermal Imaging Systems Performance Model

User's Manual & Reference Guide

March 12, 2001

DOCUMENT : Rev 5

U.S Army Night Vision and Electronic Sensors Directorate

Modeling & Simulation Division
Fort Belvoir, VA

U.S. Army Night Vision and Electronic Sensors Directorate
ATTN: AMSEL-RD-NV-MS-SPMD
FT. Belvoir, VA 22060-5677

Scope

NVTherm (Night Vision Thermal Imaging System Performance Model) is a PC based computer program which models parallel scan, serial scan, and staring thermal imagers that operate in the mid and far infrared spectral bands (3 to 12 micrometers wavelength). The model can only be used for thermal imagers which sense emitted, infrared light. NVTherm predicts the Minimum Resolvable Temperature Difference (MRTD or just MRT) that can be discriminated by a human when using a thermal imager. NVTherm also predicts the target acquisition range performance likely to be achieved using the sensor.

Figure 1-1 shows the relationship between the NVTherm model, laboratory measurements, and field performance. The model predicts the MRT that is achievable given the sensor and display design; this can be verified by laboratory measurement. The model also predicts the target acquisition performance achievable if the sensor meets design expectations; these field predictions are based on a history of both field and laboratory experiments relating the MRT to field performance. NVTherm is a system evaluation tool that uses basic sensor design parameters to predict laboratory and field performance.

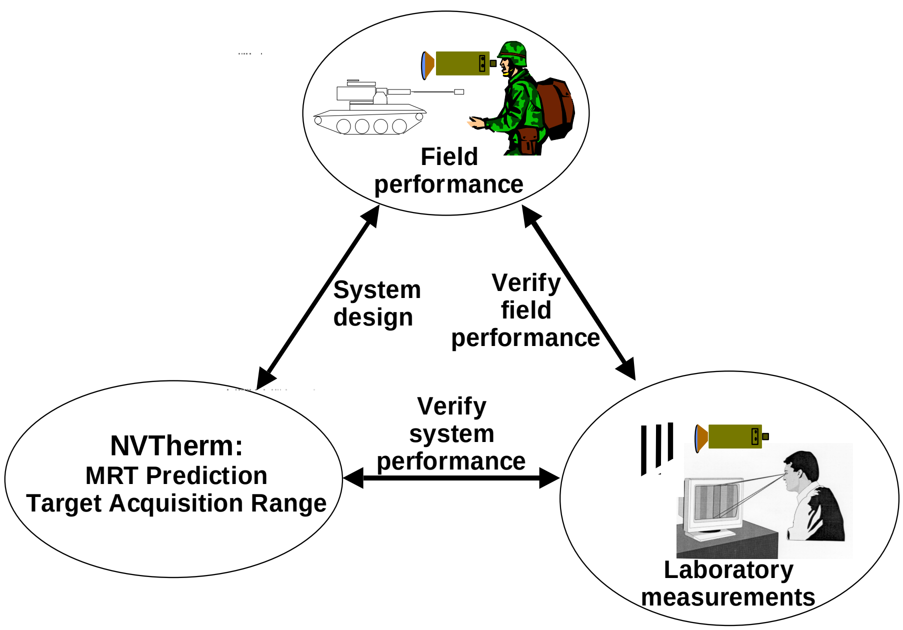

Figure 1-1 NVTherm models the MRT, which is achievable in the lab, and the target acquisition performance, which is achievable in the field.

In NVTherm, all MTFs are assumed separable: sensors are analyzed in the vertical and horizontal directions separately, and a summary performance calculated from the separate analyses. The point spread function, *psf,* and the associated Modulation Transfer Function, MTF, are assumed to be separable in Cartesian coordinates. The separability assumption reduces the analysis to one dimension so that complex calculations that include cross-terms are not required. This approach allows straight-forward calculations that quickly determine sensor performance.

The separability assumptions are almost never satisfied, even in the simplest cases. There is generally some calculation error associated with assuming separability. Generally, the errors are small, and the majority of scientists and engineers use the separability approximation. However, care should be taken in applying the model. For example, diagonal (two-point) dither cannot be modeled correctly, nor can diamond shaped detectors.

Further, in NVTherm all blurs are assumed to be symnetrical so that all MTFs are real. This means that, for example, electronics are not modeled correctly. A low pass electronic filter in this model does not result in any phase shift or time delay. Optical abberations are also not modeled rigoriously. The basic model assumption is that a region of the field of view can be selected that is isoplanatic, that that region can be modeled by a linear shift invariant process, and that some reasonable match to the MTF within that region can be achieved with a symetrical blur.

1. Introduction

NVTherm is the latest iteration of NVESD thermal models. NVESD was previously called the Night Vision Laboratory (NVL). The first NVESD thermal model "Night Vision Laboratory Static Performance Model for Thermal Viewing Systems," was published by Ratches and others in 1975.[1] Later versions of the thermal model included FLIR90 and FLIR92. The original 1975 performance model included both prediction of sensor Minimum Resolvable Temperature Difference (MRTD or just MRT) and also prediction of target acquisition performance using the Johnson criteria. FLIR90 and FLIR92 predict sensor MRT only; the MRT is an input to the Acquire computer model which uses the Johnson criteria to predict target acquisition. NVTherm returns to the original format by including range prediction and MRT prediction in the same computer program.

FLIR92 and Acquire provide target acquisition performance estimates for first and second generation thermal scanning sensors. NVTherm extends these models to provide performance estimates for thermal staring imagers as well. NVTherm generates a two dimensional MRT (2DMRT) which is used with the Johnson criteria to predict probability of target detection, recognition and identification versus range. In the current version of NVTherm, only the MRT prediction has changed from previous NVESD models like FLIR92. The Johnson criteria are still used to predict probability of task performance based on the MRT. Reference 2 describes the basic Johnson Criteria/Acquire modeling methodology.

NVTherm replaces the FLIR92 thermal model because staring arrays have two characteristics which can lead to errors in FLIR92 performance predictions. First, due to the sensitivity of the new staring arrays, the contrast limitations of the eye can be important in establishing performance limitations. Eye contrast limitations are not part of the FLIR92 theory. Second, in staring sensors, the limitations on detector size, spacing, and fill factor can result in under-sampled imagery. The resulting sampling artifacts can affect imager performance. To account for sampling artifacts, FLIR92 imposed an absolute cutoff at the half sample rate of the imager. This absolute cutoff, coupled with the use of the Johnson criteria to predict range performance, lead to pessimistic predictions for most staring imagers.

The next section describes the basic MRT prediction theory used through FLIR92. Subsequent sections describe the model changes needed to incorporate eye contrast limitations and sampling limitations on performance. Section 1.4 briefly describes the use of MRT and the Johnson criteria to predict range performance.

1.1. MRT Theory Used Through FLIR92

The basic MRT theory has not changed since the original NVESD thermal model published in 1975. The theory is described in References 1, 2, 3, and elsewhere in the literature.

1.1.1. Observer model

The theory predicts the ability of an observer to detect a single bar in a 4-bar pattern. The ability of the human visual system to detect patterns in noise is modeled by assuming that the visual system provides a matched filter to discriminate the object. The signal due to the eye integrating over the length and width of the bar is found, the expression for the eye integrated noise is derived, and the formula for MRT follows by finding the signal to noise ratio at each frequency.

The sensor and eye MTF will blur the bar pattern. The blurring effect can be modeled in frequency space by multiplying the Fourier Transform of the bar by sensor and eye MTFs. After passing through the matched filter provided by the visual system, the peak signal S_L due to the length of the bar is:

$$S_L = L\ L1 \int_{-\infty}^{\infty} H(f)\, H_e(f)\, H_L(f)\, H_{L1}(f)\, df \qquad (1\text{-}1)$$

where *H(f)* is the system MTF, $H_e(f)$ is the eye MTF, and $L \cdot H_L(f)$ is the bar Fourier Transform which is equal to sin(π·f·L)/(π·f). The factor $H(f) \cdot H_e(f) \cdot L \cdot H_L(f)$ is the Fourier Transform of the blurred bar pattern.

The factor $L1 \cdot H_{L1}$ represents the matched filter, provided by the visual system, which acts to integrate the signal over the bar area. The amplitude S_L is found by taking the inverse Fourier Transform at the center of the bar, which is the integral given in Equation 1-1.

H_{L1} equals H_L only for short bar lengths; the eye does not integrate intensity over long bars. The eye integration is limited to 4 milliradians in the NVTherm model. In the traditional model, H_{L1} equals H_L for all bar-pattern lengths.

The Equation 1-1 formulation is used in the aperiodic direction, along the length of the bar pattern. It does not work well in the periodic direction (across the bar pattern) to find the bar-space-bar modulation. At high frequencies, the bar modulation rides on a "hump" caused by the fact that sensors have better MTF at low frequencies than at high frequencies. The image of the center bars in a 4-bar pattern is brighter than the image of the two edge bars.

For the periodic direction, across the bars, the output modulation is approximated as equal to the first harmonic of the input square wave, degraded by the sensor and eye MTF. The first harmonic is (4/π) larger in amplitude than the initial square wave. Therefore:

$$\begin{aligned} S_W &= (4/\pi)\, H(f)\, H_e(f) \int_0^W \sin(\pi x/W)\, dx \\ &= (8/\pi^2)\, W\, H(f)\, H_e(f). \end{aligned} \qquad (1\text{-}2)$$

In Equation 1-2, the integral represents signal summation in the eye.

Using $H_N(f)$ to represent the noise filtering MTF, the noise filters are:

$$B_W = W1^2 \int_{-\infty}^{\infty} \left[H_N(f)\, H_e(f)\, H_{W1}(f) \right]^2 df$$
$$B_L = L1^2 \int_{-\infty}^{\infty} \left[H_N(f)\, H_e(f)\, H_{L1}(f) \right]^2 df. \qquad (1\text{-}3)$$

The system MTF $H(f)$ for thermal imagers is generally dominated by the optics MTF, the detector spatial MTF, the detector integrate and hold circuit MTF (if used) and the display MTF. The detector noise generally dominates, so that $H_N(f)$ consists of the detector integrate and hold MTF multiplied by the display MTF. Other MTF factors can be important in individual circumstances.

1.1.2. Detector Signal to Noise

The theory described below incorporates only the random noise generated within each detector; this theory will accurately predict the performance of a well-designed scanning FLIR system. As a practical matter, staring sensors are less likely to achieve detector-noise-limited performance, especially if a wide range of operating environments is considered. Detector-to-detector non-uniformity can be the dominate noise in staring sensors. The model treatment of non-ideal noise is discussed in Section 2.4.11 and 2.4.12.

Spectral detectivity ($D\lambda$) is used to specify the noise in a thermal detector.

$$D_\lambda = 1/NEP_\lambda. \qquad (1\text{-}4)$$

$NEP\lambda$ is the spectral noise-equivalent power; it is the monochromatic signal power necessary to produce an rms signal to noise of unity. Spectral D-star ($D\lambda^*$) is a normalization of $D\lambda$ to unit area and bandwidth.

$$D_\lambda{}^* = D_\lambda \left(A_{\mathrm{det}} \Delta f \right)^{1/2} \qquad (1\text{-}5)$$

where

Δf = temporal bandwidth and

A_{det} = Area of a single detector on the FPA.

The thermal model uses peak spectral D-star and relative detector response at other wavelengths to characterize detector performance.

$D^*_{\lambda peak}$ = $D_\lambda{}^*$ at wavelength of peak response and

$S(\lambda)$ = Response at wavelength λ normalized to peak response.

The spectral radiant power on the focal plane array is calculated as follows.

$$E_{fpa} = \pi \;\; \tau \;\; L_{scene} \big/ 4 \;\; F\#^2 \tag{1-6}$$

where

E_{fpa} = watt cm^{-2} u^{-1} on the detector array,

L_{scene} = watts cm^{-2}str^{-1}u^{-1} from the thermal scene, and

τ = Transmission of atmosphere and optics.

The parameters τ, L_{scene}, and E_{fpa} are all functions of wavelength λ. The spectral radiant power on a single detector of the array is:

$$E_{det} = A_{det} \;\; \pi \;\; \tau \;\; L_{scene} \big/ 4 \;\; F\#^2 \; . \tag{1-7}$$

The signal to noise in one detector (SN$_{det}$) can now be calculated.

$$SN_{det} = D^*_{\lambda peak} \left(2 \;\; t_e / A_{det}\right)^{1/2} \int_{\Delta\lambda} E_{det} \;\; S(\lambda) \;\; d\lambda$$

$$SN_{det} = \left(D^*_{\lambda peak} \left(2 \;\; t_e \;\; A_{det}\right)^{1/2} \pi \;\; \tau / 4 \;\; F\#^2 \right) \left(\int_{\Delta\lambda} L_{scene} \;\; S(\lambda) \;\; d\lambda \right) \tag{1-8}$$

where

$\Delta\lambda$ = Spectral band of sensor and

t_e = Eye integration time.

The MRT measurement is made by looking at a temperature-controlled, high-emissivity plate with a bar pattern cut into it. A blackbody cavity, temperature controlled to 300 K, is viewed through the bar cutouts. To estimate the differential spectral radiance resulting from a delta temperature near 300 K, the following equation is used.

$$L_{\substack{scene \\ (Temp)}} = \Gamma \;\; \partial L(\lambda, T) / \partial T \tag{1-9}$$

where the partial derivative is evaluated at 300 K and

$L(\lambda,T)$ = Plank's Equation for blackbody radiation,

T = Temperature, and

Γ = Amplitude of apparent blackbody temperature difference.

As long as the bars are at a temperature close to 300 K, the spectral nature of the difference signal is closely approximated by the partial derivative of the blackbody equation with respect to temperature evaluated at 300 K.

The signal to noise on one detector is now:

$$SN_{det} = \Gamma\ \delta\ D^*_{\lambda peak} \left(2\ t_e\ A_{det}\right)^{1/2} \pi\ \tau / 4\ F\#^2 \qquad (1\text{-}10)$$

where

$$\delta = \int_{\Delta\lambda} \left(\partial\, \mathrm{L}(\lambda, \mathrm{T}) / \partial \mathrm{T}\right) \mathrm{S}(\lambda)\, \mathrm{d}\lambda\,.$$

In one steradian, the signal to noise would increase by an amount $(F_0{}^2/A_{det})^{1/2}$ where F_O is the effective focal length of the afocal or objective lens.

$$SN_{rad} = \Gamma\ \delta\ F_o\ D^*_{\lambda peak} \left(2t_e\right)^{1/2} \pi\tau / 4\ F\#^2\ . \qquad (1\text{-}11)$$

1.1.3. MRT Equations.

In the following equation, SN_{sen} is the signal to noise seen by the human observer when viewing two blackbody bars at different temperatures.

$$SN_{sen} = SN_{rad}\ S_W S_L / \left(B_W B_L\right)^{1/2}$$
$$SN_{sen} = \Gamma\ \delta\ F_o\ D^*_{\lambda_{peak}} \left(2\ t_e\right)^{1/2} \pi\ \tau\ S_W S_L / \left(4F\#^2\ \left(B_W B_L\right)^{1/2}\right) \qquad (1\text{-}12)$$

This equation for SN_{sen} is for a staring sensor where the detectors fill the entire area of the image on the focal plane. If the fill factor for the detectors is less than unity, then SN_{sen} will decrease. Also, the theoretically available detector dwell time cannot be achieved by many staring detector arrays, because the 300 K background flux is too large and overfills the detector storage capacitor. An efficiency factor is needed in the signal-to-noise equation.

η_{eff} = (Fill Factor) (Actual Dwell/Available Dwell)

= Efficiency for staring sensor

$$SN_{sen} = \Gamma\ \delta\ F_o\ D^*_{\lambda_{peak}} \left(2\ t_e\ \eta_{eff}\right)^{1/2} \pi\ \tau\ S_W S_L / \left(4F\#^2 \left(B_W B_L\right)^{1/2}\right) \qquad (1\text{-}13)$$

At threshold, Γ is the MRT. Also, the signal to noise to the eye (SN_{sen}) is the signal-to-noise ratio threshold (SNRT). For a staring sensor, the MRT is given by the following equation.

$$MRT = \frac{\pi\, SNRT\;\; F\#^2\;\; f\;(B_W B_L)^{1/2}}{\delta\, F_o\;\; D*_{\lambda peak}\;(2\,t_e\;\eta_{eff})^{1/2}\,\tau\, H(f)\, S_L}\,. \tag{1-14}$$

Equation 1-14 is the MRT for a staring sensor. For a scanning sensor, the dwell time is reduced by the amount of detector area divided by the image area at the detector focal plane. Equation 1-14 can be used to find the MRT of a scanning sensor by substituting the following expression for (η_{eff}).

$\eta_{eff} = \eta_{scan}\ N_d\ A_{det}$ / (FOVH FOVV F_0^2)

= Efficiency for scanning sensor

where

η_{scan} = Scan efficiency,

N_d = Total number of detectors in parallel or Time Delay and Integrate,

FOVH = Horizontal field of view of the imager in radians, and

FOVV = Vertical field of view of the imager in radians.

1.2. Incorporating Eye Contrast Limitations

The following changes and additions to the traditional theory are incorporated into NVTherm and are not in previous versions of the NVESD thermal model.

1.2.1. Including Eye Noise

In the limit as sensor noise approaches zero and sensor MTF approaches unity, the MRT performance predicted by Equation 1-14 is unlimited; eye limitations are obviously missing from this equation. Kornfeld and Lawson suggested that quadratically adding visual noise to the sensor noise might improve model accuracy. They assumed that the noise in the eye is a fixed fraction of the measured CTF. Letting N_e represent noise in the eye, S_e represent signal to the eye, and A_L represent adapting luminance, then:

N_e = 2 A_L CTF/SNRT

= 2 S_{tmp} K_L CTF/SNRT (1-15)

S_e = Signal to eye

= Γ $H(f)$ K_L; (1-16)

where:

A_L = Average display luminance;

K_L = Converts scene temperature difference to display luminance difference (i.e., fL/K); and

S_{tmp} = A_L/K_L.

S_{tmp} is that delta temperature in the scene which results in a delta display luminance equal to the average display luminance. The thermal image arises from small variations in temperature and emissivity within the scene, and these small variations are superimposed on a large background flux. Zero luminance on the display corresponds to the minimum scene radiant energy, not to zero radiant energy. S_{tmp} is defined in terms of displayed blackbody temperature differences; S_{tmp} is not the absolute background temperature.

The total signal to noise becomes:

$$S/N_t = \left[1 \Big/ SN_{sen}^{\,2} + 4 S_{tmp}^{\,2}\, CTF^{\,2} \Big/ \left(SNRT\, \Gamma\, H(f) \right)^2 \right]^{-1/2} \qquad (1\text{-}17)$$

At threshold, S/N_t is equal to SNRT. The MRT is found by solving the above equation for Γ, because Γ equals the MRT at threshold.

$$MRT = (1/H) \left\{ \left[\frac{\pi\, SNRT\, F\#^2\, f\, (B_W B_L)^{1/2}}{\delta\, F_o D^*_{\lambda peak}\, (2 t_e \eta_{eff})^{1/2}\, \tau\, S_L} \right]^2 + 4 S^2_{tmp}\, CTF^2 \right\}^{1/2} \qquad (1\text{-}18)$$

Equation 1-18 does not predict laboratory measured MRT. Current lab procedures do not control display luminance or contrast, and S_{tmp} varies during the procedure. Laboratory MRT is not currently predicted by NVTherm.

1.2.2. Variable SNRT

Previous thermal models like FLIR92 assumed SNRT to be a fixed threshold regardless of display luminance or spatial frequency. The experiments of Rosell and Wilson demonstrated, however, that SNRT is not fixed; SNRT varies depending on both display luminance and the specific spatial frequency presented to the eye.

A variable SNRT is created using the measured CTF of the eye. CTF is proportional to visual factors which increase eye noise or detection threshold and inversely proportional to factors which improve signal detection. CTF gives a relative indication of the eye/brain ability to detect a bar pattern at a given light level and spatial frequency. We hypothesize that SNRT is proportional to CTF; this hypothesis has been shown to be true for image intensified sensors.

$$SNRT = K_{eye}\, CTF$$

where K_{eye} is a constant. Since eye MTF is included in the CTF, the $H_e(f)$ factor in Equation 1-18 is dropped. The equation for MRT becomes:

$$MRT = (1/H)\left\{\left[\frac{\pi K_{eye} CTF\ F\#^2\ f\ (B_W B_L)^{1/2}}{\delta\, F_o D^*_{\lambda peak}\ (2\ t_e \eta_{eff})^{1/2}\ \tau\, S_L}\right]^2 + 4\, S^2_{tmp}\ CTF^2\right\}^{1/2} \quad (1\text{-}19)$$

1.2.3. Contrast Loss at the Display

Contrast loss at the display can affect MRT. The following equation is used to find the MRT of a thermal imager when display contrast is degraded by the display brightness control or by ambient light reflecting from the display screen.

Let:

L_{min} = Minimum display luminance,

L_{max} = Maximum display luminance, and

$M_{disp} = (L_{max} - L_{min})/(L_{max} + L_{min})$.

Then:

$$MRT = (1/H)\left\{\left[\frac{\pi K_{eye} CTF\ F\#^2\ f\ (B_W B_L)^{1/2}}{\delta\, F_o D^*_{\lambda peak}\ (2\ \eta_{eff})^{1/2}\ \tau\, S_L M_{disp}}\right]^2 + \frac{4\, S^2_{tmp}\ CTF^2}{M^2_{disp}}\right\}^{1/2} \quad (1\text{-}20)$$

Equation 1-20 can be rewritten to yield threshold contrast for the thermal imager. This form is useful when calculating image quality metrics for thermal imagers. NVTherm has an option to calculate threshold contrast; when threshold contrast is calculated, a long, many-bar pattern is assumed consistent with the target patterns used for naked eye CTF experiments.

$$\frac{MRT}{2S_{tmp}} = (1/H)\left\{\left[\frac{\pi K_{eye} CTF\ F\#^2\ f\ (B_W B_L)^{1/2}}{\delta\, F_o D^*_{\lambda peak}\ (2\ \eta_{eff})^{1/2}\ \tau\, S_L M_{disp}\, 2S_{tmp}}\right]^2 + \frac{CTF^2}{M^2_{disp}}\right\}^{1/2} \quad (1\text{-}21)$$

1.3. Sampling

The tendency of a sampled imager to produce sampling artifacts is quantified by the spurious response function of that imager. The equations needed to calculate spurious response are provided below. The effect of spurious response on target recognition and identification were determined in two perception experiments. Based on those experiments, the *MTF Squeeze* model was developed. The degraded performance due to under-sampling was modeled as an increase in system blur or, equivalently, a contraction or "squeeze" in the system MTF. The results of these experiments were used to calibrate the MTF squeeze model for the individual recognition and identification tasks. Equations were developed for both target recognition and target identification that quantify the amount of squeeze or contraction to apply to the system MTF in order to account for the performance degradation caused by the spurious response.

Target recognition is moderately affected by both in-band spurious response (overlap of the aliased signal with the base-band) and by out-of-band spurious response (raster). Target identification, however, was not affected by base-band aliasing but was strongly affected by out-of-band spurious response. Based on the NVESD experiments and other data reported in the literature, it appears that low-level discrimination tasks (like point detection) are affected by in-band spurious response but not by out-of-band spurious response, whereas high-level discrimination tasks (like vehicle identification) are strongly affected by out-of-band spurious response but are not affected by in-band aliasing.

1.3.1. Spurious Response

The spurious response capacity of an imager can be determined by characterizing the imager response to a point source. This characterization is identical to the MTF approach for continuous systems.

The response function for a sampled imager is found by examining the impulse response of the system. The function being sampled is the point spread function of the pre-sampled image. For simplicity, the equations and examples will use one dimension, but the concepts generalize to two dimensions. Assume the following definitions:

$H(\omega)$ = Pre-sample MTF (optics and detector)

$P_{ix}(\omega)$ = Post-sample MTF (display and eye)

$R_{sp}(\omega)$ = Response function of imager

$R_{sp}(\omega)$ = Transfer response (baseband spectrum) plus spurious response

ω = spatial frequency (cycles per milliradian)

ν = sample frequency (samples per milliradian)

d = spatial offset of origin from a sample point

Then the response function $R_{sp}(\omega)$ is given by

$$R_{sp} = \sum_{n=-\infty}^{n=\infty} H(\omega - n\nu) e^{-i(\omega - n\nu)d} P_{ix}(\omega)$$

$$R_{sp} = H(\omega) e^{-i\omega d} P_{ix}(\omega) + \sum_{n \neq 0} H(\omega - n\nu) e^{-i(\omega - n\nu)d} P_{ix}(\omega). \tag{1-22}$$

The response function has two parts, a transfer function and a spurious response function. The n=0 term in Equation 1-22 corresponds to the transfer function (or baseband response) of the imager. This term results from multiplying the pre-sample blur MTF by the post-sample blur MTF. The transfer response does not depend on sample spacing, and it is the only term that remains in the limit as sample spacing goes to zero. A sampled imager has the same transfer response as a non-sampled (or a very well-sampled) imager.

A sampled imager always has the additional response terms (the n≠0 terms), which are referred to as *spurious response*. The spurious response terms in Equation 1-23 are caused by the sample-generated replicas of the pre-sample blur; these replicas reside at all multiples of the sample frequency. The spurious response of the imager results from multiplying the sample-generated replicas of the pre-sample blur MTF by the post-sample MTF. The position of the spurious response terms on the frequency axis depends on the sample spacing and the effectiveness of the display and eye in removing the higher frequency spurious signal. The phase relationship between the transfer response and the spurious response depends on the sample phase.

It was found during the perception experiments that performance could be related to a ratio of integrated spurious response to baseband response, *SR*. Three quantities have proven useful: total integrated spurious response as defined by Equation 1-23, in-band spurious response as defined by Equation 1-24, and out-of-band spurious response as defined by Equation 1-25. If the various replicas of the pre-sample blur overlap, then the spurious signals in the overlapped region are combined in quadrature before integration.

$$\begin{aligned}
SR &= \frac{\int_{-\infty}^{\infty} (\text{Spurious response})\, d\omega}{\int_{-\infty}^{\infty} (\text{Baseband signal})\, d\omega} \\
SR_{in-band} &= \frac{\int_{-\upsilon/2}^{\upsilon/2} (\text{Spurious response})\, d\omega}{\int_{-\infty}^{\infty} (\text{Baseband signal})\, d\omega} \\
SR_{out-of-band} &= SR - SR_{in-band}
\end{aligned} \tag{1-23,24,25}$$

1.3.2. MTF Squeeze Model

Experiments were conducted to determine the affect of under-sampling on tactical vehicle recognition and identification. A variety of pre-sample blurs, post-sample blurs, and sample spacings were used. Baseline data was collected for each pre-sample and post sample blur combination without any spurious response (that is, with a small sample spacing). The baseline data provided the probability of recognition and identification versus total blur when no spurious response was present.

For each spurious response case, we found the baseline case without spurious response which gave the same probability of recognition or identification. A curve fit was used to relate the actual blur (with spurious response) to the increased baseline blur (without spurious response) which gave the same recognition or identification probability.

The effect of sampling on performance was found to be a separable function of the spurious response in each dimension. For the cases where the sampling artifacts were applied in both the horizontal and vertical direction, the two dimensional relative blur increase (RI) for the recognition task is:

$$RI = \frac{1}{1 - 0.32SR} \tag{1-26}$$

where SR is the spurious response ratio defined by Equation 1-25. For cases where the sampling artifacts were applied in only the horizontal or vertical direction, the relative blur increase for recognition is:

$$RI = \frac{1}{\sqrt{1 - 0.32SR_{V\ or\ H}}}. \tag{1-27}$$

Note that, for both Equations 1-26 and 1-27, *the relative increase in blur is in two dimensions.* That is, even if the spurious response is in one direction, the relative increase shown in Equation 28 is applied to both directions.

By the Similarity Theorem, a proportional increase in the spatial domain is equivalent to a contraction in the frequency domain. This turns an equivalent blur increase into an MTF contraction, or *MTF squeeze,* and allows the equivalent blur technique to be easily applied to performance models. Instead of an increase in the effective size of the point spread function, the Modulation Transfer Function is contracted. The MTF squeeze for recognition is:

$$MTF_{squeeze} = \sqrt{1.0 - 0.32SR_H}\ \sqrt{1.0 - 0.32SR_V}. \tag{1-28}$$

Figure1-1 illustrates the application of contraction, or *MTF squeeze*, to the system MTF. The spurious response given by Equation 1-23 is calculated independently in the horizontal and vertical directions, and the squeeze factor given by Equation 1-28 is calculated. At each point on the MTF curve, the frequency is scaled by the contraction factor. The contraction is applied separately to the horizontal and vertical MTF in Equations 1-1 and 1-2. The MTF squeeze is not applied to the noise MTF in Equation 1-3.

$$f_1 = \sqrt{1.0 - 0.32 SR_H}\ \sqrt{1.0 - 0.32 SR_V}\ f_2$$

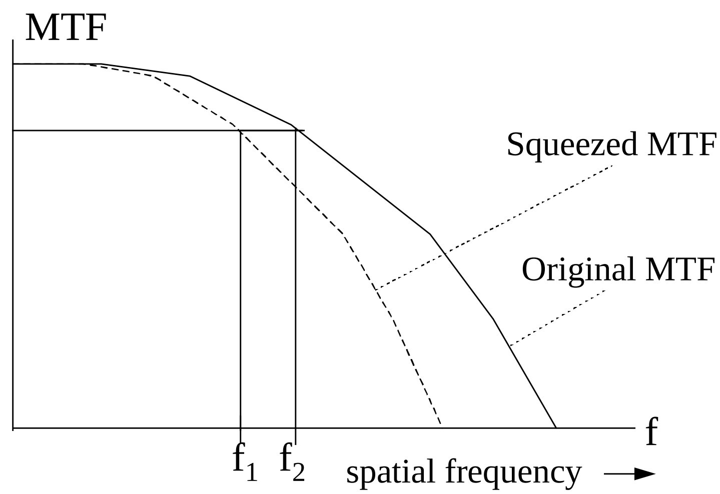

Figure 1-1. Application of the MTF Squeeze. Contraction is calculated based on total spurious response ratio in each direction. Contraction of frequency axis is applied to both horizontal and vertical MTF. Contraction is applied to signal MTF, not the noise MTF.

The results of the identification experiment using tracked vehicles suggest that target identification is strongly affected by out-of-band spurious response but is only weakly affected by in-band spurious response. The identification MTF squeeze factor is calculated using Equation 1-29. Again, the effect of sampling was found to be separable between the horizontal and vertical dimensions.

$$MTF_{squeeze} = \sqrt{1 - SR_{H-out-of-band}}\ \sqrt{1 - SR_{V-out-of-band}} \qquad (1\text{-}29)$$

where $SR_{out\text{-}of\text{-}band}$ is calculated using Equation 1-25.

1.4. Predicting Range Performance Using the Johnson Criteria

MRT quantifies the threshold vision when viewing a scene through a thermal imager. Practical interest, however, focuses on doing a task. For example, determining how far away a tank can be detected, recognized and identified. Performance metrics provide the bridge between sensor characteristics and task performance. NVTherm uses the Johnson criteria to predict the range performance expected for a given sensor MRT.

The sensor is modeled in detail, but the target, background and the observers are treated as ensembles. Targets are described by size and average contrast to the background; the models do not treat a specific target in a specific background. Only a generalized task can be modeled accurately using the Johnson criteria.

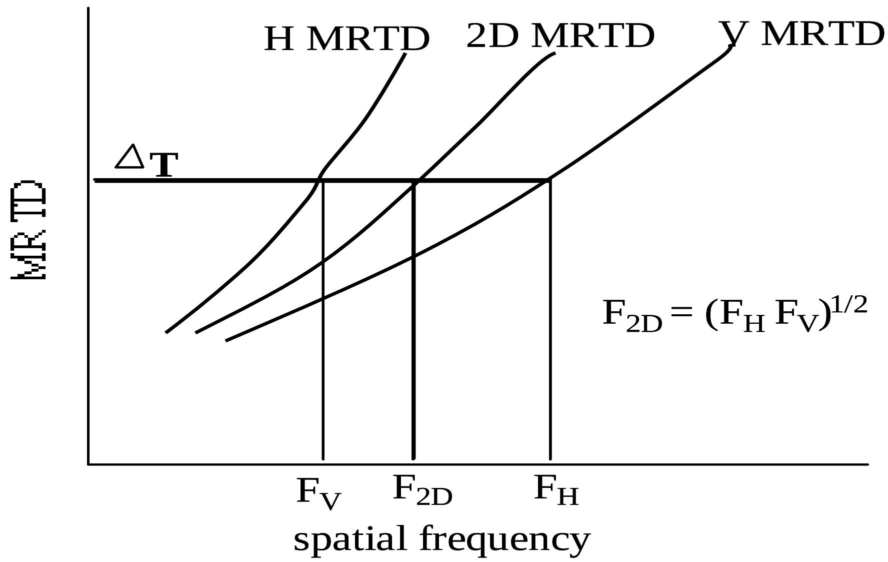

Figure 1-2. Generating 2D MRTD from the Horizontal (H MRTD) and Vertical (V MRTD).

For example, the probability of correctly identifying a T-62 Russian tank cannot be accurately predicted. One problem in making such a prediction is that the visual discrimination is not defined. A visual discrimination is *always* a comparison. Correctly identifying that a Russian tank is a T-62 rather than a T-72 is much harder than discriminating between a T-62 and an American M1 tank. Russian tanks look alike and do not look like American tanks. When it comes to identifying or recognizing tactical vehicles, task difficulty is established by the entire group of vehicles being discriminated and not by a single vehicle in the group. A second problem with using the Johnson criteria to make specific target predictions is that size and average contrast to the background is not sufficient information for a model to make target by target predictions.

Observers are also treated as a group, and the model predicts their average performance against a group of targets. A 90 percent probability of correct identification corresponds to nine observers out of ten correctly identifying all of the vehicles in a group or all of the observers correctly identifying nine out of ten vehicles. Fortunately, tactical military vehicles can be grouped by size and other characteristics. For example, the question "what is the average probability that a trained military observer, using a specified sensor system, can discriminate between Russian and American tanks at a 5 kilometer range" can be answered quite accurately by this model.

1.4.1. Two Dimensional MRT (2D MRT)

A single 2D MRT is generated by combining the sensor horizontal and vertical MRT's. This procedure is illustrated in Figure 1-2. The horizontal and vertical frequencies achieved at each temperature are geometrically averaged.

1.4.2. Range Prediction Methodology

The following methodology evolved based on John Johnson's work. Field tests and laboratory perception experiments have shown the target acquisition model presented here to be fairly accurate on the average, although the variance is quite large when specific target predictions are tried.

a. The square root of the target area and the thermal contrast between the target and local background in the spectral band of the imager are measured. Quite often, the "standard target" with square root of area equal to 2.3 meters and thermal contrast of 1.25 K is specified. In this example, the square root of target area is 1 meter and the thermal contrast is 0.5 K.

b. The apparent temperature versus range is calculated using Beer's law or an atmospheric transmission program. The atmospheric transmission for this example is assumed to be 0.7 per kilometer. The apparent temperature of the target versus range is plotted in Figure 1-3.

c. A cycle criteria is chosen based on the task, desired probability of success, and the analyst's judgment of difficulty. Assume four cycles for a 50% recognition probability.

c. For N cycles across a target minimum dimension H_{targ} in meters at a range of R_{ng} in kilometers, the spatial frequency F_{req} in cycles per milliradian at the sensor can be calculated as shown below. Using this formula, an MRT can be plotted as a function of range as shown in in Figure 1-3.

$$F_{req} = {N R_{ng}} / {H_{\mathrm{targ}}}$$

e. The range for task performance at the specified probability is given by the intersection of the apparent target temperature with the MRT curve. In this case, 50% probability of recognition occurs at a range of 1.05 kilometer.

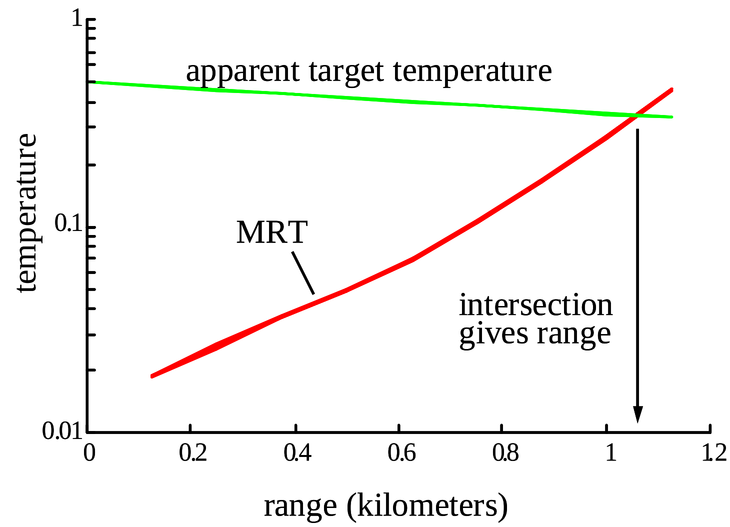

Figure 1-3. Using Johnson Criteria to find task performance range

Given a cycle criteria for 50 percent success, generally referred to as N_{50}, the following formula gives the fraction of an ensemble of observers that is likely to accomplish the task with a different number of cycles across the target. This function is called the Target Transform Probability Function (TTPF).

$$P_{rob} = \frac{\left(N/N50\right)^E}{1+\left(N/N50\right)^E} \qquad (1\text{-}30)$$

where E = 3.76

1.5. Summary of MRT Changes

Thermal models based on the traditional theory do not adequately account for the physiological characteristics and limitations of the eye. NVTherm upgrades the theory by adding a variable SNRT and by including the eye's contrast limitations when predicting MRT. These changes have a minor affect on performance predictions for first generation thermal imagers but can be significant when predicting the performance of sensitive staring array imagers.

NVTherm also incorporates the changes needed to model under-sampled sensors. The spurious response corresponding to sampling artifacts is predicted. The MTF Squeeze model is used to degrade predicted performance based on the amount of spurious response.

2. Model Inputs

This is the "Inputs" menu. Each menu item is described below.

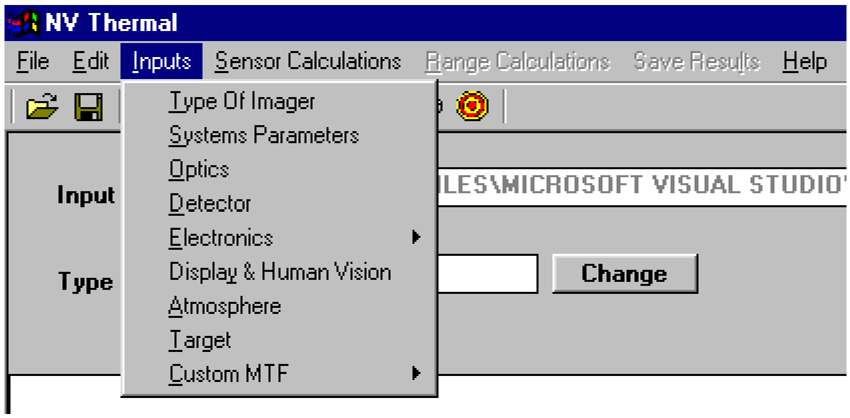

2.1. Type of Imager

This is the "Type of Imager" form. Each option is described below.

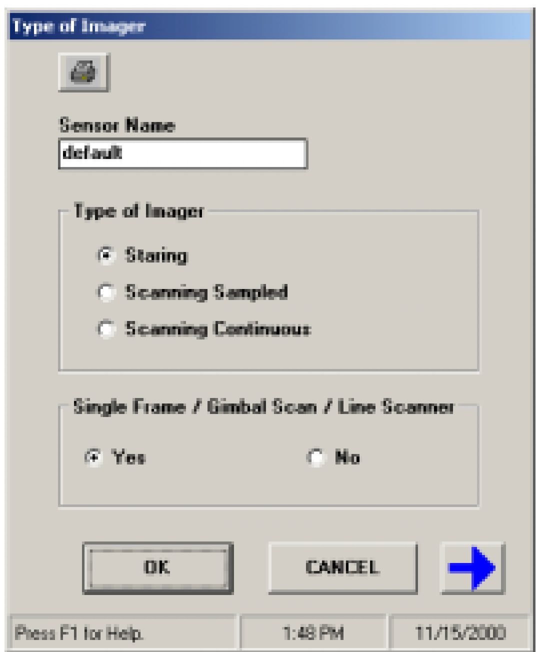

2.1.1. Input Description

NVTherm can model staring, scanning sampled, and scanning continuous imagers. In each case, the image can be framing (presenting a series of 25, 30 or 60 images of the scene per second to the eye) or single frame (a single snapshot of the scene presented to the eye). The default screen shows a staring sensor selected; the sensor is being operated in a single frame mode.

A typical FLIR operates in the framing mode, presenting imagery where motion is visible. The single frame mode is implemented with gimbals scan or line scanners. Each portion of the field of view is imaged once and that single image presented continuously to the eye. Single frame has the advantage of imaging wide areas at reduced bandwidth because each part of the field of view is imaged only once. Framing mode has the advantage of showing motion and generally provides a somewhat less noisy image because each part of the field of view is imaged a number of times per second.

A staring imager uses a two-dimensional array of detectors; see Figure 2-1. The image is not scanned over the detectors; each part of the field of view is sensed continuously by distinct detector elements.

In a scanning imager, the image is scanned over a linear detector array as shown in the left figure. The detectors are time multiplexed, sampling different parts of the scene as the frame proceeds. In the scanning sampled case also described by the left figure, the detector signal is integrated for a sample period before being readout to the signal multiplexer. Since the scene is moving over the detector during this signal integration, the image is blurred by the integration. In the scanning continuous case, the detector signal is either viewed directly or perhaps sampled quickly without integrating the signal. The left image illustrates the operation of 1st generation FLIRs which used continuous scanning.

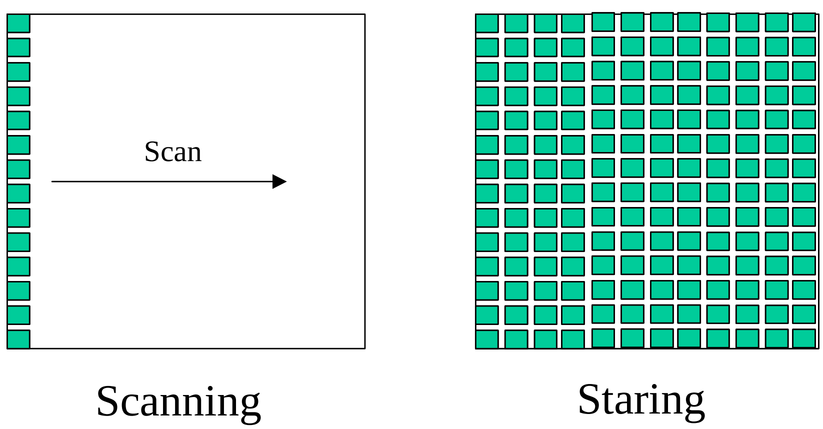

Figure 2-1

If the imager, regardless of type, is used to obtain a single image, then Single Frame/Gimbal Scan/Line Scanner should be selected. This action allows the eye to integrate only one frame of imagery and sets the eye integration time to a frame time.

2.1.2. Help and Examples

1st generation imagers like the TOW sight and the M60 Tank Thermal Sight are scanning continuous sensors. 2nd generation thermal imagers like the HTI "B-kit" are scanning sampled.

2.2. System Parameters

This is the "System Parameters" form. Each option is described below.

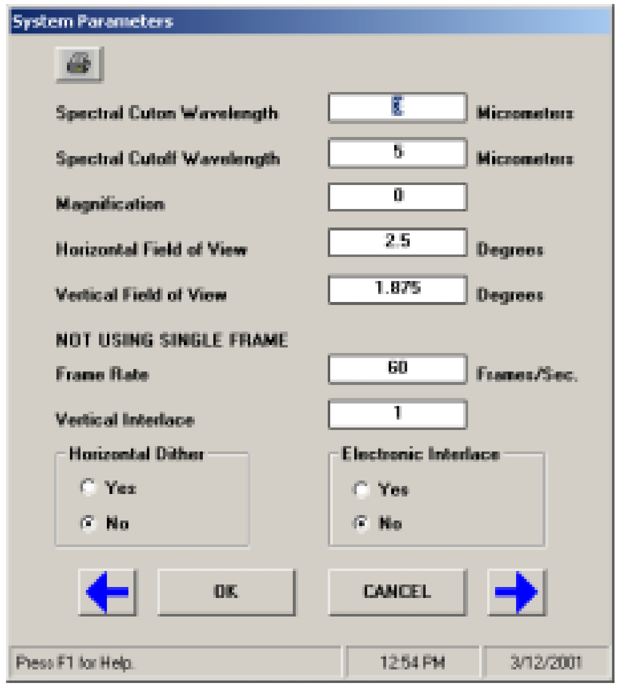

2.2.1. Spectral Cuton Wavelength

2.2.1.1. Input Description

The Spatial Cuton Wavelength is the lower wavelength limit of the system (optics, detector, and filter) spectral passband. The spectral cuton wavelength shown in the default window is 3 micrometers. λ_1 is the spectral cuton wavelength for the passband shown in figure 2-2.

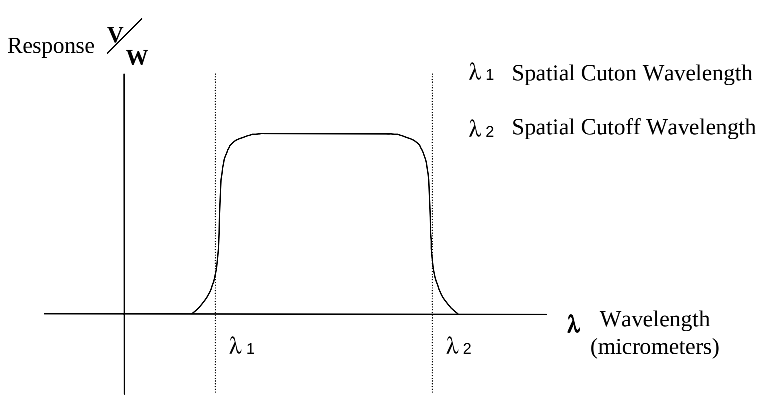

Figure 2-2

2.2.1.2. Help and Examples

This value needs to be greater than 2.4 microns and less than 25.0 microns. A Midwave value is typically 3.0 and a Longwave value is typically 8.0.

2.2.2. Spectral Cutoff Wavelength

2.2.2.1. Input Description

The Spectral Cutoff Wavelength is the upper wavelength limit of the system (optics, detector, and filter) spectral passband. The spectral cuton wavelengthshown in the default window is 5 micrometers. λ_2 is the spectral cutoff wavelength for the passband shown in figure 2-2.

2.2.2.2. Help and Examples

This value needs to be greater than 2.4 microns and less than 25.0 microns. A Midwave value is typically 5.0 and a Longwave value is typically between 12.0 and 14.0. The cutoff wavelength must be greater than the cuton wavelength.

2.2.3. Magnification

2.2.3.1. Input Description

System magnification is the ratio of the angular image size seen by the observer to the actual angular size in object space as seen by the sensor.

This can be written as:

$M = \theta_{\text{image}}/\theta_{\text{object}}$ or

$M = \dfrac{FOV_d}{FOV_v}$ where FOV_v is the sensor vertical field of view, and FOV_d is the display field of view defined by the vertical dimension of the active display area and the observer viewing distance.

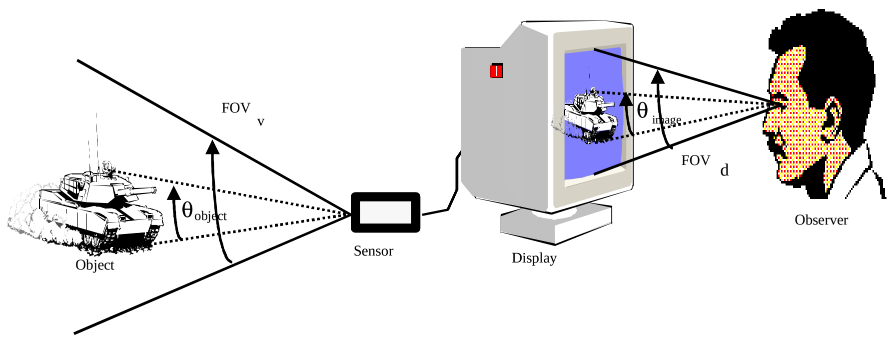

Figure 2-3

2.2.3.2. Help and Examples

Entering a value for magnification is optional, NVTherm will calculate magnification if a value is not entered. However, if a value is entered, MTFs for the display and sensor will be automatically adjusted to correspond to this magnification.

The magnification for an electronic imaging system can vary from 1/6th (extremely small) to 200 or more. Normally, magnification values range from 0.5 to 20.

2.2.4. Horizontal Field of View

2.2.4.1. Input Description

The field of view (FOV) of an imaging system is one of the most important design parameters. It is the parameter that describes the angular space in which the system accepts light. The system FOV and the distance, or range, from the sensor to the object determine the area that a system will image. Consider the optical system in Figure 2-4.

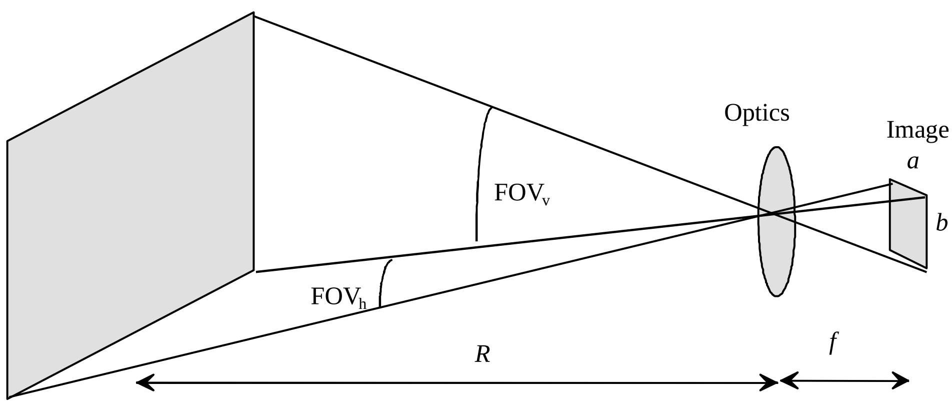

Figure 2-4. Field of View.

For the system shown, FOV_h and FOV_v are the horizontal and vertical FOVs, respectively. The FOVs are the arctangents of the image size divided by the focal length:

$$FOV_h = 2\tan^{-1}\frac{a}{2f} \qquad \text{and} \qquad FOV_v = 2\tan^{-1}\frac{b}{2f} \qquad (2\text{-}1)$$

For small angles, the FOVs can be estimated as a/f and b/f.

The image size (and field of view) is bounded by a field stop. The field stop is located in an image plane (or an intermediate image plane) and is specified by *a* and *b*. The light-sensitive material is limited to the area inside the field stop, so the field stop can be merely like a frame (like a picture frame). However, infrared and EO systems exploit light with detectors. The detectors take the form of a two-dimensional array of individual detectors called a staring array or a single detector or rows of detectors that are scanned across the image space. In these cases, the size of the image plane is defined by the light-sensitive area of the array and the possible light-sensitive positions of the scanned systems. A field stop larger than the detector array size would not limit the FOV and hence would not be required.

2.2.4.2. Help and Examples

In NVTherm, the FOV is a required input. The input units for FOV are degrees.

2.2.5. Vertical Field of View

2.2.5.1. Input Description

The vertical field of view is described in an identical manner as that of the horizontal field of view in the previous section. The FOV is the angle subtended by the light sensitive area of the detector array divided by the focal length of the imaging system. This approach works for staring arrays and linear scanning arrays such as 1st GEN FLIRs and 2nd GEN FLIRs.

2.2.5.2. Help and Examples

Vertical FOV is a required input. If the magnification of the system is not input, then the magnification is calculated based on the vertical field of view and the angle of the display subtended to the eye. The ratio of the later to the former gives the system magnification.

The input units for FOV are degrees.

2.2.6. Frame Rate

2.2.6.1. Input Description

The Frame Rate is the rate per second at which complete pictures are produced by the system and displayed to the eye. This value is taken from the sensor and is given in Frames Per Second (FPS).

2.2.6.2. Help and Examples

Real time video, such as television, is displayed at 30 FPS in the U.S. and 25 FPS in Europe. Most sensors take pictures at a rate of 30 Hz to 60 Hz. Some missile seekers operate up to 200 Hz frame rates.

2.2.7. Vertical Interlace

2.2.7.1. Input Description

Interlace improves sensor sampling without increasing detector count. A high resolution frame is comprised of two or more lower resolution fields taken sequentially in time. Between each field, a nodding mirror or other mechanical means is used to move the locations where the scene is sampled. Interlace achieves high resolution while minimizing focal plane array complexity.

Interlace generally has the connotation that the field sub-images are taken and displayed in time synchronism. That is, the pixels from sub-images taken at different times are not combined and then displayed, but rather the time sequencing of the sensor field images is maintained at the display. The reduced resolution, field sub-images are combined into a high resolution image by the human visual system. *Dither*, on the other hand, generally has the connotation that the field images are combined to form a higher resolution image prior to the display. Since this model is a static performance model, dither and interlace are equivalent and vertical interlace is used to model dither in the vertical direction.

Interlace is used to improve sensor sampling without increasing pixel rate or electronic throughput of the system. Interlace takes advantage of the eye's ability to integrate multiple fields of imagery, presented in time sequence, into a higher resolution frame.

Video display rates must be 50 or 60 Hertz in order to avoid perceptible flicker, but each 50 or 60 Hertz image need not display every pixel. Flicker is avoided in most circumstances by displaying every-other pixel in each field. Flicker can occur when the image contains lines which are one pixel wide as in graphic plots. In that case, local regions of the image do not have approximately the same intensity between fields. Most natural scenes, however, do not contain such constructs, and the sensor pre-sample blur mitigates the problem when it does occur.

Standard video uses two fields per frame and vertical interlace. That is, the video display is a vertical raster of lines, and every-other line is displayed in every-other field. In the United States, the field rate is 60 Hertz and the frame rate is 30 Hertz. In Europe, the standard rate is 50 Hertz field and 25 Hertz frame.

Figure 2-5 illustrates video interlace. Each 1/60th of a second, an interlaced sensor gathers every-other horizontal row of scene samples. The video display shows every-other horizontal line. Every-other video line is collected by the sensor in each field. Every-other video line is displayed during each field. Interlace is used because the full resolution image need only be produced and displayed 30 times a second.

With an interlaced sensor and display, the human visual system integrates the full resolution image whether the image is stationary or moving relative to the sensor. The 30 Hertz update of pixel information is more than adequate to support the perception of smooth apparent motion. Exceptions to smooth apparent motion can occur. If the scene is comprised of very simple, high contrast structures, then image breakup can sometimes be seen during scene to sensor motion. However, for natural, complex scenes, such breakup is very rare. For a human observer, interlace provides full resolution imagery at half the pixel throughput.

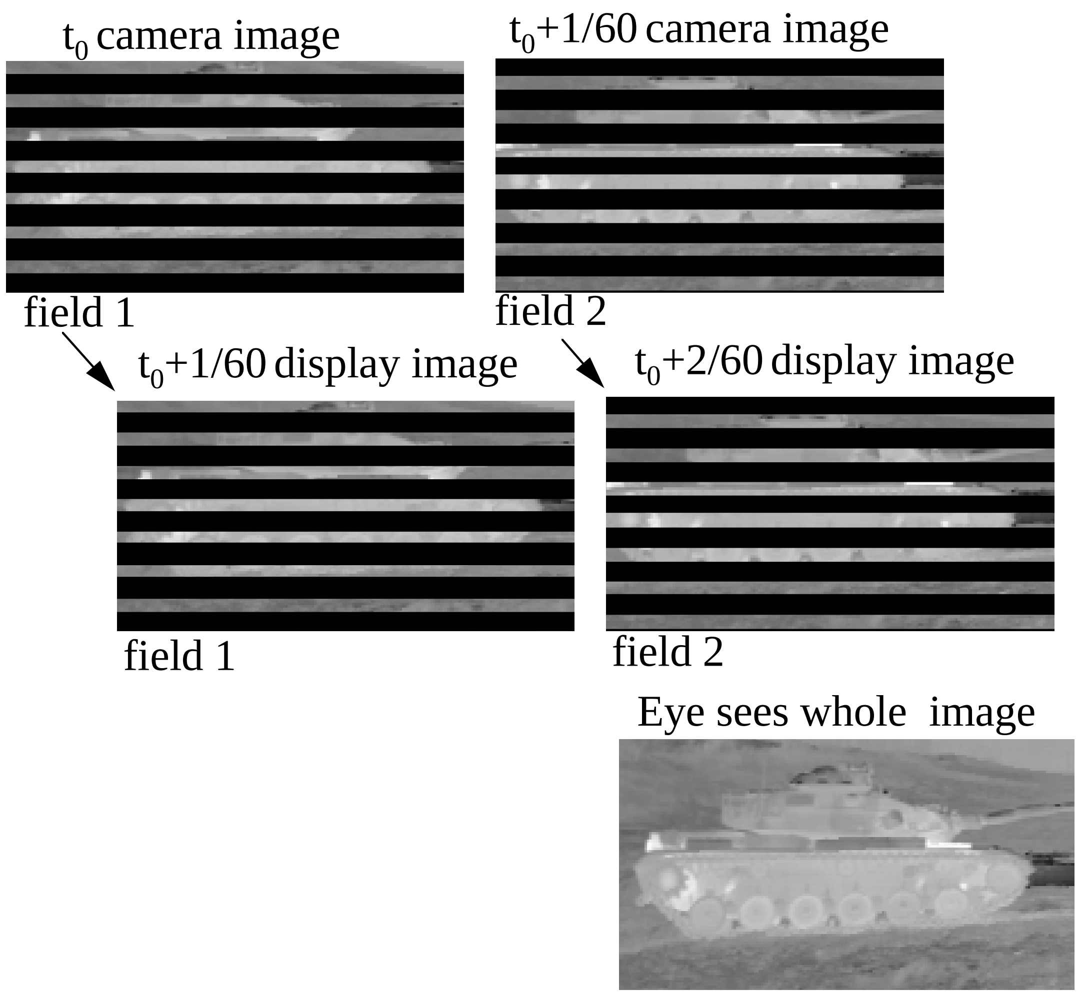

Figure 2-5 Illustration of Interlace At top, the sensor or camera collects the first field of imagery consisting of alternate horizontal lines. The first field is displayed 1/60th of a second later. The camera then collects the lines not collected in the first field and these are subsequently displayed.

2.2.7.2. Help and Examples

Vertical Interlace of greater than 1 gives an increased vertical sampling rate. Typically, first generation FLIRs have a vertical interlace of 2. A serial scanned imager using a single detector that provides 480 lines would have a vertical interlace of 480.

2.2.8. Horizontal Dither

2.2.8.1. Input Description

Dither is only applied in the horizontal direction and increases the horizontal sampling rate by a factor of 2. When dither is selected, there are 2 fields per frame in the horizontal direction (very similar to vertical interlace).

2.2.8.2. Help and Examples

Four point dither can be achieved by selecting dither as yes and setting vertical interlace to 2. Slant path dither is not supported by NVTherm.

2.2.9. Electronic Interlace

2.2.9.1. Input Description

Electronic Interlace occurs whenever the output of the detector array is formatted into two fields. Every other line from the detector output is discarded, giving a sensitivity equivalent to half the number of vertical detectors. This does not change the sampling rate. In NVTherm, electronic interlace has an action in the MRT equation of dividing the number of vertical detectors by 2. The sampling rate remains the same as that on the focal plane.

2.2.9.2. Help and Examples

Electronic interlace is common with staring arrays (480 by XXX) that are formatted in RS-170 for viewing on a monitor.

2.3. Optics

This is the “Optics” input form. Each option is described below.

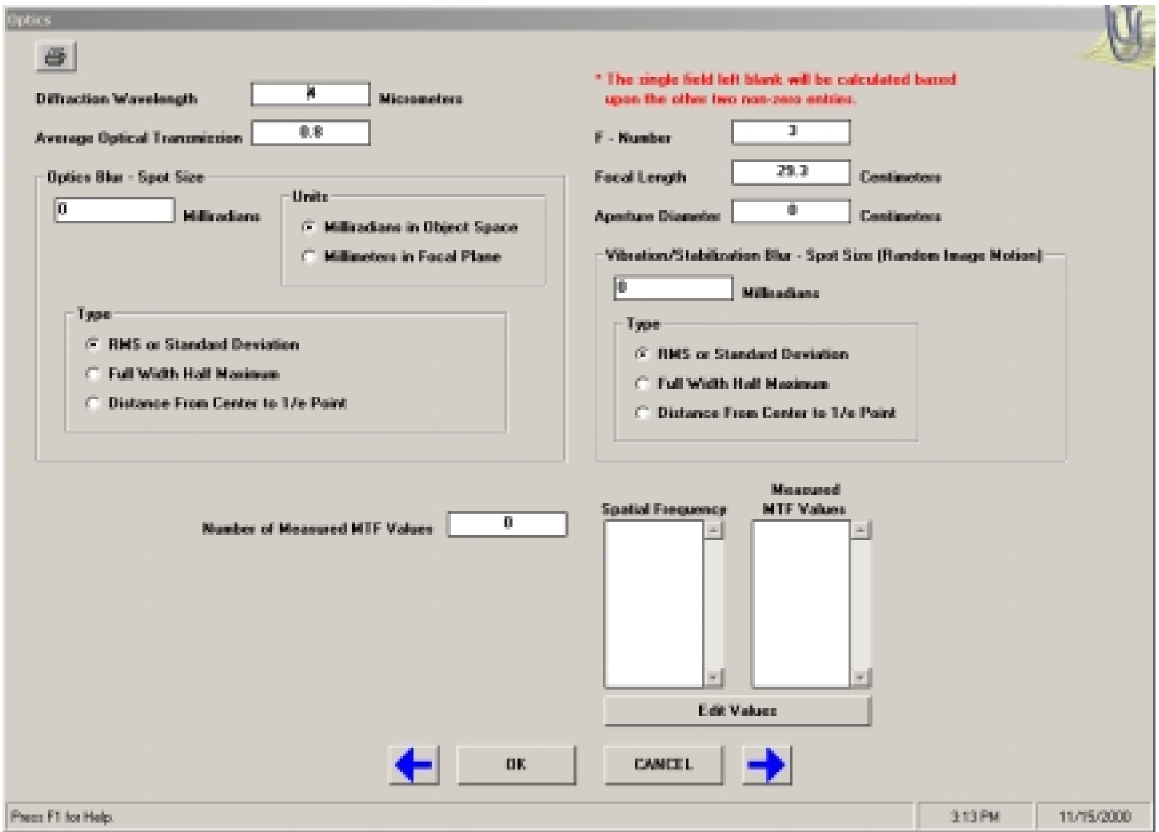

2.3.1. Diffraction Wavelength

2.3.1.1. Input Description

The diffraction wavelength is used in the diffraction MTF calculation. MTFs are described in section 3.2.

2.3.1.2. Help and Examples

In NVTHERM, the diffraction wavelength input is optional. If it is not input, then the diffraction wavelength is calculated from the spectral cuton wavelength and the spectral cutoff wavelength. The diffraction wavelength is taken to be centered between these two wavelengths.

The units on the diffraction wavelength input are micrometers.

2.3.2. Aperture Diameter

2.3.2.1. Input Description

The aperture diameter of an infrared imaging system is shown Figure 2-6. It is the clear aperture dimension of the collecting optics. Frequently, imaging systems have a large number of lenses. However, the entrance aperture size is taken as the aperture diameter and is usually specified by the company that makes the optical system.

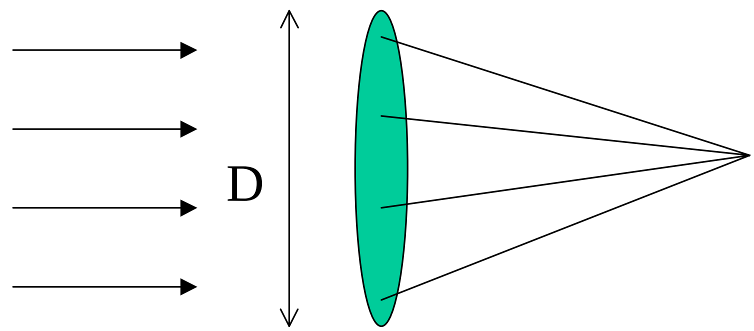

Figure 2-6 Aperture Diameter

2.3.2.2. Help and Examples

Two of the following three parameters must be input to NVTHERM: Aperture Diameter, Focal Length, and F-Number. If three are input, they must correspond such that

$$Fnumber = \frac{FocalLength}{ApertureDiameter} \tag{2-2}$$

otherwise an error is shown.

The input units for Aperture Diameter are centimeters.

2.3.3. Focal Length

2.3.3.1. Input Description

Focal Length (*f*) is the distance between a lens and its focal point. (See Figure 2-7) For multiple lens systems, use the effective focal length, usually specified by the company that makes the optical system.

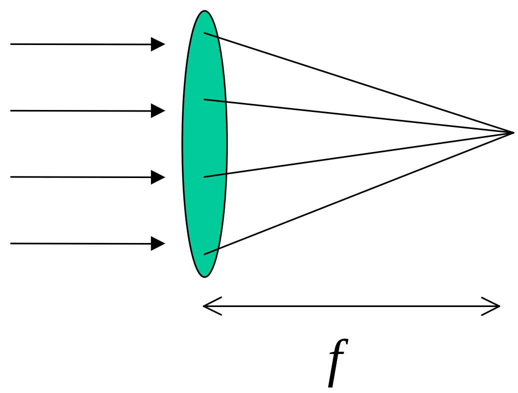

Figure 2-7

2.3.3.2. Help and Examples

The units on focal length are in centimeters.

2.3.4. F-Number

2.3.4.1. Input Description

The F-Number of an infrared imaging system describes the light collection capabilities of the system and is shown in Figure 2-8. It is the ratio of the focal length to the aperture dimension of the collecting optics. It describes the collection cone of the imaging optics.

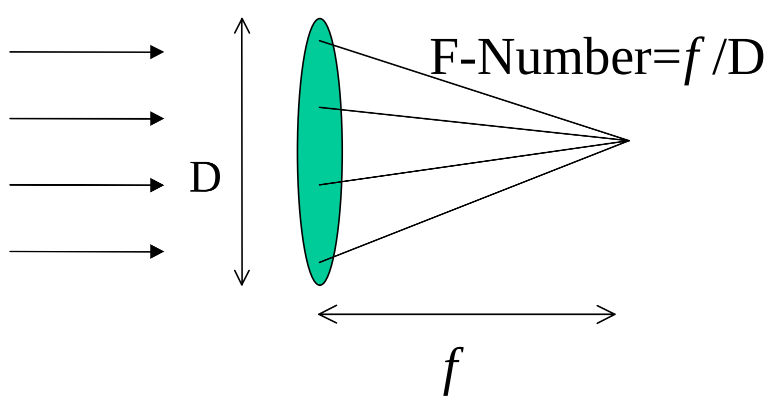

Figure 2-8. Aperture Diameter

2.3.4.2. Help and Examples

Two of the following three parameters must be input to NVTHERM: F-number, Aperture Diameter, and Focal Length. If three are input, they must correspond such that

$$Fnumber = \frac{FocalLength}{ApertureDiameter} \tag{2-3}$$

otherwise an error is shown.

F-number is unitless.

Typical F-numbers for tactical systems are between 1 and 10.

2.3.5. Average Optical Transmission

2.3.5.1. Input Description

The decimal amount of energy transmitted through the optical system in the specified spectral band. Program assumes that spectral signature is represented by differentiating Plank's blackbody equation with respect to temperature, evaluated at 300 K. Value must be between 0.0 and 1.0. Typical value for 1st generation thermal sensors is about 0.7. Typical value for 2nd generation systems range from 0.45 to 0.65. Values for staring sensors tend to be higher, typically 0.8.

2.3.5.2. Help and Examples

The optical system vendor can usually provide the average optical transmission for a given sensor spectral bandwidth. Typical values for average optical transmission are between 0.4 and 0.95.

2.3.6. Optics Blur Spot Size for Geometrical Aberrations

2.3.6.1. Input Description

A Gaussian distribution is used to describe the blur circle caused by the aberrations in the optical system. Aberrations tend to increase with field angle (as position in FOV moves away from center). Note that if the optics blur spot is larger than the diffraction spot, the lens is not considered to be diffraction limited. The following equation describes the optics blur spot.

$$h(x) = \frac{1}{b} e^{-\pi (\frac{x}{b})^2} \tag{2-4}$$

2.3.6.2. Help and Examples

The blur can be described in angular space (milliradians) or in the focal plane (millimeters).

The amount of blur can be described in three different ways, each of which is shown graphically in Figure 2-9.

- RMS (Standard Deviation) of the shape; this is the radius of the blur to 0.61 amplitude.
- Full-width, half max
- Radius of blur to 1/e amplitude

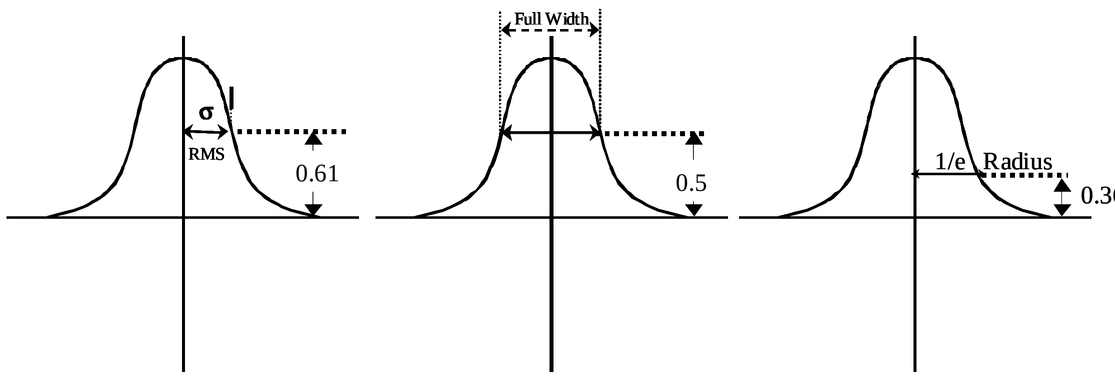

Figure 2-9

2.3.7. Stabilization/Vibration Blur Spot Size

2.3.7.1. Input Description

This blur occurs when the sensor is mounted on a platform that is vibrating or is not stabilized to well within sensor resolution. Random motion occurs between the object scene and the sensor causing a Gaussian-distributed blur. Figure 2-10 shows the random motion blur associated with imaging a point.

Motions with a period less than 5 Hz are tracked by the eye and are not included in the stabilization blur. Motions associated with gimbal stabilization are often sinsuidal in nature, not Gaussian. However, if the RMS motion is less than about 1/3 of an instantaneous field of view (IFOV), then the Gaussian MTF is a reasonable approximation for the vibration MTF.

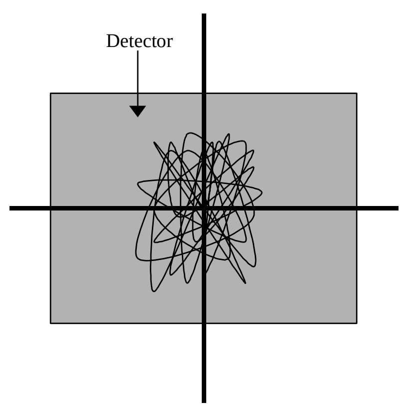

Figure 2-10

2.3.7.2. Help and Examples

The blur is described in angular space in milliradians. The blur spot is described by equation $h(x) = \frac{1}{b} e^{-\pi (\frac{x}{b})^2}$.

The blur can be described in three different ways as shown in section 2.3.6:

- RMS (Standard Deviation) of the shape
- Full-width, half max
- 1/e distance

1st GEN system attempted to hold stabilization error to about 1/3 IFOV. Newer systems often take 1/10 IFOV as a goal.

2.3.8. Measured MTF Values

2.3.8.1. Input Description

The measured MTF Values in the "Optics" input menu are the MTF values that would have been measured on the optical system. This measurement includes the diffraction effects and the aberration effects of the optical system. If this information is provided, the diffraction MTF and optics blur MTF are replaced with this measured MTF.

2.3.8.2. Help and Examples

There are three inputs that are required. First, the number of measured points is required. If this value is non-zero, then the diffraction MTF and optics blur MTF are replaced with the measured MTF values. Second, the spatial frequencies corresponding to the measured MTF points are input into an array that is provided. The units on these spatial frequencies are cycles per milliradian. Third, the measured MTFs that correspond to the input spatial frequencies are input as an array. There must be an equal number of spatial frequencies and measured MTFs. Also, the first MTF value should be 1 in the array and the last MTF value should be 0. The units on MTF are unitless, but the values must be between 0 and 1.

2.4. Detector

This is the “Detector” form. Each option is described below.

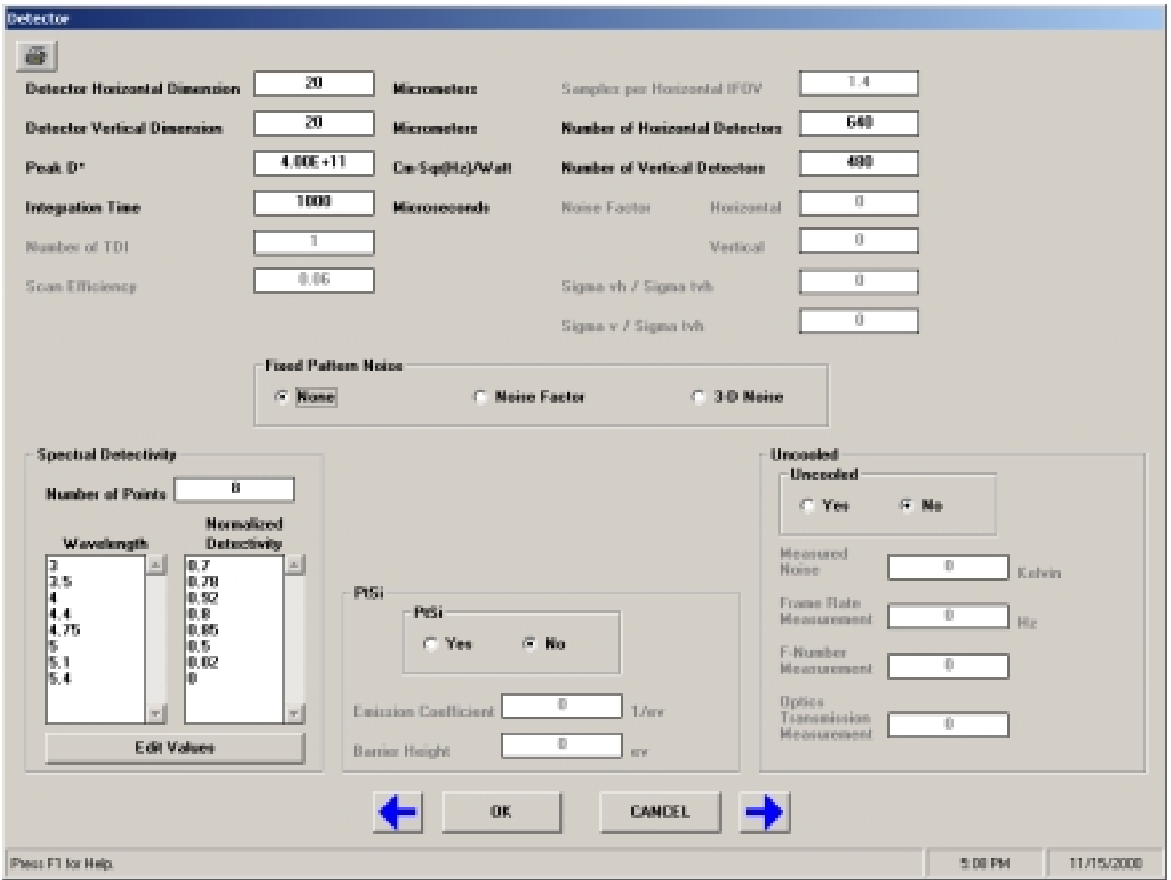

2.4.1. Detector Horizontal Dimension

2.4.1.1. Input Description

This describes the physical size of the detector in micrometers. Note that this is not the unit cell size, but the size of the light collecting material. (See Figure 2-11)

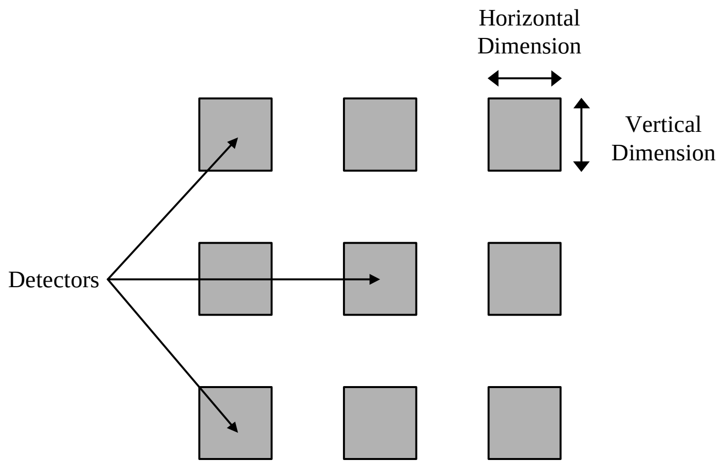

Figure 2-11

2.4.1.2. Help and Examples

Typical values are from 10 micrometers to 100 micrometers.

Input units are micrometers.

2.4.2. Detector Vertical Dimension

2.4.2.1. Input Description

This describes the physical size of the detector in micrometers. Note that this is not the unit cell size, but the size of the light collecting material. (See Figure 2-11)

2.4.2.2. Help and Examples

The typical range for this value is from 10 micrometers to 100 micrometers.

2.4.3. Peak D*

2.4.3.1. Input Description

D* (“dee star”) or normalized detectivity is the primary detector sensitivity performance parameter. The D* is a function of wavelength and frequency and can be written as

$$D^*(\lambda, f) = \frac{\sqrt{A_d \Delta f}}{NEP} \qquad \left[\frac{cm - Hz^{1/2}}{Watts}\right] \qquad (2\text{-}5)$$

where A_d is the detector area in square centimeters and Δf is the noise equivalent bandwidth of the system that limits the detector output noise. NEP is the noise equivalent power, the input power required to produce an output signal equal to the RMS noise. Peak D* is the highest detectivity in the spectral pass-band. See Figure 2-12.

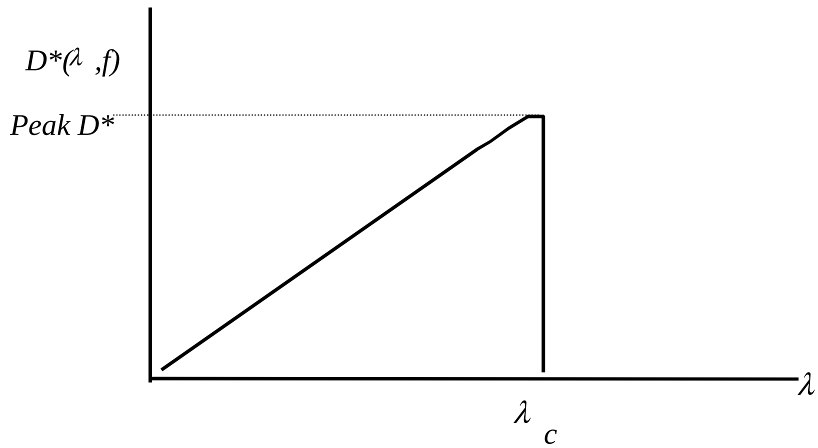

Figure 2-12

2.4.3.2. Help and Examples

The units of D* are called Jones and are given in centimeter - Hertz$^{1/2}$ per Watt.

2.4.4. Integration Time

2.4.4.1. Input Description

Integration time is the amount of time that light is integrated before reading out a detector output voltage.

Caution – Integration time may not equal a field or frame time. The reason is that the integration capacitor may fill with charge too quickly. For example, 1/60th frame time allows for 16,666 microseconds, an imager may only be able to integrate for 1000 to 2000 microseconds due to well-charge capacity.

2.4.4.2. Help and Examples

Integration Time units are in microseconds. This input is required for Staring Arrays and is optional for Scanning systems. Typical values range from 1000 microseconds to 33,333 microseconds. For Scanning systems, typical values are anywhere from 1/30th to 1/100th of a frame time. Integration time is required for staring sensors but is optional (with a 0 input) for scanned sampled imagers.

2.4.5. Number of TDI

2.4.5.1. Input Description

Time-Delay-Integration (TDI) is when two or more detectors are sampled in the in-scan direction at the same positions and the outputs of the detectors are added together. The noise adds in RMS fashion and the signal adds directly giving a $\sqrt{N_{tdi}}$ improvement in signal to noise ratio (SNR).

2.4.5.2. Help and Examples

TDI has no units.

1st GEN FLIR = 1 TDI
2nd GEN FLIR = 4 TDI

Some IRST systems can range as high as 18 TDI.

TDI does not apply to Staring Arrays, it only applies to Scanning systems

2.4.6. Number of Samples per H IFOV

2.4.6.1. Input Description

The Number of Samples Per Horizontal Instantaneous Field of View (H IFOV) is used for scanned sampled sensors only and does not apply to scanned continuous or staring sensors. It is calculated by dividing the horizontal IFOV by the horizontal Sample Spacing. This input is used to determine the horizontal sample rate of scanned sampled imagers.

2.4.6.2. Help and Examples

This value is not applicable for staring imagers or scanned continuous imagers. See Figure 2-11.

H IFOV for 2nd GEN FLIR is typically 1.7 or 2.2.

2.4.7. Scan Efficiency

2.4.7.1. Input Description

Scan Efficiency is a ratio of effective detector scan time to a field time. It describes the time lost due to overscanning the image plane. It includes the deceleration, turnaround, and acceleration of Galvanic scanners and the time passing the image plane with Polygon scanners (See Figure 2-13 and Figure 2-14). The equation that describes Scan Efficiency is $\eta_{scan} = \dfrac{t_{image}}{t_{nothing} + t_{image}}$.

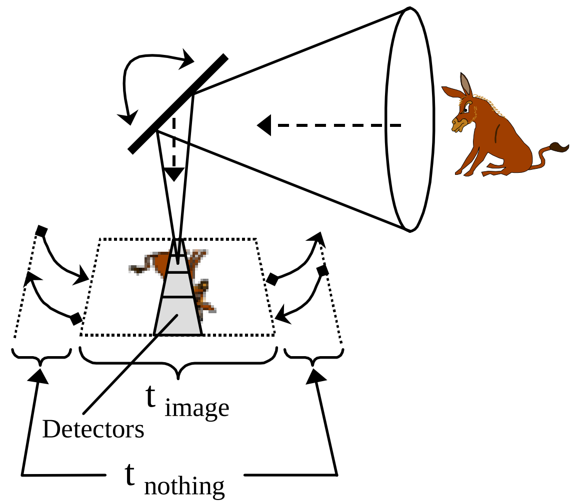

Figure 2-13 Galvanic Scanner

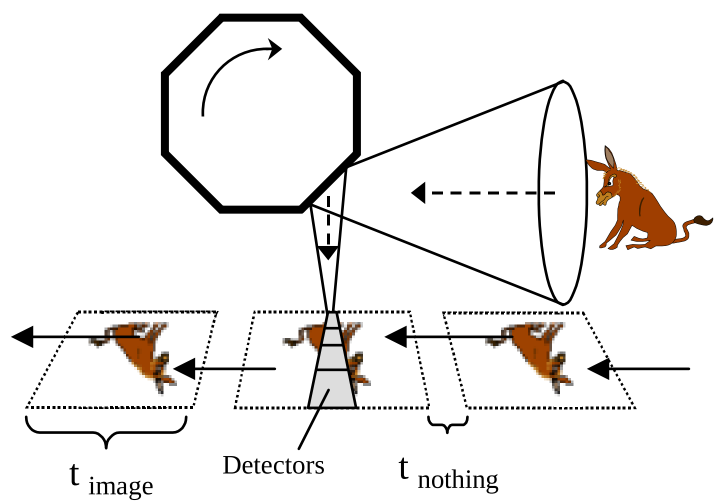

Figure 2-14 Polygon Scanner

2.4.7.2. Help and Examples

A perfect scan efficiency is a value of 1 (where overscanning ($t_{nothing}$) = 0). As the amount of overscanning increases, the scan efficiency gets smaller.

Typical scan efficiencies for a galvanic scanner are 0.6 to 0.75.

Typical scan efficiencies for a polygon scanner are 0.45 to 0.6

2.4.8. Number of Horizontal Detectors

2.4.8.1. Input Description

This input is the number or horizontal detectors in one detector row. See Figure 2-15 for an example. This input applies to both staring and scanning sensors. For a second generation FLIR, 4 should be used.

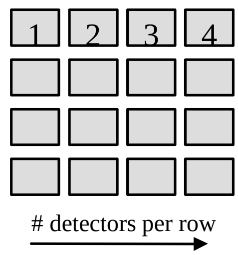

Figure 2-15

2.4.8.2. Help and Examples

Typical values for a staring sensor are from 256 to 1024.

For scanned first generation sensors, use 1. For second generation sensors, use the number of TDI detectors.

2.4.9. Number of Vertical Detectors

2.4.9.1. Input Description

This input is the number of vertical detector rows on a sensor. See Figure 2-16 for an example. This input applies to both staring and scanning sensors and has no associated unit.

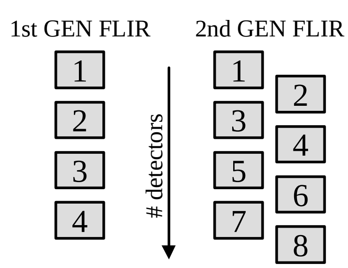

Figure 2-16 Number of Vertical detectors

2.4.9.2. Help and Examples

Typical values are:

1^{st} GEN FLIR	60, 120, 180
2^{nd} GEN FLIR	480
Staring sensor	240 to 1024

2.4.10. Fixed Pattern Noise

2.4.10.1. Input Description

Each detector has its own amplifier. Each detector/amplifier has a different gain and level offset and these variations produce fixed pattern noise (FPN). Examples of the two most common types of noise, σ_{vh} and σ_v, are shown below in Figure 2-17 and Figure 2-18.

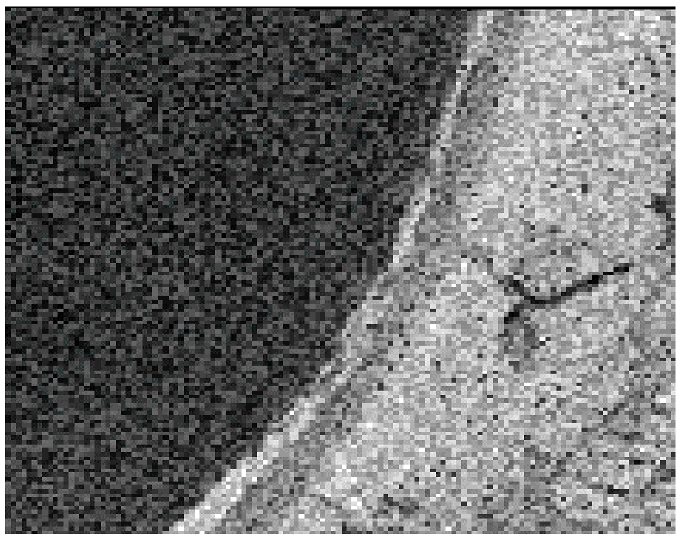

Figure 2-17 Random Spatial Noise or σ_{vh}

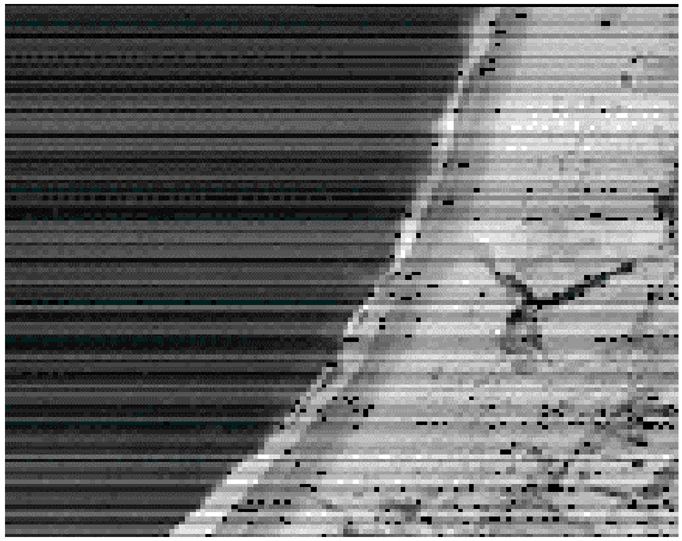

Figure 2-18 Fixed Row Noise or σ_v

2.4.10.2. Help and Examples

You must choose:

- None
- Noise Factor
- 3D Noise

Described below

  - You must enter values for σ_{vh} and σ_v if 3D Noise is chosen.

2.4.11. Noise Factor

2.4.11.1. Input Description

One option to model non-ideal performance in NVTherm is by using independent horizontal and vertical factors to multiply detector noise. These factors multiply the final horizontal and vertical MRTs. Knowledge of these factors is typically based on experience with measuring the MRT of the particular type of sensor being modeled.

2.4.11.2. Help and Examples

Typical values for Noise Factor range from 1.2 to 1.6.

2.4.12. Three Dimensional Noise

3D Noise must be understood before a selection for σ_{vh} or σ_v can be made. The description follows.

2.4.12.1. 3D Noise Description

Noise Equivalent Temperature Difference (NETD) is limited in that it only characterizes temporal detector noise, where three-dimensional noise characterizes both spatial and temporal noises that are attributed to a wide variety of sources. Consider the successive frames of acquired noise given in Figure 2-19.

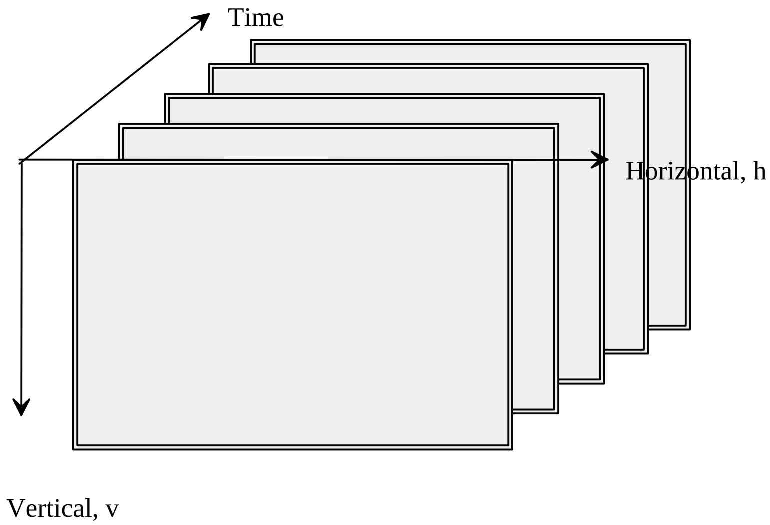

Figure 2-19 Three-dimensional noise coordinates.

A directional average is taken within the coordinate system shown in order to obtain eight parameters that describe the noise at the system's output. The noise is then calculated as the standard deviation of the noise values in the directions that were not averaged. The parameters are given in

Noise	Description	Source
σ_{tvh}	Random Spatio-Temporal Noise	Detector Temporal Noise
σ_{tv}	Temporal Row Noise, Line Bounce	Line Processing, 1/f, readout
σ_{th}	Temporal Column Noise, Column Bounce	Scan Effects
σ_{vh}	Random Spatial Noise, Bi-Directional Fixed Pattern Noise	Pixel Processing, Detector-to-Detector Non-Uniformity, 1/f
σ_{v}	Fixed Row Noise, Line-to-Line Non-Uniformity	Detector-to-Detector Non-Uniformity
σ_{h}	Fixed Column Noise, Column-to-Column Non-Uniformity	Scan Effects, Detector-to-Detector Non-Uniformity
σ_{t}	Frame-to-Frame Noise, Frame Bounce	Frame Processing
S	Mean of All Noise Components	

Figure 2-20, where the subscript that is missing gives the directions that were averaged. The directional averages are converted to equivalent temperatures in a manner similar to NETD. The result is a set of eight noise parameters that can be used as analytical tools in sensor design, analyses, testing, and evaluation. The majority of these parameters cannot be calculated like NETD with the exception of σ_{tvh}, which is similar to NETD. It is actually identical to NETD with the exception that the actual system noise bandwidth is used instead of the reference filter bandwidth. The other noise parameters can only be measured to determine the infrared sensor artifacts. In the infrared sensor models, reasonable estimates are made for these parameters based on a large database of historical measurements. The measurements were conducted on both scanning and staring-system noise parameters.

Noise	Description	Source
σ_{tvh}	Random Spatio-Temporal Noise	Detector Temporal Noise
σ_{tv}	Temporal Row Noise, Line Bounce	Line Processing, 1/f, readout
σ_{th}	Temporal Column Noise, Column Bounce	Scan Effects
σ_{vh}	Random Spatial Noise, Bi-Directional Fixed Pattern Noise	Pixel Processing, Detector-to-Detector Non-Uniformity, 1/f
σ_{v}	Fixed Row Noise, Line-to-Line Non-Uniformity	Detector-to-Detector Non-Uniformity
σ_{h}	Fixed Column Noise, Column-to-Column Non-Uniformity	Scan Effects, Detector-to-Detector Non-Uniformity
σ_{t}	Frame-to-Frame Noise, Frame Bounce	Frame Processing
S	Mean of All Noise Components	

Figure 2-20 Three-dimensional noise components from Scott, et al.

If all the noise components are considered statistically independent, an overall noise parameter can be given at the system output as

$$\Omega = \sqrt{\sigma_{tvh}{}^2 + \sigma_{tv}{}^2 + \sigma_{th}{}^2 + \sigma_{vh}{}^2 + \sigma_{v}{}^2 + \sigma_{h}{}^2 + \sigma_{t}{}^2} \qquad (2\text{-}8)$$

The frame-to-frame noise is typically negligible, so it is not included in most noise estimates.

The three-dimensional noise can be expanded further to include the perceived noise with eye and brain effects in the horizontal and vertical directions. Composite system noise (perceived) in the horizontal direction can be given by

$$\Omega = [\sigma_{tvh}^2 E_t E_v(\xi) E_h(\xi) + \sigma_{vh}^2 E_v(\xi) E_h(\xi) + \sigma_{th}^2 E_t E_v(\xi) + \sigma_h^2 E_h^2(\xi)]^{1/2} \qquad (2\text{-}9)$$

where E_t, $E_v(\xi)$, and $E_h(\xi)$ are the eye and brain temporal integration, vertical spatial integration, and horizontal spatial integration, respectively. In the vertical direction, the composite noise is given by

$$\Omega = [\sigma_{tvh}^2 E_t E_v(\eta) E_h(\eta) + \sigma_{vh}^2 E_v(\eta) E_h(\eta) + \sigma_{tv}^2 E_t E_v(\eta) + \sigma_v^2 E_v^2(\eta)]^{1/2} \qquad (2\text{-}10)$$

Note that the noise terms included in each perceived composite signal correspond to only those terms that contribute in that particular direction.

Scanning systems show a wide variety of noise values. Three different estimates of three-dimensional noise values corresponding to low, moderate, and high noise systems are provided in Figure 2-21. Staring arrays have been dominated by random spatial noise, so a single fixed pattern noise model is used. These model estimates are based on the construction of a measurement database at the U.S. Army's NVESD for infrared system characterizations. These estimates are given in Figure 2-21 in terms of a percentage of the random spatio-temporal noise.

3-D noise estimates based on historical measurements

Noise Term	**Scanning Low Noise**	**Scanning Moderate Noise**	**Scanning High Noise**	**Staring Noise**
σ_{tv}	0	0	$0.4\sigma_{tvh}$	0
σ_{v}	$0.25\sigma_{tvh}$	$0.75\sigma_{tvh}$	$1.0\sigma_{tvh}$	0
σ_{th}	0	0	0	0
σ_{h}	0	0	0	0

Figure 2-21

2.4.13. Sigma vh/Sigma tvh

2.4.13.1. Sigma vh / Sigma tvh Input Description

σ_{vh} is normalized to σ_{tvh} so the factor that is input is relative to random spatio-temporal noise.

2.4.13.2. Help and Examples

Typical values have been refined since Figure 2-21 and values range from 0.2 to 0.4 for Staring arrays and are 0 for Scanning arrays.

2.4.14. Sigma v / Sigma tvh

2.4.14.1. Input Description

σ_{v} is normalized to σ_{tvh} so the factor that is input is relative to random spatio-temporal noise.

2.4.14.2. Help and Examples

For Staring arrays, a typical value range from 0.2 to 0.4 and for Scanning arrays, values range from 1.1 to 1.4.

2.4.15. Spectral Detectivity

2.4.15.1. Input Description

Spectral Detectivity is the normalized (to D* peak) detectivity input of an array. Values are from 0 to 1. Wavelength range must cover Cuton wavelength to cutoff wavelength. The required inputs are the number of points, the wavelengths and the normalized detectivity.

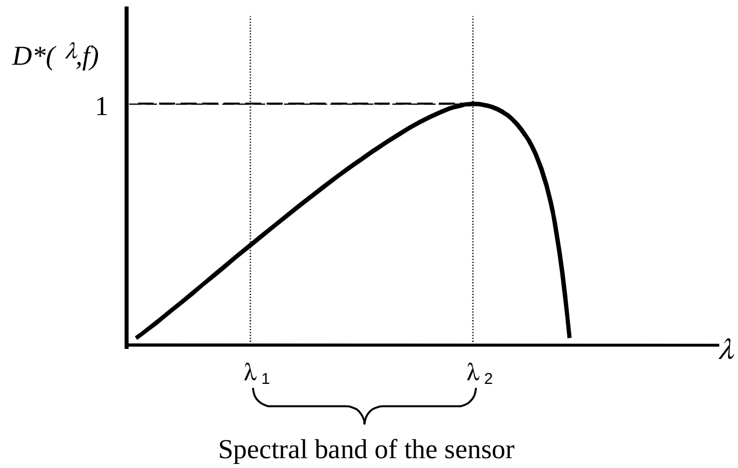

Figure 2-22

2.4.15.2. Help and Examples

Values should never exceed 1.

Wavelength range must cover spectral band of the sensor. (Figure 2-22)

2.4.16. PtSi

PtSi is a Schottky-barrier photodiode which is a metal film on a silicon substrate. It is back-illuminated through the silicon and the metal-silicide junction creates a potential energy barrier over which photogenerated holes can be excited to produce internal photoemission into the semiconductor. If PtSi is chosen, then the Peak D* and the normalized detectivity are calculated from two inputs. They are the barrier height and the emission coefficient. The barrier height for PtSi is around 0.22 electron-Volts and emission coefficients are approximately 0.25 to 0.35 eV^{-1}.

2.4.17. Uncooled

An uncooled sensor is one with a thermal detector (a bolometer or pyrometer array). If an uncooled detector is chosen, then the performance measurement of the array must be provided in terms of the measured detector noise, the frame rate, f-number, and optics transmission associated with the measured noise.

From these quantities, the peak D* of the sensor is calculated. Also, the normalized detectivity is set to 1 over the range of the sensor.

2.5. Electronics

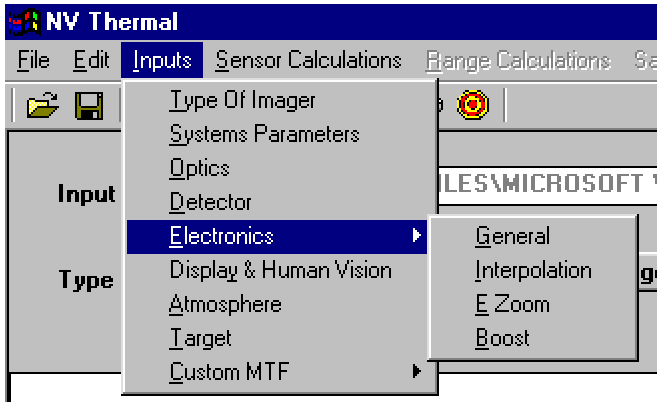

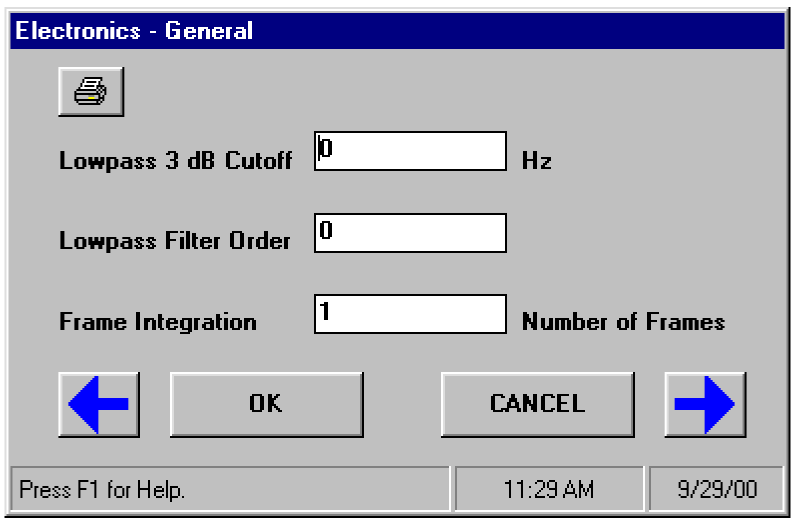

2.5.1. LowPass 3dB Cutoff Frequency (LowPass Filter)

2.5.1.1. Input Description

In scanned systems, the temporal frequency response of the electronics is given by a multiple pole RC low pass filter,

$$H_{elp}(f_t) = \left(1 + \left(\frac{f_t}{f_{elp}}\right)^{2n}\right)^{-1/2} \qquad (2\text{-}9)$$

where f_{elp} is the electronics 3dB frequency (Hz) and n is the number of filter poles (this is the filter order). This filter is used to calculate noise bandwidths and the blur associated with the filter.

2.5.1.2. Help and Examples

The LowPass filter should not be the limiting MTF of the system. If this is the case then there is an error in the system design.

Units are Hertz.

2.5.2. LowPass Filter Order

2.5.2.1. Input Description

The LowPass filter order describes the steepness of the filter MTF shape. The filter order is n in the equation given for the LowPass filter.

2.5.2.2. Help and Examples

Typically, n is 1 to 3 (1 is common).

2.5.3. Frame Integration

2.5.3.1. Input Description

Frame Integration is the temporal averaging of frames before they are displayed. Figure 2-23 shows the process for 4-frame integration. The averages shown at time t_1, t_2, t_3, …etc. are displayed on the monitor.

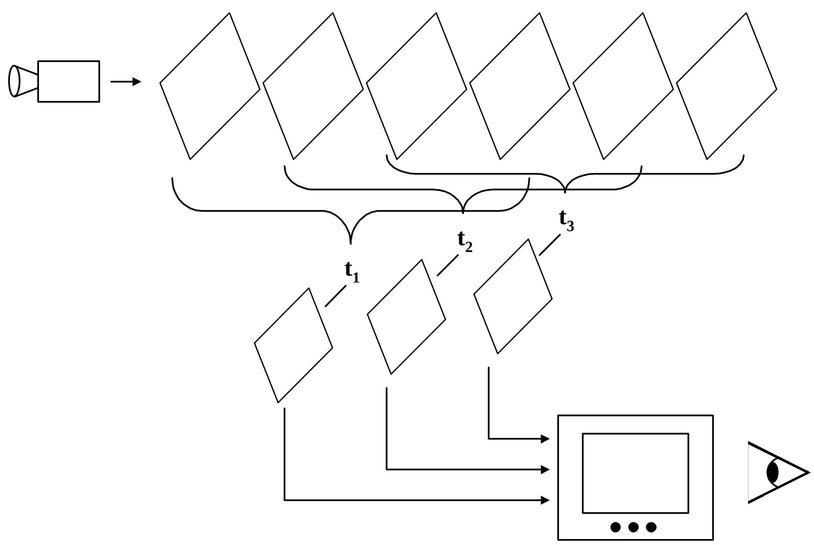

Figure 2-23 Frame Integration

The increase in S/N is

$$\frac{S}{N}_{improvement} = \sqrt{\eta} \qquad (2\text{-}10)$$

Where η is the number of frames integrated.

The increase in perceived S/N is

$$\frac{S}{N}_{perceived} = \frac{\sqrt{\eta_{FI}^2 + \eta_{eye}^2}}{\eta_{eye}} \tag{2-11}$$

Where N_{FI} is the number of frames integrated in Frame Integration and N_{eye} is the number of frames integrated by the eye.

2.5.3.2. Help and Examples

Frame Integration does not make much difference to the MRT until the number of frames integrated approaches the number of frames the eye integrates.

η_{eye} for 60 Hz display rate and a 0.2-second eye integration time associated with a dark display is 6 frames. Interpolation – Horizontal & Vertical

2.5.4. Interpolation

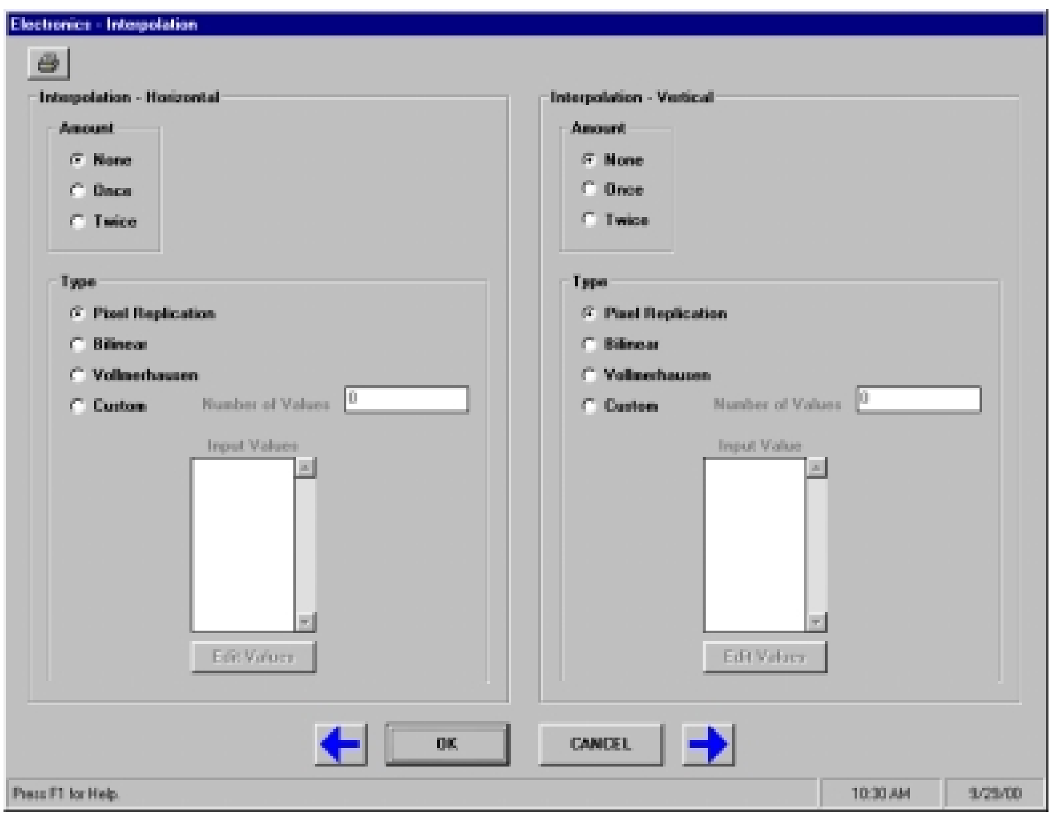

2.5.4.1. Input Description

Interpolation is the process of increasing image size via various methods of creating "filler" pixels between original pixels. Horizontal interpolation applies the different methods described below across pixels in a horizontal direction. Vertical interpolation applies them vertically. If both directions are used, NVTHERM applies one direction at a time.

The amount of interpolation refers to the number of times the specific method of interpolation is applied to an image. “Once” is applied one time. “Twice” is applied two times.

Pixel Replication Interpolation

Pixel Replication creates new pixels by copying pixels from left to right and/or top to bottom (see Figure 2-24) depending on the horizontal/vertical options that were chosen.

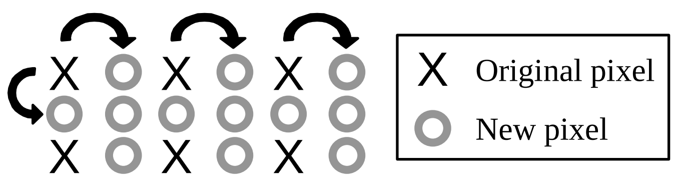

Figure 2-24 Pixel Replication Interpolation

Bilinear Interpolation

Bilinear Interpolation creates a new pixel by taking the average of the two pixels on each side of the new pixel location. (See Figure 2-25)

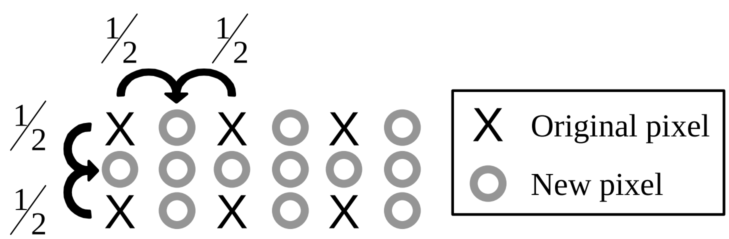

Figure 2-25 Bilinear Interpolation

Vollmerhausen Interpolation

Vollmerhausen 8-pixel interpolation creates new pixels by adding together weighted values of 8 pixels (4 on each side) surrounding the new pixel location. (See Figure 2-26) The weighted values for each location are:

(Note that these apply to both sides of the new pixel location.)

1-pixel away	0.604
2-pixels away	-0.13
3-pixels away	0.032
4-pixels away	-0.006

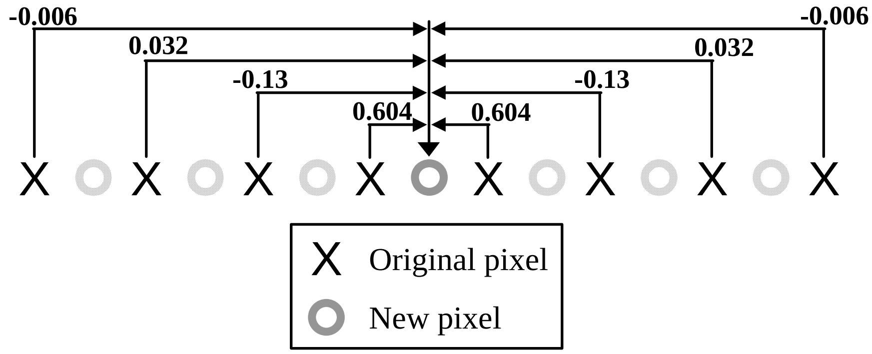

Figure 2-26 Vollmerhausen 8-pixel interpolation

Custom

The Custom interpolation input option allows the user to assign specific interpolation values in a similar way as the Vollmerhausen interpolation.

The "Number of Values" input allows the user to define how many pixels will be used *on one side* of the new pixel location to determine the new pixel value. For example, the Vollmerhausen 8-pixel would have a "Number of Values" input value of 4.

The "Input Value" input allows the user to assign different weights to each of the values entered in "Number of Values". Figure 2-27 shows what the Vollmerhausen interpolation would look like if it were entered as a Custom interpolation.

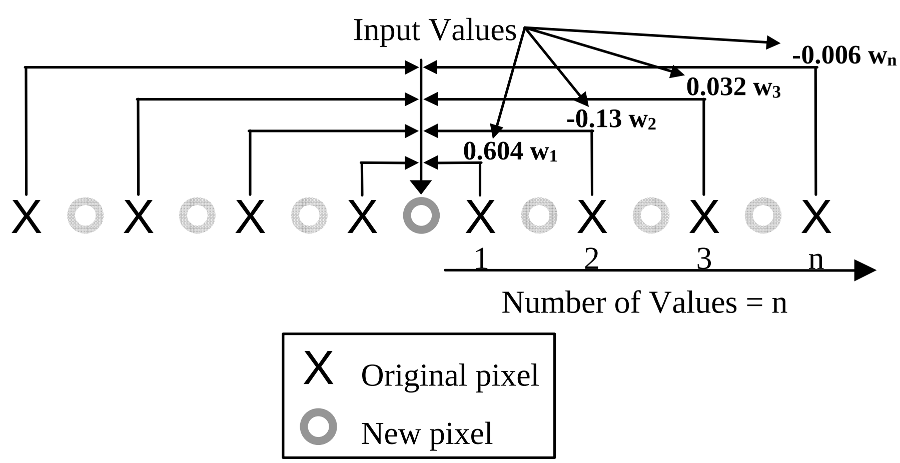

Figure 2-27 Custom Interpolation

2.5.4.2. Help and Examples

For interpolation, all of the FOV is seen on the image height (No magnification change). (See Figure 2-28)

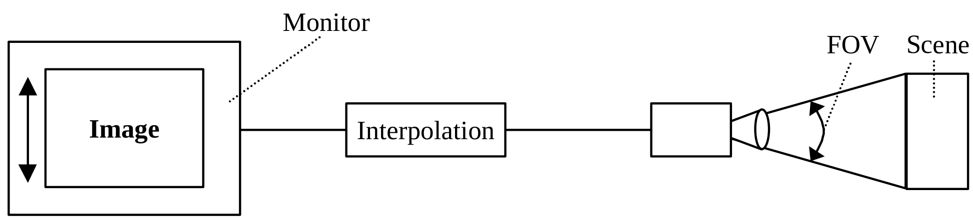

Figure 2-28 Interpolation FOV

2.5.5. Ezoom

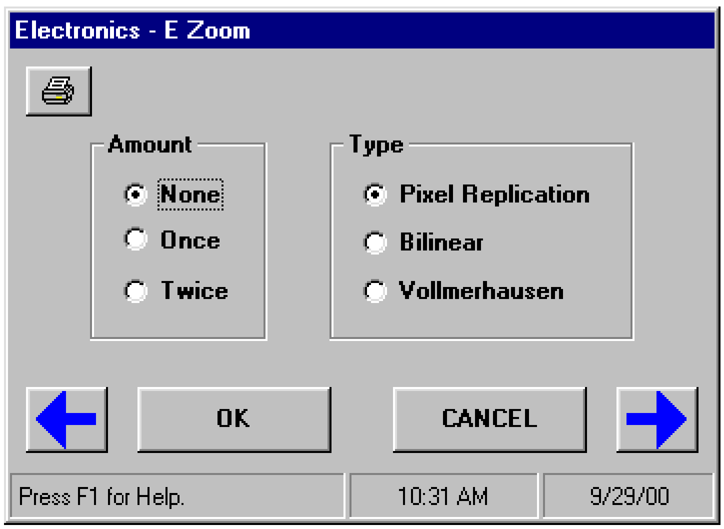

2.5.5.1. Input Description

Ezoom is really interpolation with two exceptions. 1) It assumes interpolation in both directions. 2) Magnification is increased. Generally, only part of the FOV is displayed in Ezoom.

2.5.5.2. Help and Examples

Each Ezoom doubles display magnification (one Ezoom magnification doubles and two quadruples). If the image fills the display without Ezoom, then Ezoom reduces the viewable field of view. For example, if the whole display is used to view the FOV without Ezoom, selecting “Twice” reduces system FOV by 4 in each direction. (See Figure 2-29)

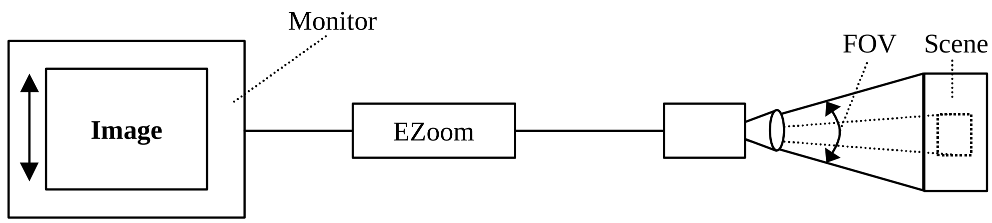

Figure 2-29

2.5.6. Boost – Horizontal

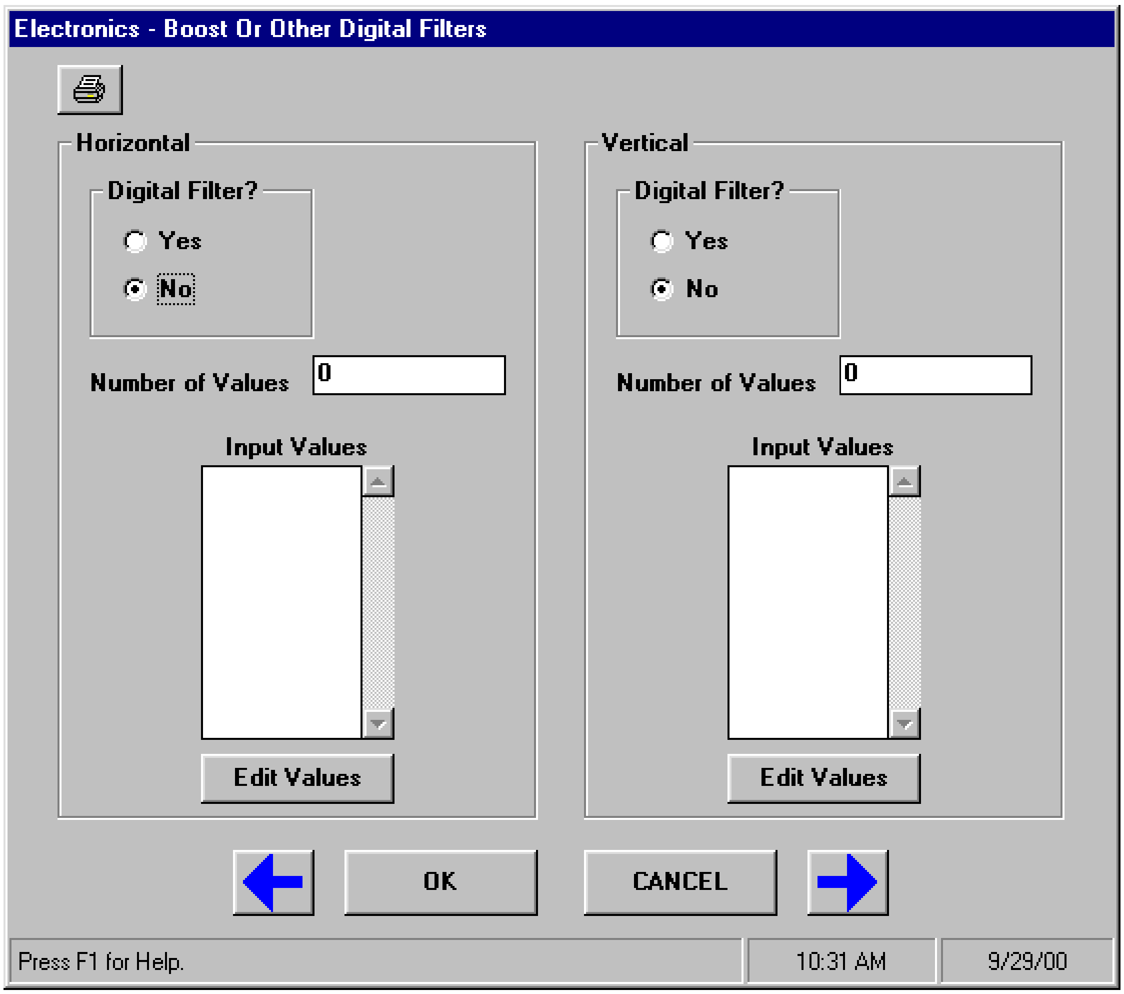

2.5.6.1. Input Description

Boost and other digital filters in NVTHERM are FIR (finite impulse response) filters. Boost calculates new pixel values in a similar fashion as an interpolation by taking weighted values of a given number of pixels and adding them together to create a new pixel. Unlike interpolation, however, boost does not create pixels to increase an image's size, it replaces existing pixels for an entirely new image. (See Figure 2-30)

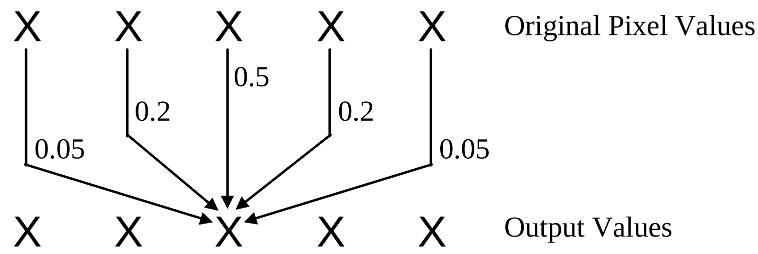

Figure 2-30 Horizontal Boost

2.5.6.2. Help and Examples

In this figure, the Number of Values is 3 (the center pixel value and the pixel values to one side of the center pixel). Input Values are 0.5 (the center value), 0.2 and 0.05 (the remaining values).

Horizontal and vertical filters do not have to be identical.

The center value (i.e. 0.5) plus twice the values of one side (i.e. 0.2 & 0.05) must equal 1.

2.5.7. Boost – Vertical

2.5.7.1. Input Description

See “Boost – Horizontal” section.

2.5.7.2. Help and Examples

See “Boost – Horizontal” section.

2.6. Display and Human Vision

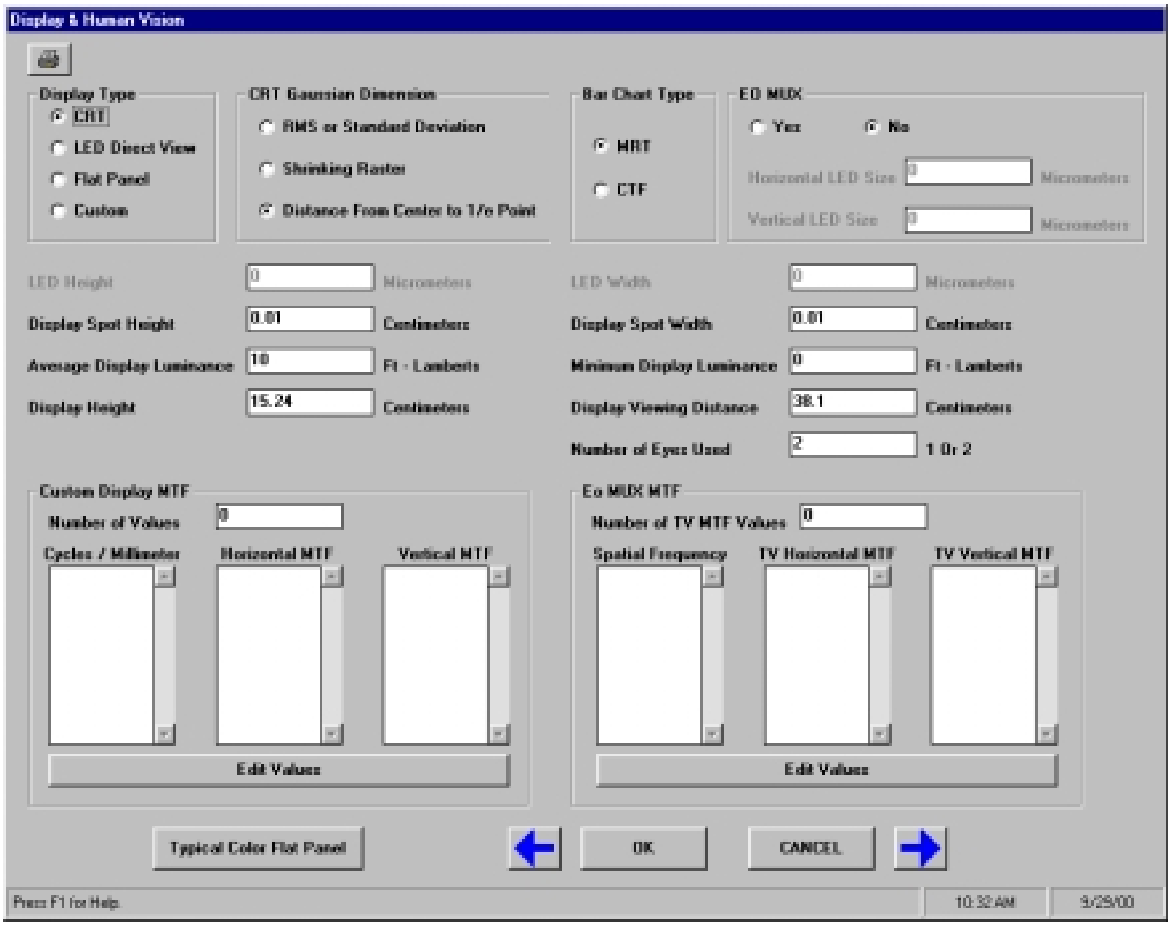

2.6.1. Display Type

2.6.1.1. Input Description

Cathode Ray Tube

Cathode Ray Tubes (CRTs) are probably the most common display component. A CRT comprises an evacuated tube with a phosphor screen. An electron beam is scanned across the phosphor screen in a raster pattern as shown in Figure 2-31. The beam direction is controlled with horizontal and vertical magnetic fields that bend the beam in the appropriate direction. The phosphor converts the electron beam into a visible point, where the visible luminance of the phosphor is related to the electron beam current (and voltage). The standard raster scan and interlace pattern are also shown in Figure 2-31. First the solid line shows a field pattern that is traced out on the screen. The dashed line shows a second field pattern that is interlaced between the first field lines.

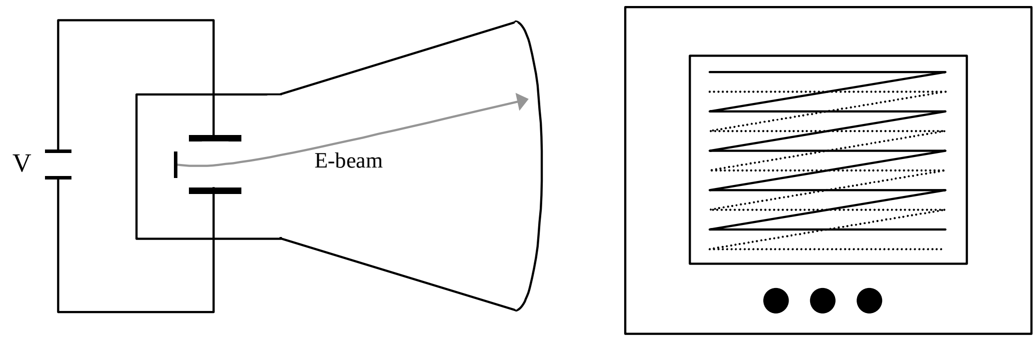

Figure 2-31 Cathode Ray Tube

LED Direct View

LED Direct View is viewed through a scan mirror as shown in Figure 2-32. The front is infrared and the back end is a scanned LED that is projected into the eye. The LED shape is rectangular and is described in the focal plane of the sensor.

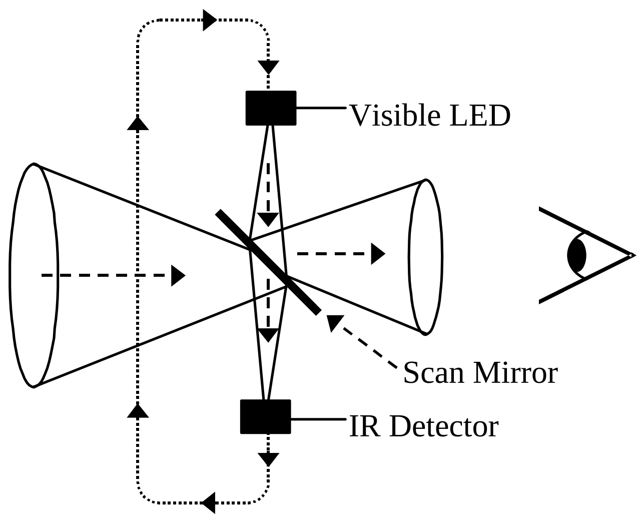

Figure 2-32 LED Direct View

Flat Panel

A Flat Panel display is a display of rectangular elements: liquid crystals, active matrix, photo emissive, and any other display with rectangular pixels. These systems are modeled as arrays of rectangular display elements shown in Figure 2-33.

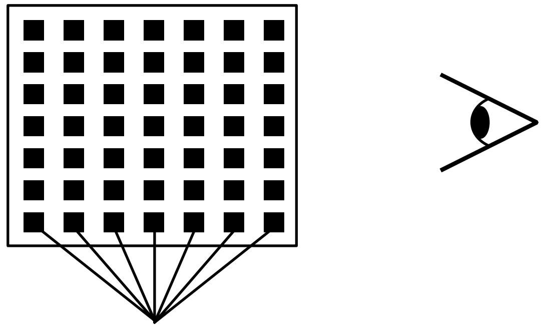

Figure 2-33 Flat Panel

Custom

Custom is used when the MTF of the monitor is known by measurement or more sophisticated modeling. Number of values, the spatial frequencies in cycles per millimeter, and the corresponding MTFs are input.

2.6.1.2. Help and Examples

2.6.2. EO MUX & EO MUX MTF

2.6.2.1. Input Description

An EO Multiplexer (or EO MUX for short) is shown in Figure 2-38 . It includes a visible LED system and a camera that converts the LED output to a video or digital signal. If EO MUX is selected, Horizontal LED Size and Vertical LED Size must be non-zero and EO MUX TV MTF values must be input. LED sizes (Horizontal and Vertical) are input in micrometers. The TV MTF Values require: Number of TV MTF Values, Spatial Frequency, TV Horizontal MTFs, and TV Vertical MTFs.

2.6.2.2. Help and Examples

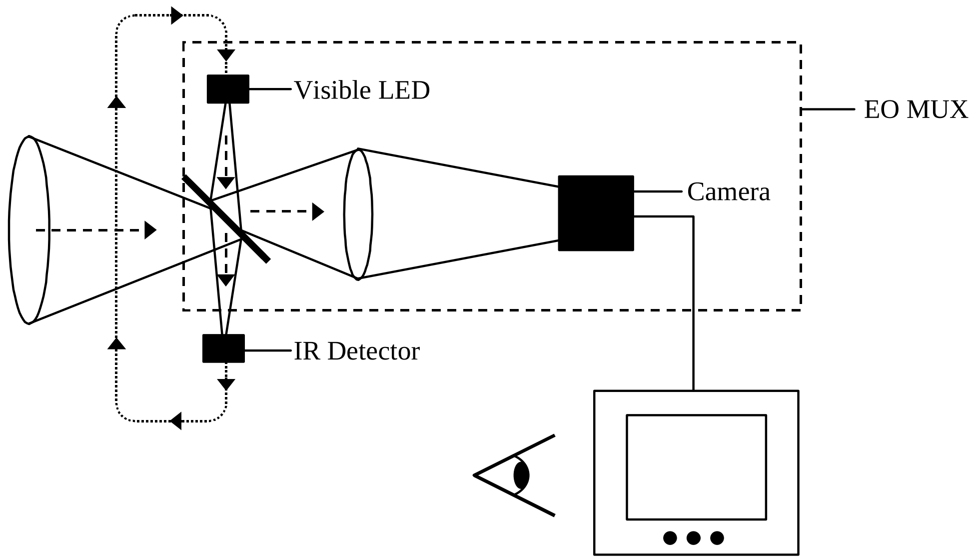

Figure 2-34

2.6.3. CRT Gaussian Dimension

2.6.3.1. Input Description

There are three ways to describe the CRT. They are:

- RMS (Standard Deviation) of the shape
- Distance from center to 1/e point
- Shrinking Raster Distance

The details on these sizes are given in section 2.3.6 (optics blur) and 2.6.7 below.

If a CRT display is selected for a staring or scanning, sampled imager, then a sample and hold at the sample rate is included in the display MTF.

2.6.4. Bar Chart Type

2.6.4.1. Input Description

MRT

An MRTD bar chart is generally used for range prediction; this is the standard four bar pattern with the length of the bars equal to seven times the width of one bar. When this bar-pattern is selected, the program output will be MRT calculated using Equation 21. This is the appropriate choice when the MRT is used with Acquire for range performance predictions. See Figure 2-35.

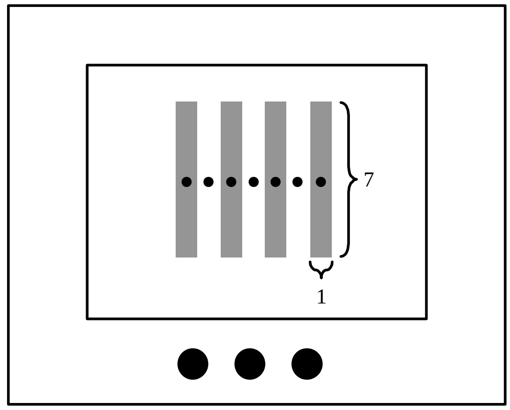

Figure 2-35

CTF

A CTF bar-pattern can also be selected; this bar-pattern is 2 degrees in length regardless of the spatial frequency. When the CTF pattern is selected, minimum resolvable contrast (at the display) is calculated as given by Equation 22. This output is provided for use in image quality metrics. See Figure 2-36.

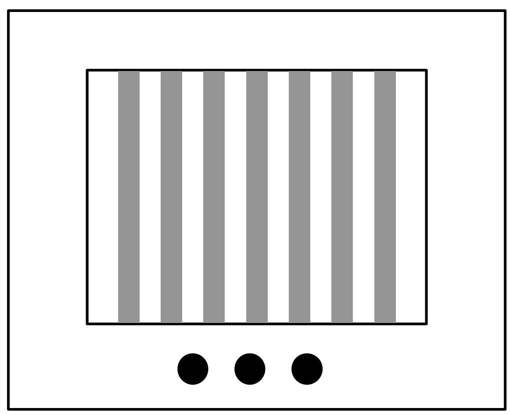

Figure 2-36

2.6.5. Custom Display MTF

2.6.5.1. Input Description

The custom MTF, if selected, overrides all other MTF inputs. This MTF array is in place of, not in addition to, any other display MTFs. Four inputs are needed: Number of MTF Values, Spatial frequency on the display in cycles/mm, Horizontal MTF Values, and Vertical MTF Values. The MTF Values both correspond to the spatial frequencies that are input.

2.6.5.2. Help and Examples

Custom Display MTF values are given by the displays measurement group or from the display manufacturer. However, there is a button on the display page that gives the custom MTF values for a typical color flat panel display as measured by NVESD ("Typical Color Flat Panel").

2.6.6. LED Height and Width (micrometers)

2.6.6.1. Input Description

LED Height and Width is the dimension of the active (emitting) area in micrometers. These values are applicable to direct view LED displays only.

2.6.6.2. Help and Examples

Common module LEDs are 19.05 micrometers horizontally and 95.25 micrometers vertically.

2.6.7. Display Spot Height & Width (micrometers)

2.6.7.1. Input Description

Display Spot Height and Display Spot Width describe the physical size of the display spot (Gaussian spot for CRT or rectangular spot for a flat panel display). The parameter is only used for these displays.

The display spot can only be described as a dimension on the display. The spot size can be described in three different ways. RMS and 1/e (center to 1/e distance) are shown in Figure 2-37. Shrinking Raster Distance is described below.

- RMS (Standard Deviation) of the shape
- Distance from center to 1/e point
- Shrinking Raster Distance

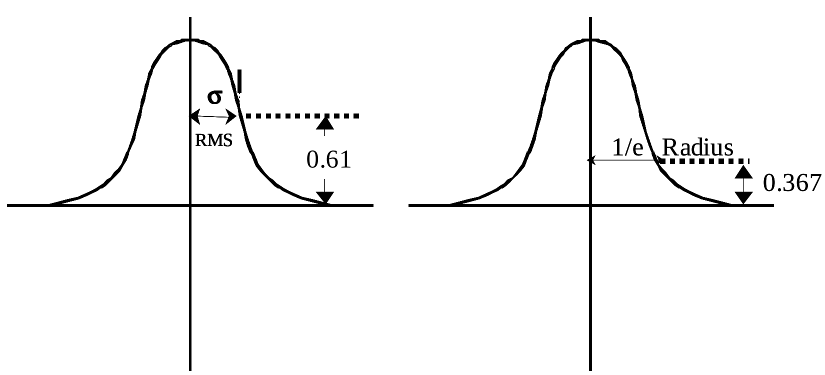

Figure 2-37

To determine Shrinking Raster Distance, the raster scan itself (no image) is shrunk until an observer can no longer detect the individual scan lines. This seems to occur at a reasonably constant value for all observers. Larger spot sizes (larger σ values) lead to larger separation for the occurrence of this condition. So poor resolution displays are characterized by large values of shrinking raster line separation, and high resolution by small values. Shrinking Raster Distance can be described by

$$\sigma = .54s$$

Where s is the raster distance and σ is the RMS distance of the spot.

The raster distance, s, is described by

$$s = \frac{h}{\#TVLines}$$

where h is the shrunken raster scan height. See Figure 2-38 below.

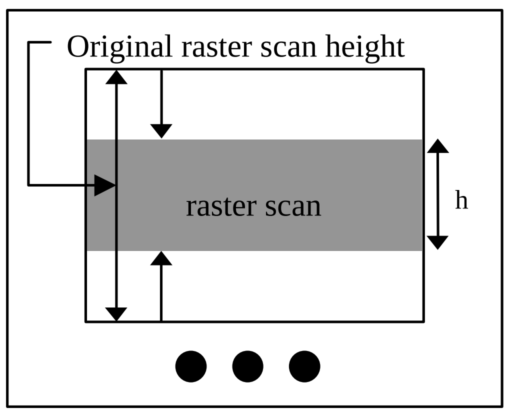

Figure 2-38

2.6.7.2. Help and Examples

Typical values range from 0.01 centimeters to 0.05 centimeters. These values can vary dramatically for different display sizes.

2.6.8. Average Display Luminance (fL)

2.6.8.1. Input Description

The average brightness of the display in footLamberts.

2.6.8.2. Help and Examples

For tactical systems on a dark night, if the user has an option, the display would typically be set between 0.1 and 0.3 footLamberts. For dimly lighted conditions use 1 to 10 fL. For normal room light use 30fL or more. The unit "millilamberts" used in some programs is very nearly equal to a footLambert.

2.6.9. Minimum Display Luminance (fL)

2.6.9.1. Input Description

The minimum display brightness in footLamberts. This is the brightness of the minimum intensity on the display. A minimum brightness other than zero might occur for several reasons. For example, ambient light might reflect off the display, reducing display contrast. Also, if the imager is producing a low contrast image, the display brightness control might be used to brighten the image to the eye; this would also reduce contrast.

2.6.9.2. Help and Examples

It is best to use actual values if measurements are available. If not, and if the display is not anticipated to be used in high ambient lighting conditions, a value of 0 can be assumed.

2.6.10. Display Height (centimeters)

2.6.10.1. Input Description

The Display Height input is the height of the image shown on the display/monitor given in centimeters. If the displayed image is less in height than the display height, then the image height is used instead of the display height.

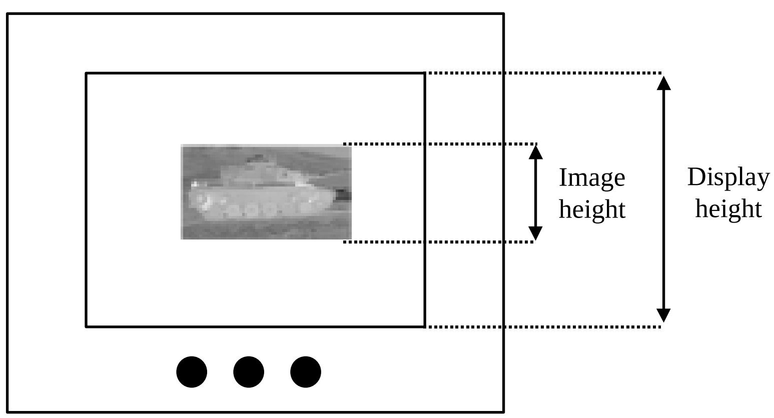

Figure 2-39

2.6.10.2. Help and Examples

Typical display heights range from 5 centimeters to 50 centimeters, althought smaller and large displays are available. A standard display height is 15.24 cm.

2.6.11. Display Viewing Distance (cm)

2.6.11.1. Input Description

Display Viewing Distance is the distance from the monitor/display to the user's eye(s) given in centimeters.

2.6.11.2. Help and Examples

Figure Figure 2-40 demonstrates Display Viewing Distance. For a standard display height of 15.24 cm, a typical viewing distance would be 38.1cm.

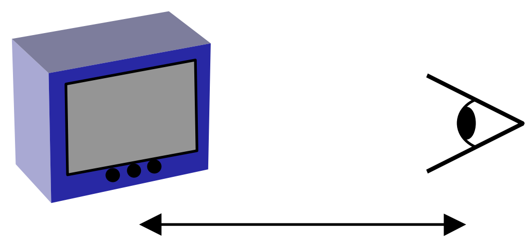

Figure 2-40 Display Viewing Distance

2.6.12. Number of Eyes Used

2.6.12.1. Input Description

Number of Eyes Used refers to the number of eyes the observer uses to view the image.

2.6.12.2. Help and Examples

On a system using a monocle, this input would be one. Otherwise, this input would typically be 2

2.7. Atmosphere

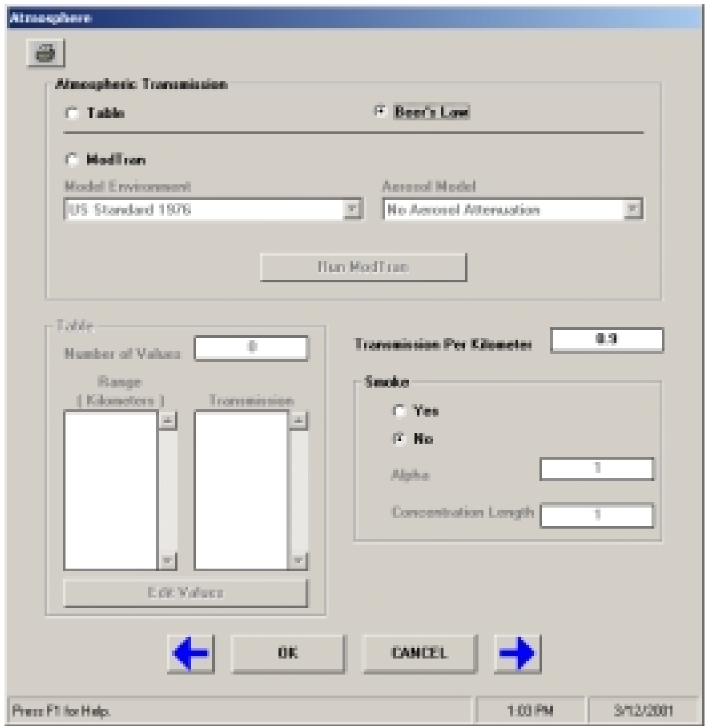

2.7.1. Atmospheric Transmission

2.7.1.1. Input Description

The three options here are Beers Law, a Table, or MODTRAN. Beers Law assumes that a 1-kilometer transmission is uniform over all ranges. Therefore, the transmission at Range, R, is

$$T(R) = (T_{km})^R \tag{2-12}$$

The second option is a table, where transmission can be entered as a function of range. The third option is to run MODTRAN and this option uses the Model Environment, the Aerosol Model, the Cuton Wavelength, The Cutoff Wavelength, and the Maximum Range (from the target form) to run a table. When Run Modtran is selected, parameters are passed to MODTRAN and the table is filled with Range and Transmission. These table values are used in the range calculations.

2.7.1.2. Help and Examples

Note: Beers Law is not a bad approximation for longwave winter. Errors of around 20 percent can be seen with longwave summer over ranges of 10 km. In the midwave, use of a table is recommended because errors can be large.

2.7.2. Transmission Per Kilometer

2.7.2.1. Input Description

This is the per kilometer transmission value that is used if Beers Law is chosen.

2.7.2.2. Help and Examples

Input a unitless value between 0.0 and 1.0. Typical value can range from .2 to .95.

2.7.3. MODTRAN

2.7.3.1. Input Description

MODTRAN is a reduced version of the atmospheric program distributed by ONTAR Corp. The program uses the Model Environment, the Aerosol Model, the Cuton Wavelength, The Cutoff Wavelength, and the Maximum Range (from the target form) to run a table. NVTherm calls the MODTRAN program through a shell:

NVmod.exe is the MODTRAN shell program that uses modin.nvl and modout.nvl files.

mod4v1r1.exe – this contains the MODTRAN executable program

The MODTRAN 4 executable and data file are the "latest versions" released by AFRL.

Example Files

NVMod input file MODIN.NVL

The input file, modin.nvl, is a small ASCII file with the following content

Cuton, 3	(Micrometers)
Cutoff, 5	(Micrometers)
Height, 0	(Kilometers)
Max Range, 5	(Kilometers)
Model Environment, 6	(MODTRAN Variable #)
Aerosol Model, 1	(MODTRAN Variable #)

The information in the parathenses are the units, and are not part of the file. These are the ONLY parameters that a user of NVTherm is allowed to set. All the other MODTRAN input variables are set to defaults. The Height is the sensor altitude and is not available currently through NVTherm, but will be added in version 2.

NVMod Output File MODOUT.nvl is a file created for NVTherm that has an array of atmospheric transmission values at different ranges and difference wavenumbers. The resolution of MODTRAN is 50 wavenumber for NVTherm.

NVMod Assumptions

Below are the assumptions we used in creating the MODTRAN input file.

Initial and Final Frequency: we use the “Cuton” and “Cutoff” values.

Geometry Parameters: we allow two type of geometry: Horizontal path, and Slant Path. If “Height” = 0 we use a horizontal path at altitude 0. The path length then starts at 0 and increments up to the “Max Range”, using the table shown below. Again, slant path will only be available in version 2.

The following table determines the range increment. This was arrived at as a trade-off between the maximum number of points allowed (20) and execution time considerations (the main runtime of NVmod.exe is waiting for MODTRAN to finish).

“Max Range” Km	**Inc Km**
0 – 4	0.2
4 – 10	0.5
10 – 20	1

Model Atmosphere: The allowable values are:

Tropical Model = 1

MidLatitude Summer = 2

Midlatitude Winter = 3

SubArctic Summer = 4

SubArctic Winter= 5

1976 U S Standard = 6

The following parameters are not allowed:

Meteorologic Data Input = 0

New Model Atmosphere = 7

Aerosol Models: The allowable values are:

No Aerosol Attenuation = 0

Rural - VIS=23km = 1

Rural - VIS=5km = 2

Navy Maritime = 3

Maritime - VIS=23km = 4

Urban - VIS=5km = 5

Tropospheric - VIS=50

Fog advection - VIS=.5km = 8

Fog radiation - VIS=.2km = 9

Desert extinction = 10

The following parameter is not allowed:

User Defined - VIS=23km = 7

No other aerosol options are available, eg. the Army VSA model, or wind speed with Navy Maritime, clouds/rain etc, as this significantly complicates the interface.

The spectral output is read by NVTherm and a weighted (for source strength and detector detectivity) transmission is calculated for each range. The calculation is

$$T(R) = \frac{\int_{\lambda_1}^{\lambda_2} \frac{\partial L(\lambda)}{\partial T} D^*(\lambda)\tau(\lambda)d\lambda}{\int_{\lambda_1}^{\lambda_2} \frac{\partial L(\lambda)}{\partial T} D^*(\lambda)d\lambda} \qquad (2\text{-}13)$$

where T is the weighted transmission, L is the radiance of the source at 300 Kelvin, D^* is the detector detectivity, and τ is the spectral transmission.

2.7.3.2. Help and Examples

When MODTRAN is run, the table of transmission values are replaced with the MODTRAN results. These can be saved and MODTRAN does not have to be run again for these conditions. WARNING: A maximum range on the target input page must be specified to run MODTRAN.

2.7.4. Table of Values

2.7.4.1. Input Description

Number of Range Values, Ranges, and Transmission of these ranges are required. This table is only used if the Table option is selected. These values can be obtained by running MODTRAN or LOWTRAN (the full versions for more sophisticated conditions) at multiple ranges and compiling a table.

2.7.4.2. Help and Examples

All ranges are in kilometers and all transmission values are between 0 and 1.

2.7.5. Smoke

2.7.5.1. Input Description

This input is intended to address intentional battlefield obscurants. The transmission is given by

$$T = e^{-\alpha CL}$$

where

α is the extinction coefficient and

CL is the concentration length.

2.7.5.2. Help and Examples

	α		CL	
	3-5mm	8-12mm	Light	Heavy
Fog Oil	.25		8	16
		.02	100	200
Hexachloroethane	.19		10.52	21.05
		.03	66.67	133.33
Phosphorus	.29		6.89	13.79
		.38	5.26	10.52

Figure 2-41

2.8. Target

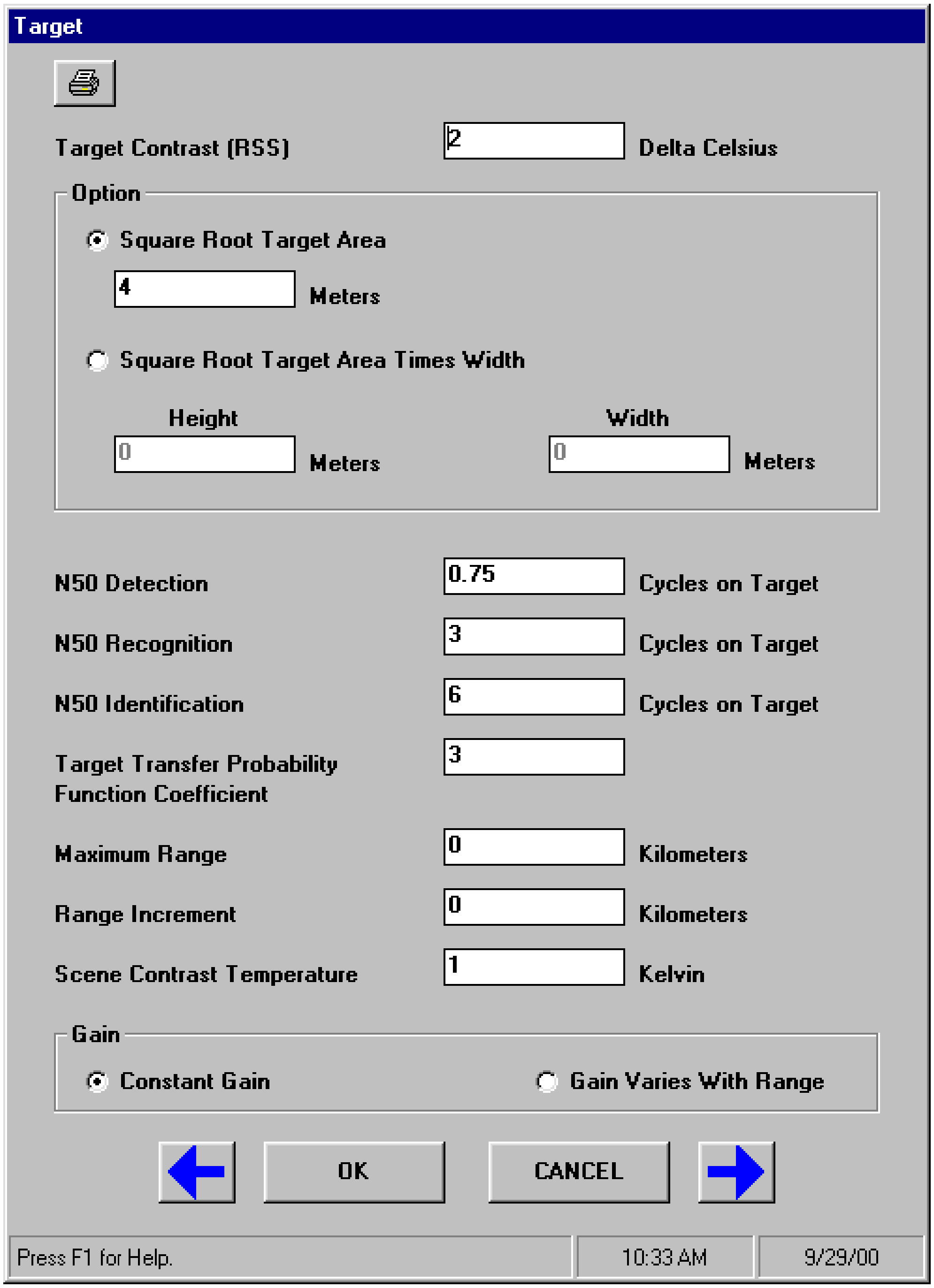

The model is only acccurate in predicting ensemble probabilities. That is, the fraction of correct choices when a group of observers is asked to discriminate a group of vehicles. A probability prediction is not provided for a single observer or a single target vehicle. For example, 10 observers are tasked to correctly identify 3 different tanks. These are assumed to be highly trained observers. All observers get 1 of the vehicles correct, 5 of the 10 observers get another of the tanks correctly dientified, and none of the observers correctly identify the last tank. The probability of ID given by the model is 0.5. Half of all possible choices were correct.

Various target sizes and contrasts are given in tables below. The idea is to calculate an average vehicle contrast and size for a defined task. For example, if the task is identifying Russian versus Americal tanks for nose aspects, then an average size and contrast for nose-on Russian T55, T62, and T72 tanks and nose-on American M1, M60 and Sheridan tanks might be used in the model. The N50 chosen would depend on the identification task: discriminating between Russian vehicles requires an N50 of about 9 whereas discriminating between the Russian and American vehicles requires an N50 of about 6.

2.8.1. Target Contrast

2.8.1.1. Input Description

RSS (Root Sum-of-Squares) is the contrast metric that NVTHERM uses to describe Target Contrast. RSS is determined by measuring the intensity difference between a target and its local background. The local background is usually taken to be a box with dimensions (width and height) the square root of 2 multiplied by the dimensions (maximum width and height) of the target. The RSS is given by:

$$RSS = \left[\frac{1}{POT} \sum_{pixel(i,j) \in tgt} \left(t_{i,j} - \mu_{bkg} \right)^2 \right]^{1/2} \qquad (2\text{-}13)$$

where $t_{i,j}$ is the temperature corresponding to the pixel (i,j) and POT is the number of pixels on target. The RSS can be calculated readily from the target and background means and the target standard deviation by the following alternative formula:

$$RSS = \left[\left(\mu_{tgt} - \mu_{bkg} \right)^2 + \sigma_{tgt}^2 \right]^{1/2} \qquad (2\text{-}14)$$

where σ_{tgt} indicates the standard deviation of the target.

The Area Weighted Average Temperature (AWAT) is sometimes used to represent target contrast instead of RSS.

$$AWAT = \left[\frac{1}{POT} \sum_{pixel(i,j) \in tgt} \left(t_{i,j} - \mu_{bkg} \right) \right] \qquad (2\text{-}13a)$$

Another typical contrast metric is the JAR (named after James Ratches).

$$JAR = \left[\frac{1}{POT} \sum_{pixel(i,j) \in tgt} ABS\left(t_{i,j} - \mu_{bkg}\right) \right] \qquad (2\text{-}13b)$$

Normally, the RSS, AWAT, and JAR are close in value and provide very similar performance results. There are cases, however, when the AWAT is near zero but the target is still quite obvious; in these cases, the RSS and JAR provide superior results. In experiments conducted at NVESD, RSS provided the most accurate performance predictions.

2.8.1.2. Help and Examples

Target Signatures: ΔTs				
Tank Type:	Central Europe		Southwest Asia	
	Front	Side	Front	Side
	Summer Day			
	1.75	3.00	3.00	3.00
	Summer Night			
	2.00	4.00	4.50	5.00
	Raining			
Static	1.00	1.50	1.50	1.75
Dynamic	2.50	3.50	2.75	3.75

2.8.2. Target Characteristic Dimension

2.8.2.1. Input Description

If the target is treated as a silhouette, then the target characteristic dimension is the square root of the silhouette area. Units are meters.

2.8.2.2. Help and Examples

Target	Characteristic Dimension Front	Characteristic Dimension Side
M109	2.99	4.19
M113	2.16	2.90
2S3	2.79	3.94
M551	2.45	3.55
BMP	2.12	3.16
M1A	2.72	4.12
M2	2.84	3.74
M60	2.78	3.80
T55	2.75	3.71
T62	2.39	3.49
T72	2.49	3.46
ZSU	2.64	3.62

2.8.3. Target Height and Width

2.8.3.1. Input Description

Characteristic Dimension is recommended, but if height and width is all you have, the dimension is taken as $\sqrt{(height)(width)}$.

Note: Target height and width is relative to the vehicle aspect. For instance, the equation for a top-down perspective would be $\sqrt{(length)(width)}$ and a side view (90° aspect) would be $\sqrt{(length)(height)}$.

2.8.3.2. Help and Examples

Target	Length	Width	Height
2S3	8.4	3.2	3
BMP	6.7	2.94	2.15
M109	9.8	3.14	3.2
M113	4.8	2.7	2.5
M1A	9.83	7.92	3.65
M2	6.55	3.61	2.56
M551	6.3	2.8	2.95
M60	9.4	3.6	3.3
T55	9	3.27	2.35
T62	9.335	3.3	2.4
T72	9.5	3.6	2.22
ZSU	6.5	2.75	2.25

2.8.4. N_{50} Detection

2.8.4.1. Input Description

The number of resolvable cycles (by the sensor/observer) across the target determines the probability of discrimination. See Figure 2-42. This number of cycles is determined with sensor sensitivity, resolution, target contrast and atmospherics. N_{50} Detection is defined as the number of resolved bar pairs or cycles required across the target for a 50% probability of detection.

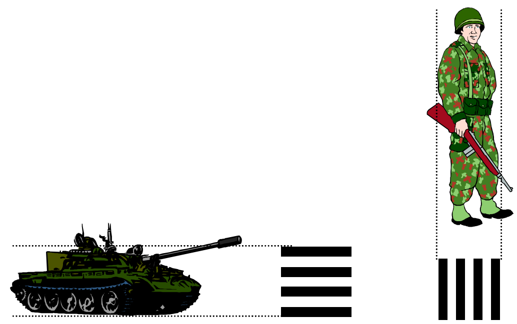

Figure 2-42

2.8.4.2. Help and Examples

Task	Description	Cycles across two-dimensional object N_{50}
Detection	Reasonable probability that blob is something of interest: further action will be taken (like change FOV) The 0.75 is for low clutter (target very hot compared to background). For high clutter, the target must be recognized to be detected, and the cycle criteria must be increased accordingly.	0.75 to 3.0
Recognition	Class discrimination (human, truck, tank, etc.)	1 to 2 for soft truck versus tracked 4 to 5 for APC versus tank
Identification	Object discrimination (M1A, T-62, or T-72 tank)	6.0 for Russian versus American 9.0 for specific vehicle ID when the group of vehicles includes tough confusers like discriminating T62 from T72

Figure 2-43

2.8.5. N_{50} Recognition

2.8.5.1. Input Description

The number of resolvable cycles (by the sensor/observer) across the target determines the probability of discrimination. See Figure 2-42 and Figure 2-43. N_{50} Recognition is defined as the number of resolved bar pairs or cycles required across the target for a 50% probability of recognition. Recognition involves discriminating the class of the vehicle but not the specific vehicle. That is, recognizing a tank as a tank and not an APC generally requires about 4 or 5 cycles across the target (the average target size and contrast). Correctly recognizing a tank is a tank and not a soft (logisitcs) truck generally requires 1.5 or 2 cycles across the (average) target.

2.8.6. N_{50} Identification

2.8.6.1. Input Description

The number of resolvable cycles (by the sensor/observer) across the target determines the probability of discrimination. See Figure 2-42. N_{50} Identification is defined as the number of resolved bar pairs or cycles required across the target for a 50% probability of correctly identifying the correct vehicle, not just vehicle type. That is T62 or T72, not just tank. See examples in table above.

.

2.8.7. Target Transfer Probability Function Coefficient

2.8.7.1. Input Description

The TTPF determines the probability of discrimination (detection, recognition, and identification) given a number of resolvable cycles across the target and the specified N_{50}.

$$P(N) = \frac{\left(\frac{N}{N_{50}}\right)^{C}}{1+\left(\frac{N}{N_{50}}\right)^{C}}$$

C is the input coefficient. The default value for NVTherm is 3.8; this is the recommended value for C.

2.8.8. Maximum Range and Range Increment (km)

2.8.8.1. Input Description

Maximum Range is the maximum distance for which the sensor target acquisition calculations are determined. Range Increment is the distance of one unit for which the distance between the maximum and minimum range is divided. See Figure 2-44.

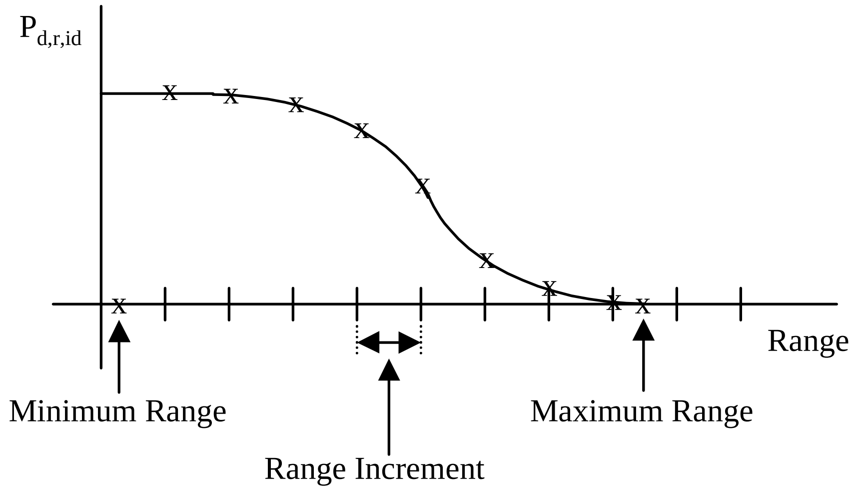

Figure 2-44

2.8.8.2. Help and Examples

Units are kilometers.

2.8.9. Scene Contrast Temperature (K)

2.8.9.1. Input Description

Scene Contrast Temp is the temperature variation in the scene (in effective blackbody temperature degrees C) that results in a display luninance change from minimum luminance to average luminance. The program uses this input to calculate the change in luminance at the display that results from a thermal contrast difference in the scene. This is not the absolute temperature of the scene. The thermal imager converts differences in thermal radiance within the field of view into differences in luminance on the display screen. Assuming that the display minimum luminance is zero, then the scene thermal contrast which results in the average display luminance is the Scene Contrast Temperature. The Scene Contrast Temp is determined rigorously from the gain and level settings of the sensor and the manner in which the sensor output is mapped to the display.

2.8.9.2. Help and Examples

When the imager is optimized for a specific target, the Sscene Contrast Temp is probably 3 to 5 times the target thermal contrast (Scene Contrast Temp for a 2 degree target between 6 and 10 K). An optimum condition is achieved when the sensor gain and level are ajusted for a specific target at a specific range, and some kind of histogram equilization has reduced the impact of extreme thermal contrast excursions. During search or other conditions under which optimum is not achieved, the sensor is probably adjusted for the background scene. An input of 1.0 degrees C represents poor scene thermal contrast. Inputs of 1 to 10 degrees C represent fair thermal contrast and inputs of 10 degrees or more represent high thermal contrast.

2.8.10. Gain

Range performance can be calculated using the same scene temp for all ranges. For example, during search where the range and position of the target are unknown, the sensor gain is probably set based on the general scene and is not optimized for the taget itself. In that case, “constant gain” is selected. On the other hand, for target ID, the target image is probably optimized. In that case, “gain varies with range” is selected. When the gain is varied with range, the target apparent contrast on the display is held constant. That is, as the assumed target range increases, the target temperature contrast decreases. It is assumed that sensor gain is increased to keep the displayed contrast constant. When the gain is adjusted with range, the range performance is enhanced.

2.9. Custom MTFs

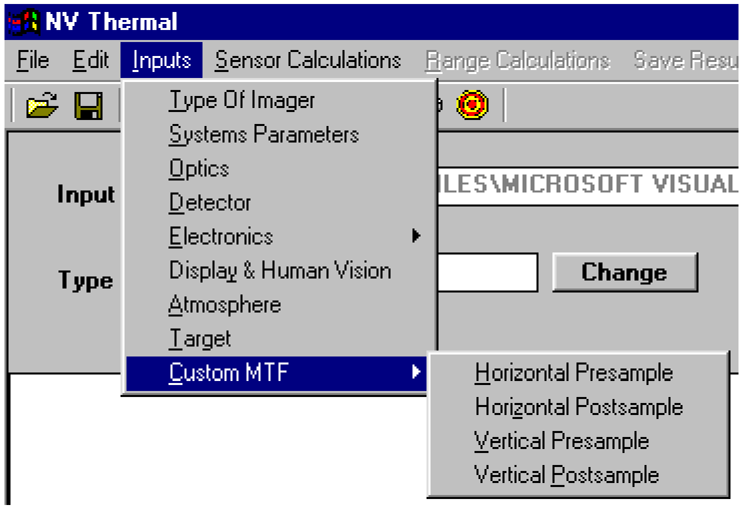

2.9.1. Horizontal Pre-Sample MTF

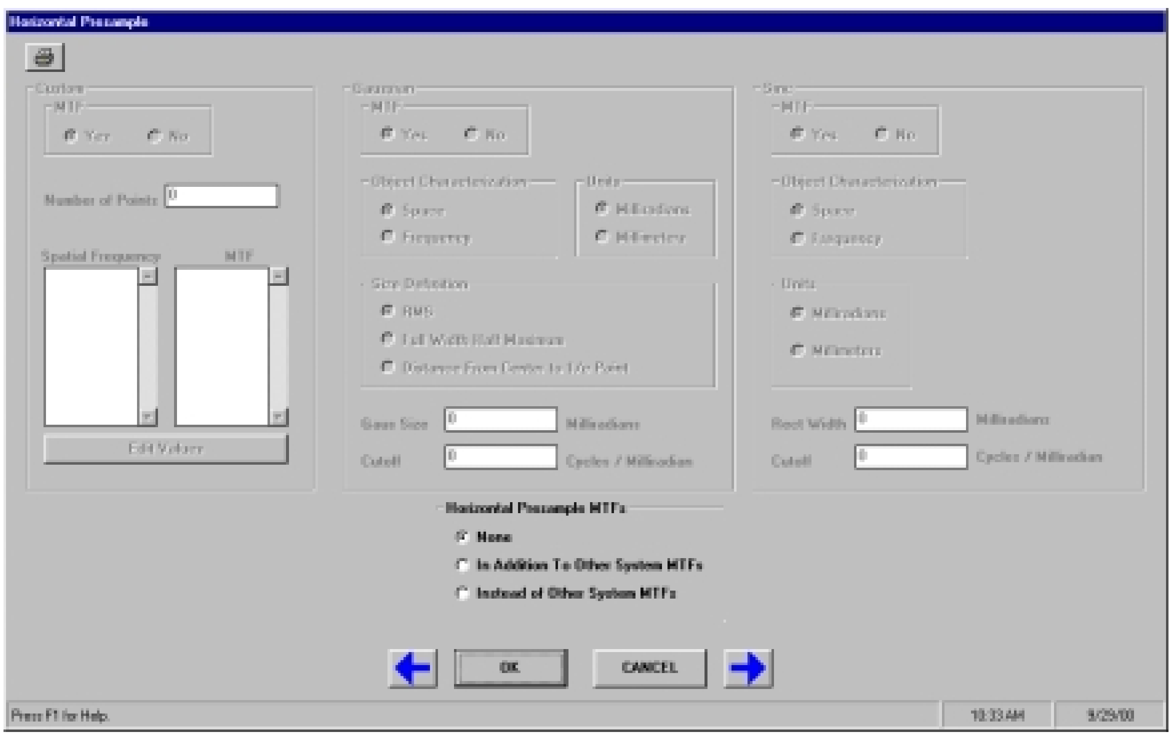

2.9.1.1. Input Description

There are three initial choices: “None”, “In addition to other system MTFs”, and “Instead of other system MTFs”. If “None” is chosen, the Horizontal Pre-Sample MTFs are defined by the sensor configuration given on all other input panels (e.g. diffraction and aberration blur). If “In addition to other MTFs” is chosen, a custom, Gaussian or Sinc (or all three if chosen) MTF is given in addition to all other sensor Horizontal Pre-Sample MTFs. If “Instead of other system MTFs” is chosen, then all sensor Horizontal Pre-Sample MTFs are set to

1 and only the custom, Gaussian, or Sinc on this form are used. If more than one MTF is chosen on this form, then the MTFs are combined as “User defined” in the Horizontal Pre-Sample MTF graph.

Custom MTF

This MTF is applied if “Yes” is chosen. In this case, “Number of Points”, “Spatial Frequencies”, and “MTFs” are required as inputs.

Gaussian

This MTF is applied if “Yes” is chosen. The MTF can be specified in “Space” or “Frequency” (as chosen). The units are Gaussian shape size in object space (milliradians) or focal plane (millimeters). The size definition gives the method of the Gaussian scale (RMS, Full width Half Max, or distance from center to 1/e point). The Gaussian size is given in milliradians or millimeters and is used if “Space is selected. The cutoff frequency is given in cycles/mrad or cycles/mm and is used if “Frequency” is selected.

Sinc

This MTF is applied if “Yes” is chosen. The Sinc MTF can be specified in space (as a rectangle size) or frequency. The units can be in milliradians (object space) or millimeters (focal plane). If “Space” is selected, the Rect width is used (milliradians or millimeters). If frequency is selected, then cutoff frequency (cyc/mrad or cyc/mm) is used.

2.9.2. Horizontal Post-Sample

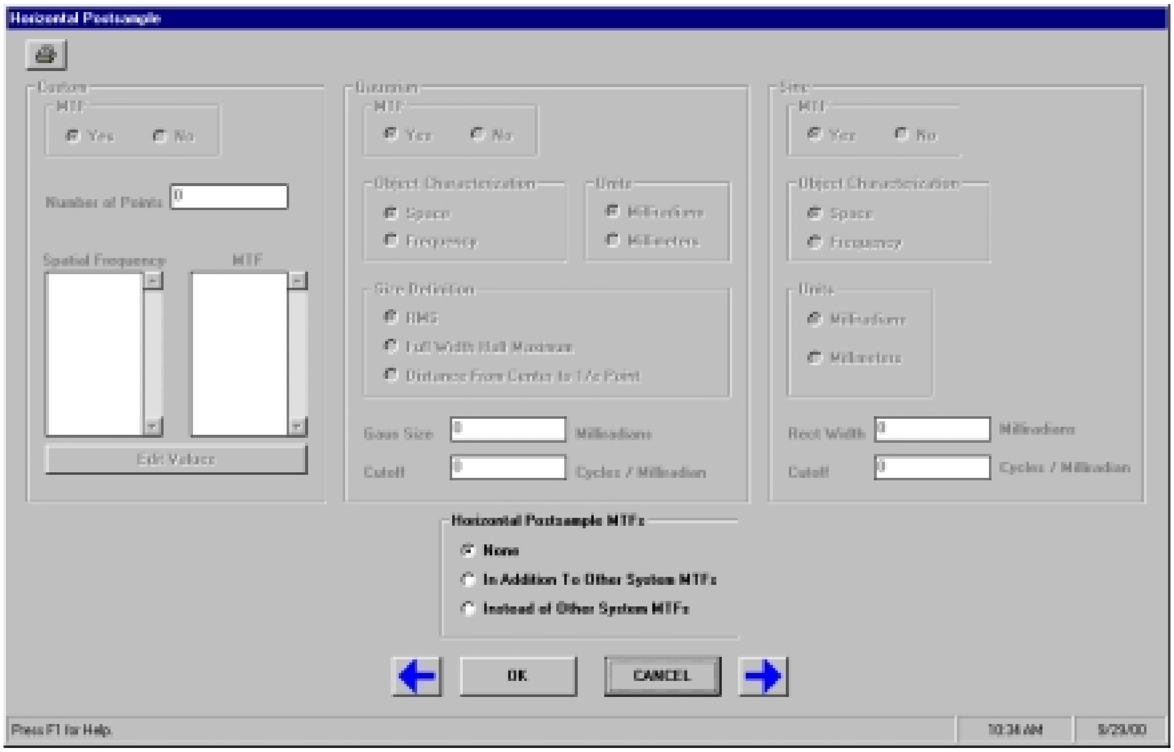

2.9.2.1. Input Description

There are three initial choices: “None”, “In addition to other system MTFs”, and “Instead of other system MTFs”. If “None” is chosen, the Horizontal Post-Sample MTFs are defined by the sensor configuration given on all other input panels (e.g. diffraction and aberration blur). If “In addition to other MTFs” is chosen, a custom, Gaussian or Sinc (or all three if chosen) MTF is given in addition to all other sensor Horizontal Post-Sample MTFs. If “Instead of other system MTFs” is chosen, then all sensor Horizontal Post-Sample MTFs are set to 1 and only the custom, Gaussian, or Sinc on this form are used. If more than one MTF is chosen on this form, then the MTFs are combined as “User defined” in the Horizontal Post-Sample MTF graph.

Custom MTF

This MTF is applied if “Yes” is chosen. In this case, “Number of Points”, “Spatial Frequencies”, and “MTFs” are required as inputs.

Gaussian

This MTF is applied if “Yes” is chosen. The MTF can be specified in “Space” or “Frequency” (as chosen). The units are Gaussian shape size in object space (milliradians) or focal plane (millimeters). The size definition gives the method of the Gaussian scale (RMS, Full width Half Max, or distance from center to 1/e point). The Gaussian size is given in milliradians or millimeters and is used if

"Space" is selected. The cutoff frequency is given in cycles/mrad or cycles/mm and is used if "Frequency" is selected.

Sinc

This MTF is applied if "Yes" is chosen. The Sinc MTF can be specified in space (as a rectangle size) or frequency. The units can be in milliradians (object space) or millimeters (focal plane). If "Space" is selected, the Rect width is used (milliradians or millimeters). If frequency is selected, then cutoff frequency (cyc/mrad or cyc/mm) is used.

2.9.3. Vertical Pre-Sample

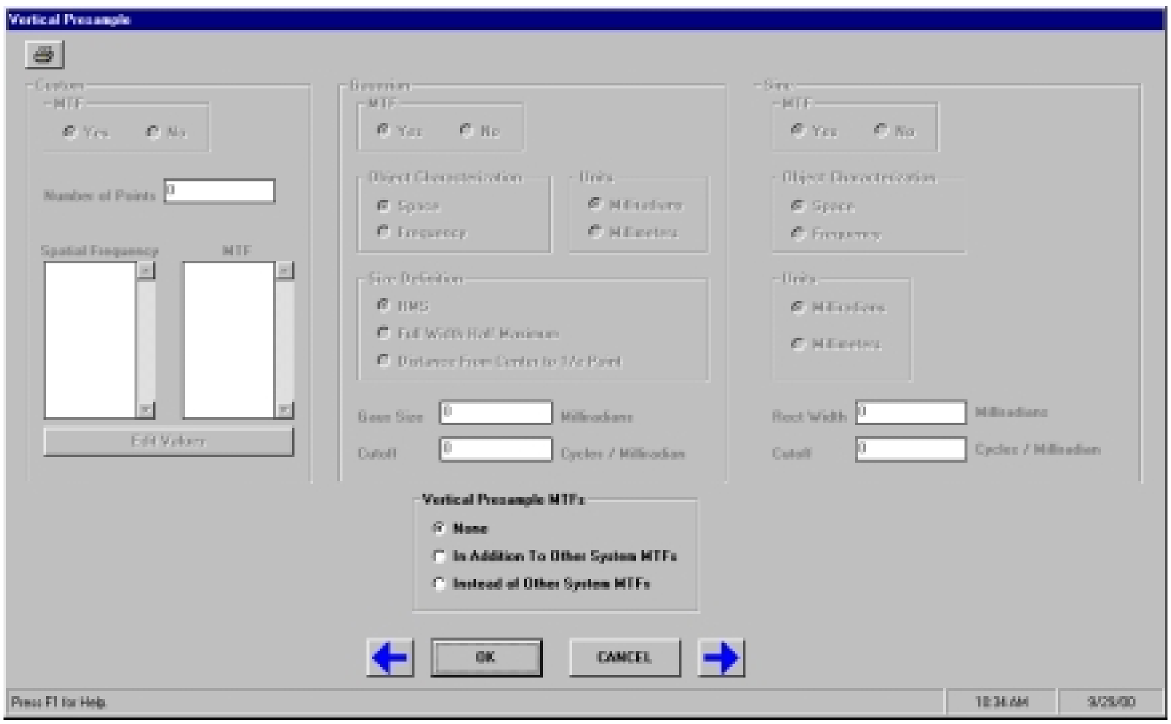

2.9.3.1. Input Description

There are three initial choices: "None", "In addition to other system MTFs", and "Instead of other system MTFs". If "None" is chosen, the Vertical Pre-Sample MTFs are defined by the sensor configuration given on all other input panels (e.g. diffraction and aberration blur). If "In addition to other MTFs" is chosen, a custom, Gaussian or Sinc (or all three if chosen) MTF is given in addition to all other sensor Vertical Pre-Sample MTFs. If "Instead of other system MTFs" is chosen, then all sensor Vertical Pre-Sample MTFs are set to 1 and only the custom, Gaussian, or Sinc on this form are used. If more than one MTF is chosen on this form, then the MTFs are combined as "User defined" in the Vertical Pre-Sample MTF graph.

Custom MTF

This MTF is applied if “Yes” is chosen. In this case, “Number of Points”, “Spatial Frequencies”, and “MTFs” are required as inputs.

Gaussian

This MTF is applied if “Yes” is chosen. The MTF can be specified in “Space” or “Frequency” (as chosen). The units are Gaussian shape size in object space (milliradians) or focal plane (millimeters). The size definition gives the method of the Gaussian scale (RMS, Full width Half Max, or distance from center to 1/e point). The Gaussian size is given in milliradians or millimeters and is used if “Space is selected. The cutoff frequency is given in cycles/mrad or cycles/mm and is used if “Frequency” is selected.

Sinc

This MTF is applied if “Yes” is chosen. The Sinc MTF can be specified in space (as a rectangle size) or frequency. The units can be in milliradians (object space) or millimeters (focal plane). If “Space” is selected, the Rect width is used (milliradians or millimeters). If frequency is selected, then cutoff frequency (cyc/mrad or cyc/mm) is used.

2.9.4. Vertical Post-Sample

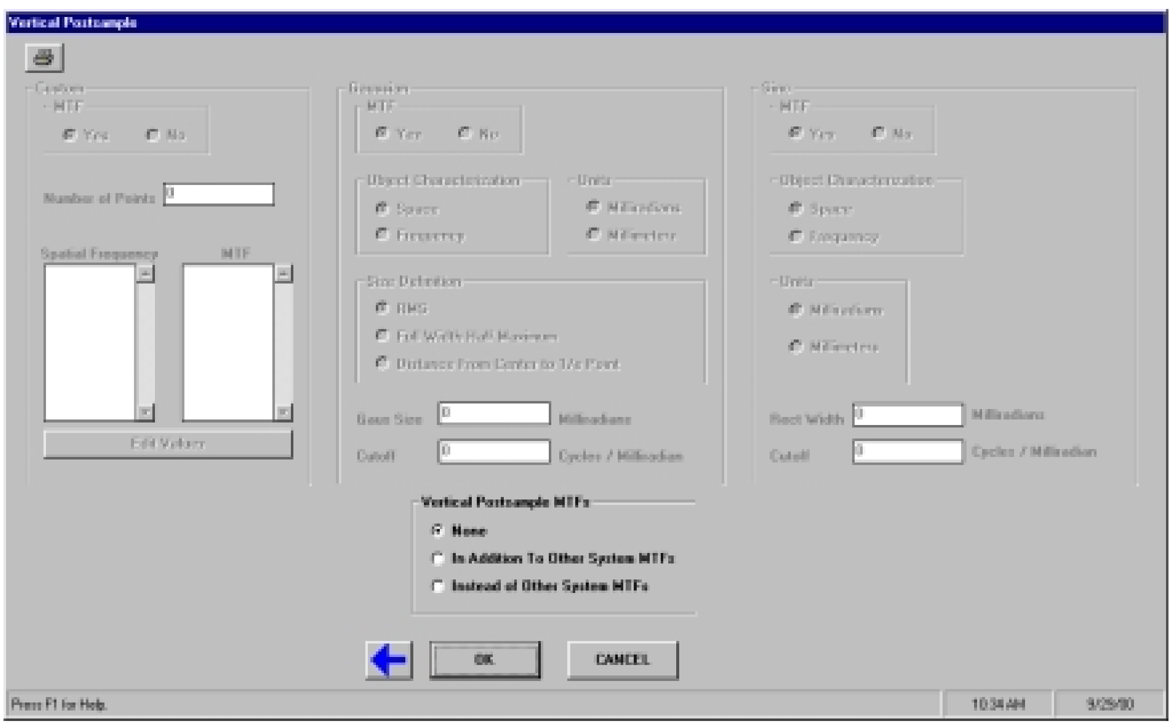

2.9.4.1. Input Description

There are three initial choices: “None”, “In addition to other system MTFs”, and “Instead of other system MTFs”. If “None” is chosen, the Vertical Post-Sample MTFs are defined by the sensor configuration given on all other input panels (e.g. diffraction and aberration blur). If "In addition to other MTFs" is chosen, a custom, Gaussian or Sinc (or all three if chosen) MTF is given in addition to all other sensor Vertical Post-Sample MTFs. If "Instead of other system MTFs" is chosen, then all sensor Vertical Post-Sample MTFs are set to 1 and only the custom, Gaussian, or Sinc on this form are used. If more than one MTF is chosen on this form, then the MTFs are combined as "User defined" in the Vertical Post-Sample MTF graph.

Custom MTF

This MTF is applied if "Yes" is chosen. In this case, "Number of Points", "Spatial Frequencies", and "MTFs" are required as inputs.

Gaussian

This MTF is applied if "Yes" is chosen. The MTF can be specified in "Space" or "Frequency" (as chosen). The units are Gaussian shape size in object space (milliradians) or focal plane (millimeters). The size definition gives the method of the Gaussian scale (RMS, Full width Half Max, or distance from center to 1/e point). The Gaussian size is given in milliradians or millimeters and is used if "Space is selected. The cutoff frequency is given in cycles/mrad or cycles/mm and is used if "Frequency" is selected.

Sinc

This MTF is applied if "Yes" is chosen. The Sinc MTF can be specified in space (as a rectangle size) or frequency. The units can be in milliradians (object space) or millimeters (focal plane). If "Space" is selected, the Rect width is used (milliradians or millimeters). If frequency is selected, then cutoff frequency (cyc/mrad or cyc/mm) is used.

3. Calculations

3.1. Basic System Calculations

3.1.1. Field of View (FOV) (degrees)

The system field of view (FOV) is a required input to NVTherm.

3.1.2. Magnification

The magnification of the system is also described in the "Input" section. However, if this value is given as zero on the input of the program, it is calculated with the information given. The definition, again, is the angle of the image to the eye normalized to the field-of-view of the system. It is assumed here that an interpolation up causes a larger image at the display, but that this larger image size is the size that is measured when a display height is given on the display inputs. However, for E-Zoom, only a portion of the image is given at the display, so E-zoom is a factor in the magnification. For a system without E-zoom, the Magnification is given by

$$Magnification = \frac{EyeImageAngle}{FOV_{vert}} \tag{3-1}$$

where *EyeImageAngle* is the angle of the displayed image that is subtended to the eye. If the image fills the entire display monitor then

$$EyeImageAngle = 2\tan^{-1}\left(\frac{DisplayHeight}{2 \bullet DisplayViewingDistance}\right) \tag{3-2}$$

If the displayed image is less in height than the display height, then the image height is used instead of the display height.

For E-zoom, it is assumed that only a portion of the full FOV is seen on the display. For a single E-zoom (a factor of 2 enlargement), it is assumed that only one-half of the vertical FOV is seen and only one-half of the horizontal FOV is seen (or a quarter of the entire FOV area). For a double E-zoom, only a quarter of the vertical FOV is viewed and a quarter of the horizontal FOV is viewed (or a 16^{th} of the FOV area).

3.1.3. Space Calculations

The Detector Angular Subtense, Airy Disc Diameter, and Sample Spacing summarize the space limitations of the detector size, optical blur, and sample spacing, respectively. Roughly speaking, the larger one of these calculations is the limiting aspect of the sensor. Fill factor is included for a light-collection quantity.

3.1.3.1. Detector Angular Subtense (DAS) or Instantaneous Field of View (IFOV)

The detector angular subtense (DAS) describes the spatial resolution limitations of the detector size. For a rectangular detector, there are two DASs: a horizontal DAS and a vertical DAS. Figure 3-1 shows that the DAS is the detector width or height divided by the focal length.

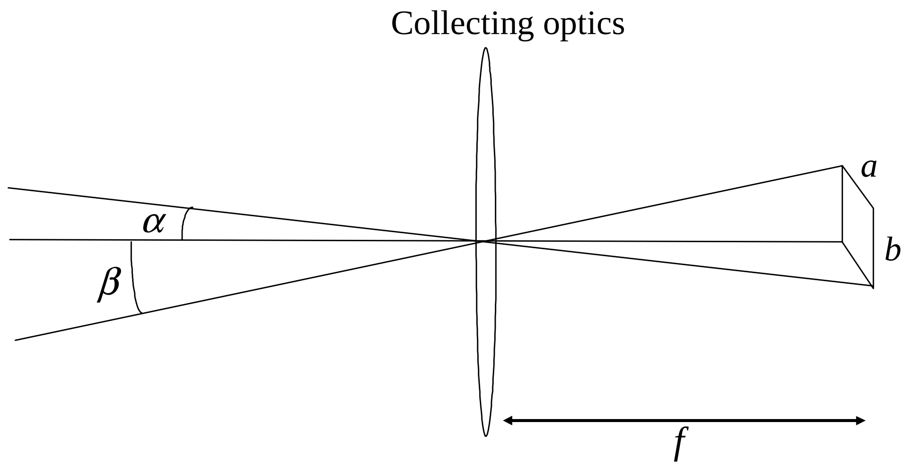

Figure 3-1. Detector angular subtenses.

For the horizontal DAS of a rectangular detector, the DAS is the detector width divided by the effective focal length of the optics:

$$\alpha = \frac{a}{f} \qquad \text{[angle is converted to milliradians]} \qquad (3\text{-}3)$$

and the vertical DAS is the detector height divided by the effective focal length:

$$\beta = \frac{b}{f} \qquad \text{[angle is converted to milliradians]} \qquad (3\text{-}4)$$

The horizontal and vertical DASs are usually specified in milliradians; the quantities described must therefore be multiplied by 1,000. The DAS describes the very best resolution that can be achieved by an infrared system due to the detector size limitations.

Help and Examples

Typical DASs for tactical infrared systems can be less than 0.1 milliradians up to 1 milliradian. Please note that DAS is sometimes called the instantaneous field-of-view (IFOV). In the origins of sensor modeling, IFOV had units of steradians in solid angle and DAS was a single angle. We use DAS and IFOV interchangeably.

3.1.3.2. Airy Disc Size

The airy disc size is calculated so that the optical blur due to diffraction can be compared to the DAS. A spot intensity slice caused by diffraction is shown in Figure 3-2. This is the intensity distribution seen in the focal plane of an imager if a point were imaged by a diffraction limited optical system with a circular aperture. Note that the Airy disc size is the distance between the two “zeroes” in the intensity pattern. This disc size can be projected out into angular space in front of the sensor. The distance between the two zeros is

$$\theta_{Airy} = 2.44\frac{\lambda}{D} \qquad (3\text{-}5)$$

where λ is the average wavelength of the imaging system and *D* is the aperture diameter of the collecting optics. Really, we know that since the wavelength sensed by most infrared sensors are a wide band, this Airy disc would be a collection of Airy patterns caused by the various bands, however, this diffraction spot gives us a rough idea of the diffraction point spread function of the system.

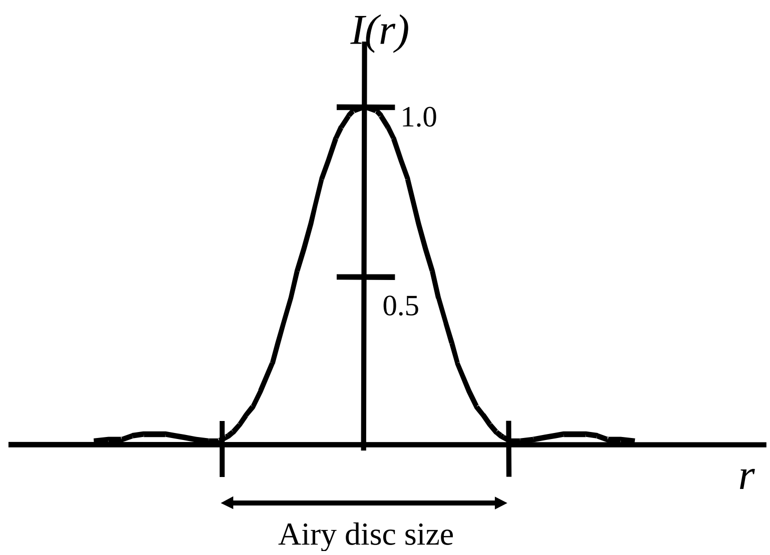

Figure 3-2.

Help and Examples

NVTherm converts that angle to milliradians for direct comparison to the DASs of the system.

3.1.3.3. Sample Spacing

The sample spacing of the imaging system describes the limitations of an imaging system due to sampling. The sample spacing is given in angular space (milliradians) and is calculated a number of different ways depending on the input parameters.

Sample Spacing for a staring array.

The sample spacing is set by the FOV and the number of vertical and horizontal detectors. The angular sample spacing is taken as

$$AngSS_v = \frac{FOV_v}{NumDetectors_v} \qquad AngSS_h = \frac{FOV_h}{NumDetectors_h} \tag{3-6}$$

where the FOV was converted to milliradians before the division

Sample Spacing for a Scanning Array

The vertical sample spacing is calculated exactly as described in the staring array case above. That is,

$$AngSS_v = \frac{FOV_v}{NumDetectors_v} \tag{3-7}$$

However, this method does not work for the horizontal, or scanning direction, of the imager. For a continuous scanned system, there is no sample spacing in the horizontal direction and the sample spacing is set to 0. For a scanned – sampled imager, detector pitch is taken as

$$DetectorPitch_h = \frac{DAS_h}{SamplesPerHIFOV} \tag{3-8}$$

where Samples Per HIFOV are a required input for a scanned – sampled system. Now that we have the detector pitch, we can calculate the horizontal sample spacing

$$AngSS_h = \frac{DetectorPitch_h}{FocalLength}. \tag{3-9}$$

Sample Spacing Modifications (interlace and dither)

If the sensor has vertical interlace or four-point dither as an option on the detector input form, then the vertical sample spacing is divided by the number of vertical interlaces. If the sensor has dither, the horizontal sample spacing is divided by 2.

3.1.3.4. Fill Factor

The fill factor is only calculated for the staring array imager. For this case, the fill factor is the ratio of the area of the detector to the area of a unit cell. A unit cell is defined as the rectangular area bounded by the centers of four adjacent detectors. The fill factor is then

$$FillFactor = \frac{DAS_v DAS_h}{DetectorPitch_v DetectorPitch_h} \tag{3-10}$$

For staring arrays, this value should always be less than or equal to 1 (for a 100% fill factor). Otherwise, an error message is given.

3.1.4. Frequency Calculations

The sensor aspect with the lowest frequency limit is the limiting aspect of the sensor.

3.1.4.1. Detector Cutoff Frequency

The shape of the detector is assumed to be rectangular and this shape can be projected into angular space in front of the sensor as the detector angular subtense (DAS). The impulse response of the detector is an angular rectangle shape. The frequency response (Fourier Transform) of this rectangular shape is the sinc function that is scaled by the DAS. This sinc function is the Modulation Transfer Function of the detector. The first zero of this transfer function (see the Detector MTF section for more details) is considered the detector cutoff frequency

$$DetectorCutoff_h = \frac{1}{DAS_h} \qquad DetectorCutoff_v = \frac{1}{DAS_v} \tag{3-11}$$

Since the DAS is in milliradians, the cutoffs are in cycles per milliradian.

3.1.4.2. Diffraction Cutoff Frequency

If the optics are diffraction-limited, then the cutoff frequency of the optics occurs where the diffraction MTF goes to zero (see the optics MTF section for more details). This frequency is

$$DiffractionCutoff = \frac{D}{1000\lambda} \tag{3-12}$$

where D is the optics aperture diameter and λ is the wavelength. In the above equation, they are in the same units and the 1000 factor is for the conversion to cycles per milliradian.

3.1.4.3. Sample Frequency and Half Sample Frequency

The sampling frequency is calculated from the sample spacing. The sampling frequency is given as

$$SamplingFrequency = \frac{1}{SampleSpacing} \tag{3-13}$$

where the sample spacing and corresponding frequency may be different in the horizontal and vertical direction. The half sample frequency, or half sample rate (sometimes called the Nyquist rate), is one-half the sampling frequency described above. The sampling frequency is the location of the first order replication of the sampled signal. The half-sample rate is the location where the sampled spectrum baseband signal and the first order replica overlaps. For more information, see the section on spurious response calculations.

3.1.5. Temporal Calculations

3.1.5.1. Integration Time

For a staring array, the integration time is required as an input. For a scanned – continuous system, there is no integration time parameter. However, for a scanned - sampled system there is an integration time calculation that can be performed, so the integration time input is optional. The integration time is calculated by

$$IntegrationTime = \frac{AngSS_h}{ScanVelocity} \tag{3-14}$$

The angular sample spacing in the horizontal direction is in milliradians and the scan velocity is given in milliradians per second, so the integration time in the above equation is in seconds. The conversion to microseconds involves multiplying the above ratio by 1×10^6. The calculations for dwell time and then scan velocity are given below.

3.1.5.2. Dwell Time

The dwell time of a sensor is the average amount of time that a detector will cover a single point in the field of view during a frame time. Dwell time does not apply to staring sensors, but is used frequently for both scanned – continuous and scanned – sampled sensors. The dwell time is calculated by

$$DwellTime = \frac{NumVertDetectors \bullet DAS_h \bullet DAS_v \bullet ScanEfficiency}{FrameRate \bullet FOV_h \bullet FOV_v \bullet SamplesPerVIFOV} \tag{3-15}$$

where the FOVs given above are first converted to milliradians. The DASs are in milliradians and all but the frame rate parameter are unitless. Since the frame rate is in frames per second, the dwell time given is in seconds. Usually, this value is converted to microseconds.

3.1.5.3. Scan Velocity

The scan velocity is a simple calculation that is the horizontal detector angular subtense divided by the dwell time

$$ScanVelocity = \frac{DAS_h}{DwellTime} \tag{3-16}$$

in milliradians per second. This value corresponds with the velocity that the scan mirror scans the image across the detector array.

3.1.5.4. Eye Integration Time

The eye integration time is calculated based on the luminance of the monitor. The equation was a curve fit derived at NVESD base on data in the literature. The equation is

$$T_{eye} = 0.0191715 + 0.062536\left(\frac{AveDispLum}{1.076}\right)^{-0.1699484}$$

This eye integration time affects both the MRT calculation and the characteristics of frame integration.

3.1.6. Efficiency Factor

The efficiency factor is a measure of detector light collecting ability compared to the theoretical maximum. For a 100% fill factor detector material that integrates for an entire frame time, the efficiency factor is 1. For a scanning system, the efficiency factor is much less since the detectors are shared over points in the field of view. The efficiency factor for a staring array is

$$\eta_{eff} = FillFactor\,\frac{ActualDwell}{AvailableDwell} \tag{3-17}$$

where the fill factor is described above. The actual dwell is the integration time of the detectors and the available dwell is 1/framerate. For a scanning system, the efficiency factor is

$$\eta_{eff} = \eta_{scan}\,\frac{NumDetectors \bullet DetectorArea}{FOV_h \bullet FOV_v \bullet FocalLength^2} \tag{3-18}$$

where η_{scan} is the scan efficiency and the field of views are given in the comparable units to the detector area (i.e. milliradians or micrometers) over the square of the focal length. NumDetectors is the total number of detectors in the focal plane array.

3.2. Modulation Transfer Functions

In NVTHERM, we assume that the imaging system is a linear system (we do not assume the system is shift invariant). However, in this section, let us assume that there is no sampling (we will consider sampling later) and that the system is LSI (linear shift-invariant). In Figure 3-3, a simple optical system is imaging a clock onto a screen. For simplicity, unity magnification is assumed (that is, the image is the same size as the object). As illustrated in the lower left corner of the image, each point source in the object becomes a *point spread function* (*psf*) in the image. The point spread function is also called the *impulse response* of the system. Each point in the scene is blurred by the optics and projected onto the screen. This process is repeated for each of the infinite number of points in the scene. The image is the sum of all the individual blurs.

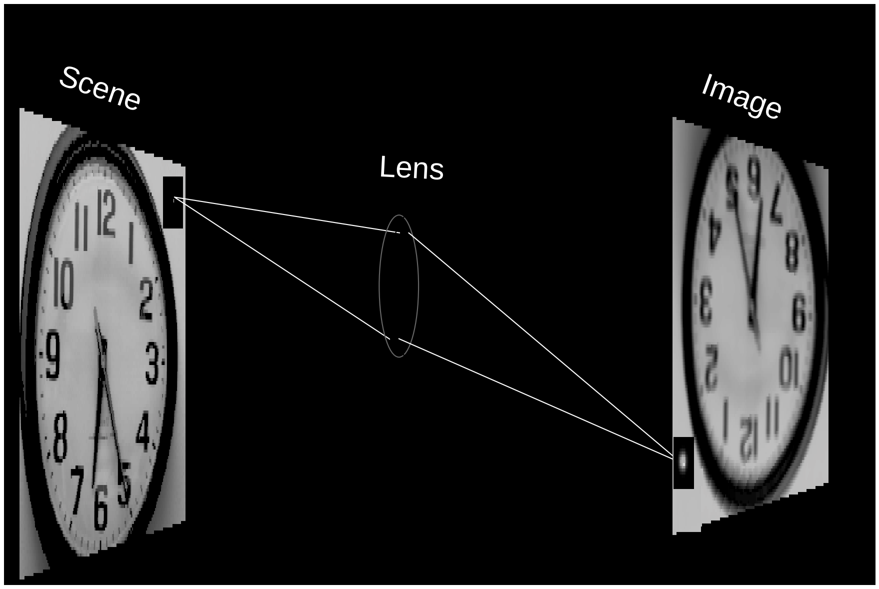

Figure 3-3

Clock being imaged by a lens onto a screen; a point source in the scene (upper right) becomes a point spread function blur in the image (lower left).

Two considerations are important here. First, the process of the lens imaging the scene is linear and therefore superposition holds. The scene is accurately represented by the sum of the individual points of light in the scene. Also, the image is accurately represented by the sum of the blurs resulting from the lens imaging each individual scene point.

Second, it is assumed that the shape of the optical blur (that is, the shape of the PSF) does not depend on position within the field of view. This is typically not true for optical systems. Typically, optical aberrations vary depending on position in the field of view. The optical blur is generally smaller at the center of an image than at the edge. However, the image plane can generally be sub-divided into regions within which the optical blur is approximately constant. A system with constant blur is sometimes called *isoplanatic*.

The assumption here is that the blur caused by the optics (the optical PSF) is the same anywhere within the region of the image being analyzed. The image of a point source does not change with position. The system is shift-invariant.

Given that the PSF is constant over the image, then the image can be represented as a convolution of the PSF over the scene. If h(x,y) represents the spatial shape (the intensity distribution) of the point spread function, then h(x-x’,y-y’) represents a point spread function at location (x',y') in the image plane. If $s_{cn}(x',y')$ describes the brightness of the object scene, and $i_{mg}(x, y)$ is the brightness of the image, then:

$$i_{mg}(x,y) = \int_{-\infty}^{\infty}\int_{-\infty}^{\infty} h(x-x', y-y')\, s_{cn}(x',y')\, dx'dy' \tag{3-19}$$

Each point in the scene radiates independently and produces a point spread function in the image plane with corresponding intensity and position. The image is a linear superposition of these point spread functions. Mathematically, that result is obtained by convolving the optical PSF over the scene intensity distribution to produce the image.

Since a convolution in space corresponds to a multiplication in frequency, the optical system can be considered to be a spatial filter.

$$I_{mg}(\xi,\eta) = H(\xi,\eta) S_{cn}(\xi,\eta) \tag{3-20}$$

where:

$I_{mg}(\xi,\eta)$ = Fourier transform of image

$S_{cn}(\xi,\eta)$ = Fourier transform of scene

$H(\xi,\eta)$ = the Optical Transfer Function (OTF)

ξ *and* η are spatial frequencies in x and y directions, respectively. The units of ξ *and* η are cycles per millimeter or cycles per milliradian.

The OTF is the Fourier transform of the point spread function *h(x,y)*. However, in order to keep image intensity proportional to scene intensity, the OTF of the optics is normalized by the total area under the PSF blur spot.

$$H(\xi,\eta) = \frac{\int_{-\infty}^{\infty}\int_{-\infty}^{\infty} h(x,y) e^{-j2\pi\xi x} e^{-j2\pi\eta y} dxdy}{\int_{-\infty}^{\infty} h(x,y) dxdy} \tag{3-21}$$

The Modulation Transfer Function (MTF) of the optics is the magnitude of the function $H(\xi,\eta)$, $\left|H(\xi,\eta)\right|$. The Phase Transfer Function (PTF) can be ignored if the PSF is symmetrical.

Note that the above relationship applies between the scene and the image plane of a well-corrected optical system. The optical system is considered to be "well-corrected" because the PSF, the optical blur, is reasonably constant over the image plane (i.e., isoplanatic).

The above describes the filtering process where one process is in the space domain and the other is in the frequency domain. In space, the output of a linear-shift-invariant (LSI) system is the input convolved with the system impulse response (in this case, the optical PSF). Take the example given in Figure 3-4. The system shown is a simple imaging system with an input transparency of a four-bar target, an imaging lens, and an output image. Given that the system shown is an LSI system, the output is simply the object convolved with the imaging system impulse response or point spread function. The convolution of the point spread function with the transparency gives a blurred image, as shown.

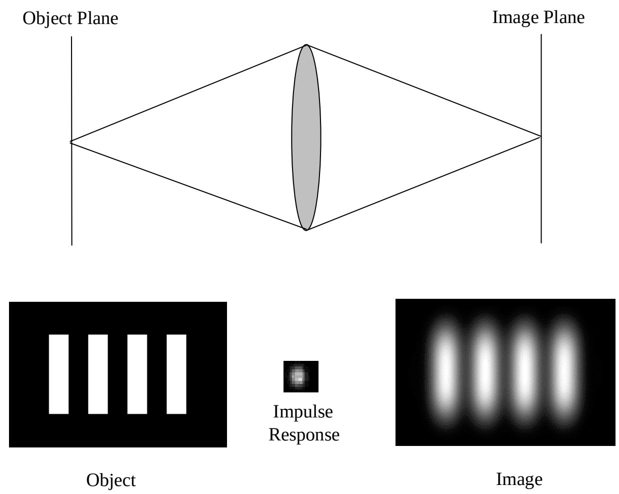

Figure 3-4. Spatial Filtering in an Optical System.

The spatial domain filtering process shown in Figure 3-4 is equivalent to frequency domain filtering process shown in Figure 3-5. The two dimensional Fourier transform of the input function is taken. The input spectrum clearly shows the fundamental harmonic of the four bar target in the horizontal direction. The higher order harmonics are difficult to see in the transform image because the higher order harmonics have much less amplitude than the fundamental.

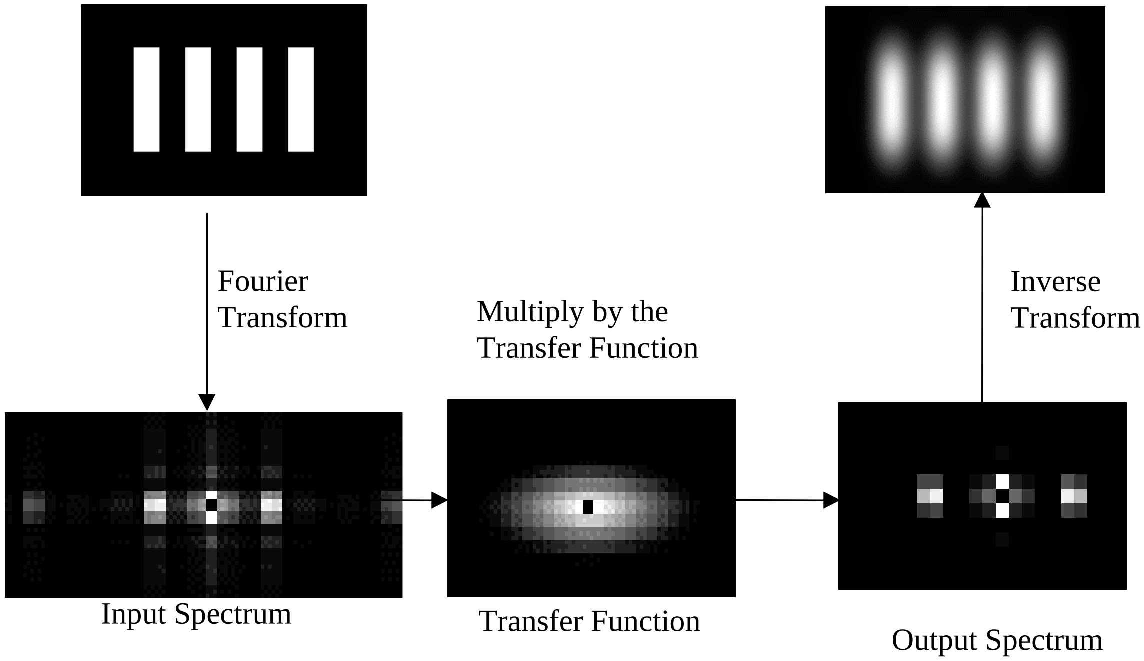

Figure 3-5. Frequency Domain Filtering in an Optical System.

The transform of the point spread function gives the transfer function of the system. Next, the output spectrum is given by the input spectrum multiplied by the transfer function. Finally, the output image is found by taking the inverse transform of the output spectrum. The resulting image is identical to that given by the spatial convolution of the point spread function in the space domain.

To summarize, LSI imaging system analysis can be performed using two methods: spatial-domain analysis and frequency-domain analysis. The results given by these analyses are identical. In NVTHERM, we treat filters associated with each of the components in the frequency domain.

Reducing Analyses to One Dimension

It is common in imaging system analysis to analyze sensors in the horizontal and vertical directions. The point spread function, *PSF*, and the associated modulation transfer function, MTF, are assumed to be separable in Cartesian coordinates. The separability assumption reduces the analysis one dimension so that complex calculations that include cross-terms are not required. This approach reduces processing time in calculations and quickly determine sensor performance.

The separability assumptions are almost never satisfied (even in the simplest case, there is generally some calculation error associated with assuming separability). Generally, the errors are small, and the majority of scientists and engineers use the separability approximation.

Separability in Cartesian coordinates requires that

$$f(x,y) = f(x)f(y)$$
(3-22)

and separability in polar coordinates requires

$$f(r,\theta) = f(r)f(\theta)$$
(3-23)

However, the optical PSF is a combination of the diffraction spot and the geometric aberrations. Usually, these functions can be characterized by a function that is separable in polar coordinates. The detector PSF is a rectangular shape that is separable in Cartesian coordinates, but is not separable in polar coordinates. The collective PSF of the detector and the optics is not separable in either polar or Cartesian coordinates!

The analysis of imaging systems is usually performed separately in the horizontal and vertical directions. These one-dimensional analyses allow a great simplification in sensor performance modeling. Although the separability assumption is not error-free, the errors usually turn out to be small. NVTHERM is a two (horizontal and vertical) one-dimensional model in terms of transfer functions. The one-D model is applied successively in horizontal and vertical directions. The MTFs are combined in a the MRT model for overall system performance.

The MTF associated with typical imager components

The impulse response or point spread function of an imaging system is comprised of component impulse responses as shown in Figure 3-6. Each of the components in the system contributes to the blurring of the scene. The blur attributed to a component may be comprised of more than one physical effect. For example, the optical blur is a combination of the diffraction and aberration effects of the optical system. The point spread function of the system is a convolution of the individual impulse responses:

$$h_{system}(x,y) = h_{atm}(x,y) ** h_{optics}(x,y) ** h_{\det}(x,y) ** h_{elec}(x,y) ** h_{disp}(x,y) ** h_{eye}(x,y)$$
(3-24)

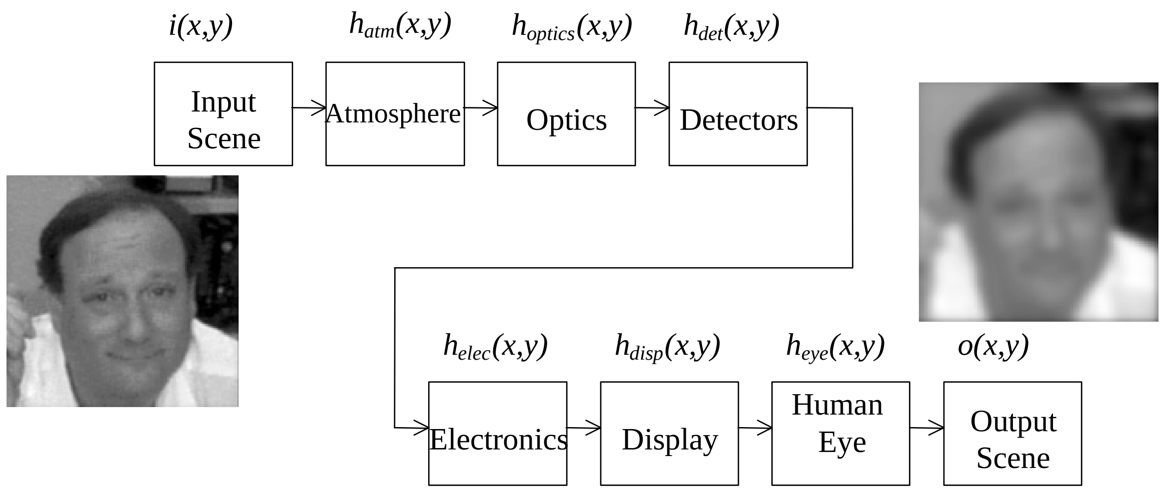

Figure 3-6. System psf results from convolving the individual psf of all of the system components.

The Fourier transform of the system impulse response is called the *transfer function* of the system. Since a convolution in the spatial domain is a product in the frequency domain:

$$O(\xi,\eta) = I(\xi,\eta)H_{atm}(\xi,\eta)H_{optics}(\xi,\eta)H_{\det}(\xi,\eta)H_{elec}(\xi,\eta)H_{disp}(\xi,\eta)H_{eye}(\xi,\eta) \quad (3\text{-}25)$$

The system transfer function is the product of the component transfer functions.

Detailed descriptions of the point spread functions and modulation transfer functions for typical imager components are given below. These MTFs are computed in NVTHERM.

3.2.1. Optical Diffraction MTF

The diffraction filter accounts for the spreading of the light as it passes an obstruction or an aperture. The diffraction impulse response for an incoherent imaging system with a circular aperture of diameter *D* is

$$h_{diff}(x,y) = \left(\frac{D}{\lambda}\right)^2 somb^2\left(\frac{Dr}{\lambda}\right) \quad (3\text{-}26)$$

where λ is the average band wavelength and r is the square root of x^2 plus y^2. The *somb* (for sombrero) function is:

$$somb(r) = \frac{J_1(\pi r)}{\pi r} \quad (3\text{-}27)$$

where J_1 is the first order Bessel function of the first kind. The MTF corresponding to the above impulse response is the optical diffraction MTF and is obtained by taking the Fourier transform of the function given. The Fourier transform of the *somb* is (one dimensional case):

$$H_{diff}(\xi) = \frac{2}{\pi}\left[\cos^{-1}\left(\frac{\xi\lambda}{D}\right) - \frac{\xi\lambda}{D}\sqrt{1-\left(\frac{\xi\lambda}{D}\right)^2}\right] \qquad (3\text{-}28)$$

and ξ in units of cycles per milliradian.

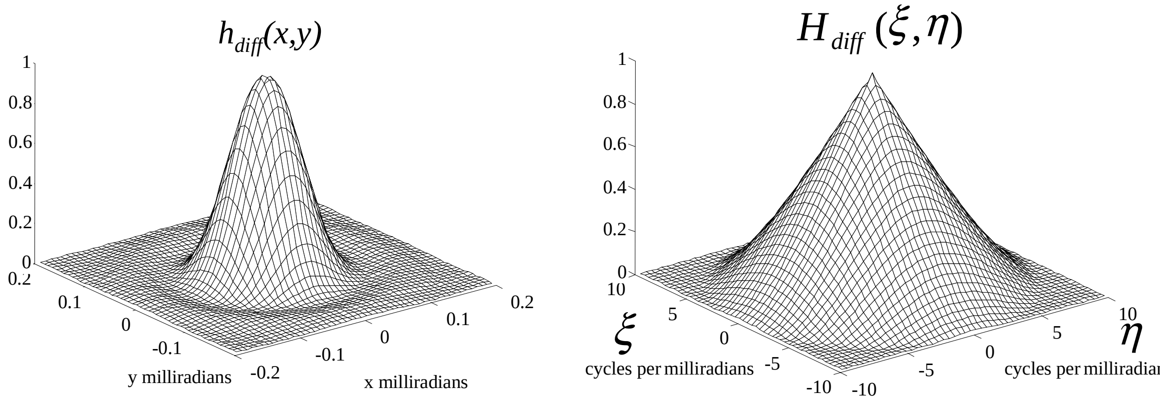

Figure 3-7. Spatial representations of the diffraction blur (left) and the MTF of the diffraction blur (right)

3.2.2. Optical Blur MTF

The filtering associated with the optical aberrations is sometimes called the geometric blur. There are many ways to model this blur and there are numerous commercial programs for calculating geometric blur at different locations on the image. However, a convenient method is to consider the geometric blur collectively as a Gaussian function

$$h_{geom}(x,y) = \frac{1}{b^2} Gaus\left(\frac{r}{b}\right), \qquad (3\text{-}29)$$

where r_{geom} is the geometric blur scaling factor. The Gaussian function, *Gaus*, is

$$Gaus(r) = e^{-\pi r^2} \qquad (3\text{-}30)$$

Note that the scaling values in front of the space functions are intended to provide a functional volume (under the curve) of unity so that no gain is applied to the image. The Fourier transform of the *Gaus* function is simply the *Gaus* function, with care taken on the scaling property of the transform. The transfer function corresponding to the aberration effects is

$$H_{geom}(\xi) = Gaus(b\xi) \,. \tag{3-31}$$

Blur can be specified in NVTHERM three different ways: (Case 0) RMS or standard deviation of the blur spot, (Case 1) Full Width Half Max, or (Case 2) Distance from the center to the 1/e point. The conversions for b (OpticsBlurScaleFactor) are the following where the blur listed below corresponds to these three cases:

If (OpticsBlurType = 0), OpticsBlurScaleFactor = Sqr(2 • 3.14159) • OpticsBlur

If (OpticsBlurType = 1), OpticsBlurScaleFactor = OpticsBlur / 2 • Sqr(3.14159 / 0.693)

If (OpticsBlurType = 2), OpticsBlurScaleFactor = OpticsBlur • Sqr(3.14159)

In addition, the blur, *b*, can be specified in milliradians in object space or in millimeters in the focal plane of the imager. If the blur is specified in millimeters, it is converted to milliradians by dividing by the focal length in meters (millimeters divided by meters gives milliradians).

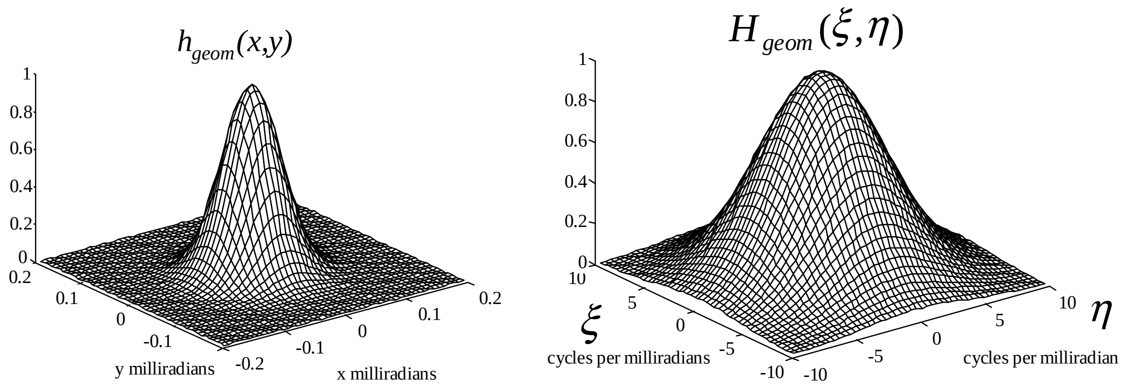

Figure 3-8. Spatial representations of the geometric blur (left) and the MTF of the geometric blur (right)

3.2.3. Measured Optical MTF

If the optical vendor supplies measured optical MTF information, it can be input to the model under the optics input form. Required information is “Number of Measured MTF Values”, “Spatial Frequencies” in cycles per milliradian, and “MTF Values”. Rest results are obtained if the MTF ranges from 1 to 0. If the “Number of Measured MTF Values” in not equal to 0, then the measured MTF is used and the Optical Diffraction MTF and Optical Blur MTFs are set to 1.

3.2.4. Vibration/Stabilization Blur MTF

Vibration/stabilization MTF describes the blur associated with random motion between the sensor and the scene. The equation for the vibration/stabilization blur MTF is identical to that of the optical blur given in the previous section. It is a

Gaussian model that can be specified with RMS (standard deviation), FWHM, or the 1/e distance. The only difference is that the vibration blur cannot be specified in the image plane in millimeters. It must be described in milliradians in object space.

3.2.5. Detector Shape

Two spatial filtering effects are normally associated with the detector. The first is associated with spatial integration over the detector active area. Spatial integration over the detector area occurs for both scanning and staring sensors. The second occurs in sensors where the detector is scanned across the scene. In this case, the relative motion between scene and detector results in a motion blur. The extent of the blur depends on how far the detector moves while the signal is being integrated by the electronic circuitry. Typically, the detector signal is integrated for a period of time, the integrated signal is sampled, and the then integrator is reset. The integrate and hold circuit is generally called a "sample and hold" circuit.

$$h_{\det}(x,y) = h_{\det\_sp}(x,y) ** h_{\det\_sh}(x,y) \tag{3-32}$$

Other effects can be included, but are usually negligible. For example, variation in detector responsivity will affect the spatial MTF of the detector, but responsivity is generally uniform over the active area of the detector.

The detector spatial impulse response is due to the spatial integration of the light over the detector. Since most detectors are rectangular, the rectangle function is used as the spatial model of the detector

$$= \left[\frac{1}{DAS_x} rect\left(\frac{x}{DAS_x}\right)\right]\left[\frac{1}{DAS_y} rect\left(\frac{y}{DAS_y}\right)\right] \tag{3-33}$$

where DAS_x and DAS_y are the horizontal and vertical detector angular subtenses in milliradians. The detector angular subtense is the detector width (or height) divided by the sensor focal length.

The MTF corresponding to the detector spatial integration is found by taking the Fourier transform of the above equation.

$$H_{\det\_sp} = \mathrm{sinc}(\mathrm{DAS_x}\xi)\,\mathrm{sinc}(\mathrm{DAS_y}\eta) \tag{3-34}$$

where the *sinc* function is defined as

$$\mathrm{sinc}(\pi \mathrm{x}) = \sin(\pi \mathrm{x}) / (\pi \mathrm{x}) . \tag{3-35}$$

The impulse response and the transfer function for a detector with a 0.1 by 0.1 milliradian detector angular subtense is shown in Figure 3-9.

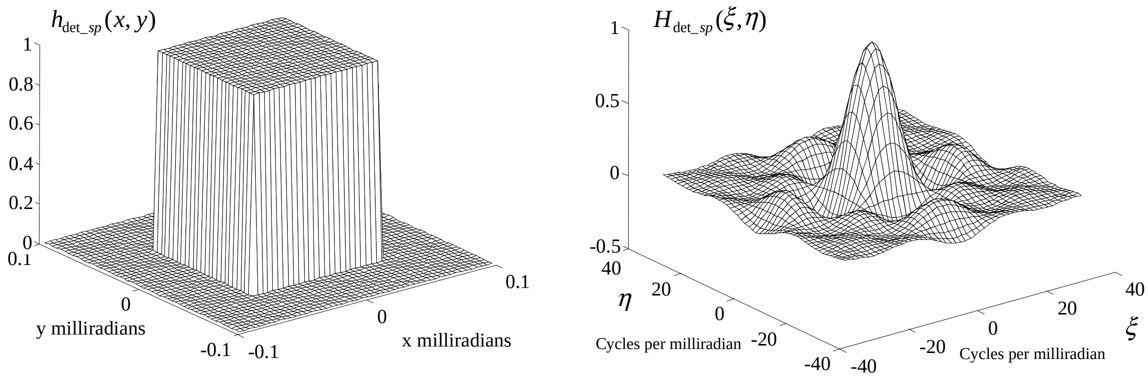

Figure 3-9. Detector Spatial Impulse Response and Transfer Function.

3.2.6.   Integrate & Hold

In parallel scan thermal imagers, the scene is mechanically scanned across a linear array of detectors. Each detector generates a line of video as the field of view of the sensor is scanned. In older sensors, the analog detector outputs were amplified and then processed in various ways to construct the displayed image. In most modern parallel scan imagers, circuitry on the detector focal plane integrates the photoelectron signal for a sample time period. At the end of the sample period, the integrator voltage is read out by a integrate and hold circuit. The integrator is then reset in preparation for the next sample.

The detector integrate and hold function is an integration of the light as the detector scans across the image. This integrate and hold function is not present in staring arrays, but is present in most scanning systems where the output of the integrated signal is sampled. The sampling direction is assumed to be the horizontal or x direction. Usually, the distance, in milliradians, between samples is smaller than the detector angular subtense by a factor called *samples per IFOV* or *samples per DAS*, ϑ. The integrate and hold function can be considered a rectangular function in x where the size of the rectangle corresponds to the distance between samples. In the spatial domain y direction, the function is an impulse function. Therefore the impulse response of the integrate and hold function is

$$h_{\det\_sh}(x,y) = \frac{\vartheta}{DAS_x} rect(\frac{x\vartheta}{DAS_x})\delta(y) \qquad (3\text{-}36)$$

The Fourier transform of the impulse response gives the transfer function of the integrate and hold operation

$$H_{\det\_sh}(\xi,\eta) = \mathrm{sinc}(\frac{DAS_x \xi}{\vartheta}) \qquad (3\text{-}37)$$

The Fourier transform of the impulse function in the y direction is 1. The impulse response and the transfer function for a integrate and hold (two samples per detector DAS) associated with the detector shown in Figure 3-9 are shown in Figure 3-10.

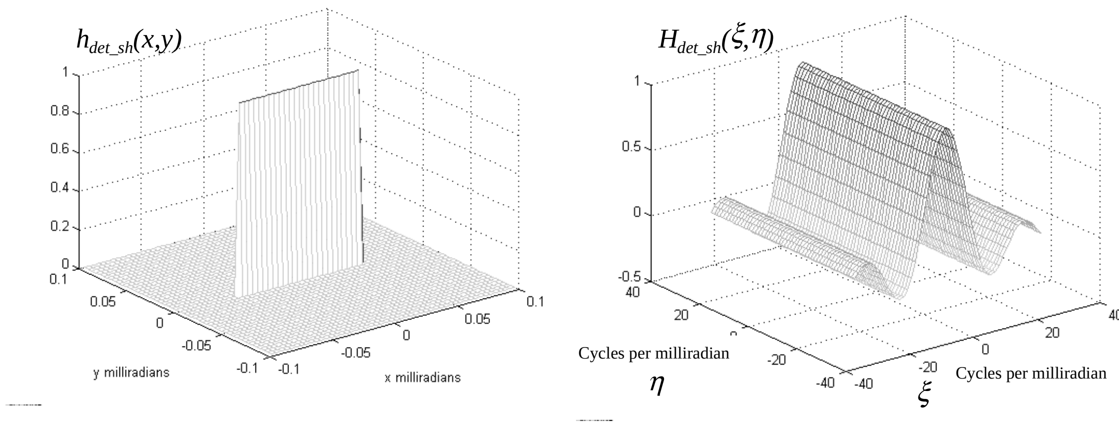

Figure 3-10. Detector Sample and Hold Impulse Response (left) and Transfer Function (right).

3.2.7. User Defined (Custom Pre-Sample MTF)

There are four custom (user-defined) MTFs: Horizontal Pre-Sample, Horizontal Post-Sample, Vertical Pre-Sample and Vertical Post-Sample. They are all applied in the same manner. One must choose:

- "None" (where no user defined MTF is used)
- "In Addition to Other System MTFs"
- "Instead of Other System MTFs"

If "Instead of Other System MTFs" is used, then all other MTFs are set to 1. There are three user defined MTFs that can be applied:

- Custom (where MTF values are input)
- Gaussian
- Sinc

Any one, two, or three of these MTFs make up the User Defined MTFs.

Custom

"Yes" must be checked to include custom. The number of MTF values, spatial frequencies and MTFs must be input.

Gaussian

The scaling factor is described in the input section. The equation is

$$H(\xi) = e^{-\pi(b\xi)^2} \tag{3-38}$$

where b is the scaling factor. b is determined from the user selected inputs in frequency or space.

Sinc

The scaling factor is described in the input section. The equation is

$$H(\xi) = \frac{\sin(\pi b\xi)}{\pi b\xi} \tag{3-39}$$

where b is the scaling factor. b is determined from the user selected inputs in frequency or space.

“Yes” must be checked on any user defined MTF in order to include it. A single MTF is used that includes all “Yes” checked MTFs.

3.2.8. Electronic Low Pass Filter

The Electronic Low Pass filter response is given by a multiple pole RC low pass filter,

$$H_{elp}(f_t) = \left(1 + \left(\frac{f_t}{f_{elp}}\right)^{2n}\right)^{-1/2} \tag{3-40}$$

where f_{elp} is the electronics 3 dB frequency (Hz), and n is the number of filter poles. Both of these parameters are required inputs for scanning systems. The Low Pass transfer function is converted to a spatial blur by using the scan velocity to convert cyc/sec (Hz) to cyc/mrad.

3.2.9. Digital Boost

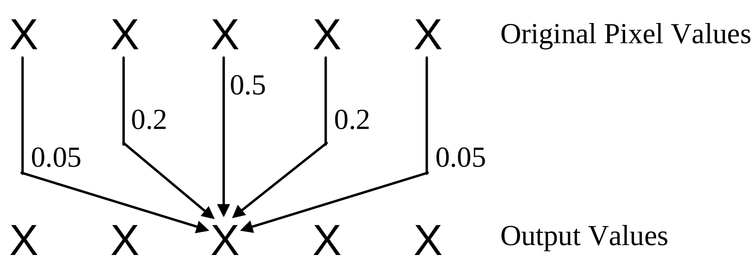

Figure 3-11 Digital Boost

The digital boost filter can be any digital filter, it does not have to be boost. It can be any finite impulse response (FIR) filter that is an even function (symmetric around the center pixel value) and an odd number of pixels. See the input definition in section 2.5.6 Boost – Horizontal on page 54. The transfer function is

$$H(\xi) = w_1 + \sum_{n=2}^{N} 2w_n \cos(2\pi ss(n-1)\xi) \tag{3-41}$$

Note that the sample spacing, ss, is in milliradians for a frame. For a field digital filter set w_2, w_4, $w_6 = 0$ and set w_1, w_3, w_5… to non-zero values.

3.2.10. Interpolation

Interpolation does not change the magnification. The image size on the screen is assumed to be the whole image. Interpolation occurs after dither or interlace and is the process of estimating double the number of pixels in one direction. An interpolation of "once" gives twice the number of pixels in that direction. An interpolation of "twice" gives 4 times the number of pixels in that direction. See Figure 3-12.

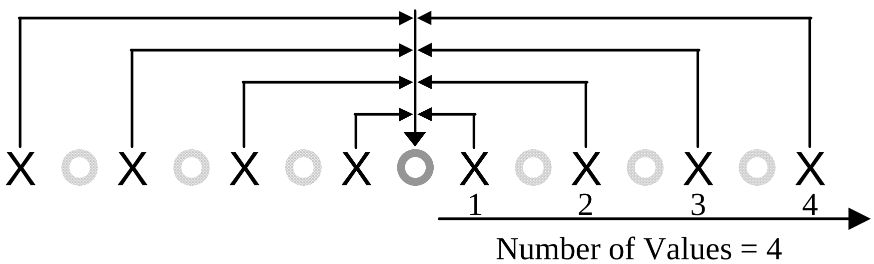

Figure 3-12 Interpolation (values are examples)

The impulse response of this process looks like h(x)

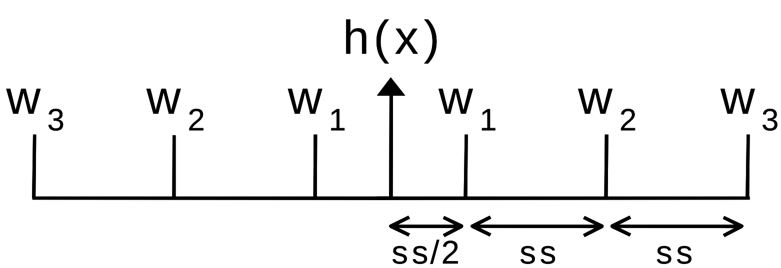

Figure 3-13

The general transfer function is Fourier transform of the impulse response shown

$$H(\xi) = 0.5\left[1 + \sum_{n=1}^{N} 2w_n \cos(\pi(2n-1)ss\xi)\right] \tag{3-42}$$

where ss is the original frame sample spacing in milliradians. For an interpolation of once

$$H(\xi) = 0.5\left[1 + \sum_{n=1}^{N} 2w_n \cos(\pi(2n-1)ss\xi)\right] \quad (3\text{-}43)$$

For an interpolation of twice

$$H(\xi) = (0.5)^2\left[1 + \sum_{n=1}^{N} 2w_n \cos(\pi(2n-1)ss\xi)\right]\left[1 + \sum_{n=1}^{N} 2w_n \cos\left(\pi(2n-1)\frac{ss}{2}\xi\right)\right] \quad (3\text{-}44)$$

For custom, w_1, w_2, w_3,… w_n are input in the table given along with the number of values, n. For pixel replication, the above transfer functions do not work, but can be altered by removing the constant (the DC term), setting $w_1 = 0.5$, and setting ss to ss/2. This is what is performed in NVTHERM. For bilinear, the above equations do work with $w_1 = 0.5$. For the Vollmerhausen case, $w_1 = 0.604$, $w_2 = -0.13$, $w_3 = 0.032$, and $w_4 = -0.006$.

3.2.11. Ezoom

The MTF for Ezoom is exactly that described in the interpolation section. Not as many options are available (i.e. custom Ezoom is not available). There is one exception. If interpolation is used, then the sample spacing, ss, is smaller in the MTF equation. For one interpolation, the Ezoom $ss = \frac{ss_{old}}{2}$. For twice, Ezoom $ss = \frac{ss_{old}}{4}$.

3.2.12. EO Mux

There are two parts of the MTF:

$$MTF_{EO\_Mux} = MTF_{LED} \bullet MTF_{EO\_Mux\_Tv} \quad (3\text{-}45)$$

The LED height and width are given. The angular subtense of the LED is

$$\alpha_{LED} = \frac{LED\_Width}{Focal\_Length} \text{ and } \beta_{LED} = \frac{LED\_Height}{Focal\_Length} \quad (3\text{-}46)$$

The MTF of the LED is

$$MTF_{Horizontal\_LED}(\xi) = \frac{\sin(\pi\alpha_{LED}\xi)}{\pi\alpha_{LED}\xi} \quad MTF_{Vertical\_LED}(\xi) = \frac{\sin(\pi\beta_{LED}\xi)}{\pi\beta_{LED}\xi} \quad (3\text{-}47)$$

The MTF of the EOMux Tv is input to a table. The number of values, spatial frequency in cycles per millimeter, and MTF values are given.

3.2.13. Display

The display can be a CRT, an LED Direct View, Flat Panel or Custom. If CRT is chosen, the spot size is determined from the CRT Gaussian Dimension selection, the display spot height and display spot width.

3.2.13.1. CRT

The finite size and shape of the display spot also corresponds to a spatial filtering, or *psf*, of the image. The *psf* of the display is simply the size and shape of the display spot and is Gaussian as shown in Figure 3-14. The display has a Gaussian display spot. The spot is shown in the lower right hand corner of the display. This spot is convolved with the scene to obtain the CRT output image as shown.

Figure 3-14. CRT Display with a Gaussian *psf*.

The finite size and shape of the display spot must be converted from a physical dimension to the sensor angular space. For the Gaussian spot, the spot size dimension in centimeters must be converted to an equivalent angular space in the sensor's field-of-view

$$\sigma_{disp\_angle} = \sigma_{disp\_cm} \frac{FOV_v}{L_{disp\_v}} \tag{3-48}$$

where L_{disp_v} is the length in centimeters of the display vertical dimension and FOV_v is field-of-view of the sensor in milliradians. Once these angular dimensions are obtained, the *psf* of the display spot is simply the size and shape of the display element

$$h_{disp}(x,y) = \frac{1}{\sigma_{disp\_angle}^{2}} Gaus\left(\frac{r}{\sigma_{disp\_angle}}\right) \quad \text{for a Gaussian spot} \tag{3-49}$$

where the angular display element shapes are given in milliradians. The transfer functions associated with the display spot is determined by taking the Fourier transform of the above *psf* equation.

$$H_{disp}(\xi,\eta) = Gaus(\sigma_{disp\_angle}\rho) \qquad \text{Gaussian display} \qquad (3\text{-}50)$$

3.2.13.2. LED Direct View

The LED direct view assumes that an EO Mux is viewed directly on the visible side and that the LED is in the focal plane of the sensor. Therefore, the angular dimension of the LED is

$$\alpha_h = \frac{LED\_width \bullet 10^{-6}}{Focal\_length \bullet 10^{-2}} \bullet 1000 \text{ mrads} \qquad (3\text{-}51)$$

$$\alpha_v = \frac{LED\_height \bullet 10^{-6}}{Focal\_length \bullet 10^{-2}} \bullet 1000 \text{ mrads} \qquad (3\text{-}52)$$

where the LED height and width are in micrometers and the Focal length in cm.

The point spread function is

$$h(x.y) = \frac{1}{\alpha_h \alpha_v} rect\left(\frac{x}{\alpha_h}, \frac{y}{\alpha_v}\right). \qquad (3\text{-}53)$$

The MTF is

$$H(\xi, w) = \sin(\alpha_n \pi \xi) \big/ \alpha_h \pi \xi \bullet \sin(\alpha_v \pi \eta) \big/ \alpha_v \pi \eta \,. \qquad (3\text{-}54)$$

3.2.13.3. Flat Panel

Liquid Crystal Devices (LCDs) and Light Emitting Diode (LEDs) displays are rectangular in shape and can be considered flat panel devices. The *psf* of the display is simply the size and shape of the display spot. Consider the display in Figure 3-15. The spot is shown in the lower right hand corner of the display. Flat panel displays have rectangular display elements that can impose display artifacts on the image. This is especially true if the rectangular elements are so large that the edges of the elements are not filtered by the eye.

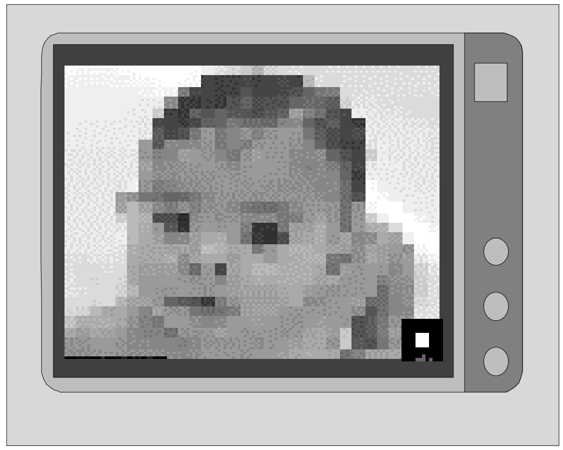

Figure 3-15. Flat panel display with a rectangular *psf*.

The finite size and shape of the display spot must be converted from a physical dimension to the sensor angular space. For the rectangular display element, the height and width of the display element must also be converted to the sensor's angular space. The vertical dimension of the rectangular shape is obtained using

$$\sigma_{disp\_angle} = LED\_Height \frac{FOV_v}{L_{disp\_v}} \qquad (3\text{-}55)$$

and the horizontal dimension is similar with the horizontal display length and sensor field-of-view. Once these angular dimensions are obtained, the *psf* of the display spot is simply the size and shape of the display element

$$h_{disp}(x,y) = \frac{1}{W_{disp\_angle\_h} H_{disp\_angle\_v}} rect\left(\frac{x}{W_{disp\_angle\_h}}, \frac{y}{H_{disp\_angle\_v}}\right) \qquad (3\text{-}56)$$

for flat panel where the angular display element shapes are given in milliradians. The transfer functions associated with these display spots are determined by taking the Fourier transform of the above *psf* equations.

$$H_{disp}(\xi,\eta) = \sin c(W_{disp\_angle\_h}\xi, H_{disp\_angle\_v}\eta) \quad \text{Flat panel display} \qquad (3\text{-}57)$$

3.2.13.4. Custom

For custom display MTF, four parameters must be provided: Number of MTF values, Spatial Frequencies and Horizontal and Vertical MTFs that correspond to the spatial frequencies.

3.2.14. Human Eye

The human eye has a *PSF* that is a combination of three physical components: optics, retina, and tremor (see Overington). In terms of these components, the *PSF* is

$$h(x,y) = h_{eye\_optics}(x,y) ** h_{retina}(x,y) ** h_{tremor}(x,y) \tag{3-58}$$

The transfer function of the eye is important in calculating human performance when using a sensor system.

The transfer function of the eye is:

$$H_{eye}(\xi,\eta) = H_{eye\_optics}(\xi,\eta) H_{retina}(\xi,\eta) H_{tremor}(\xi,\eta) \tag{3-59}$$

The transfer function of the eye optics is a function of display light level. This is because the pupil diameter changes with light level. The number of foot-Lamberts, fL, at the eye from the display is Ld/0.929 where Ld is the display luminance in milli-Lamberts. The pupil diameter is then

$$D_{pupil} = -9.011 + 13.23 \exp\{-\log_{10}(fL)/21.082\} \,[\mathrm{mm}] \tag{3-60}$$

This equation is valid if one eye is used as in some targeting applications. If both eyes view the display, the pupil diameter is reduced by 0.5 millimeters. There are two parameters, *io* and *fo*, that are required for the eye optics transfer function. The first parameter is

$$io = (0.7155 + 0.277/\sqrt{D_{pupil}})^2 \tag{3-61}$$

and the second is

$$fo = \exp\{3.663 - 0.0216 * D_{pupil}{}^2 \log(D_{pupil})\} \tag{3-62}$$

Now, the eye optics transfer function can be written

$$H_{eye\_optics}(\rho) = \exp\{-(43.69(\rho/M)/fo)^{i_0}\} \tag{3-63}$$

where ρ is the radial spatial frequency,

$\sqrt{\xi^2 + \eta^2}$, in cycles per milliradian.

and M is the imaging system magnification. In Figure 3-16, the magnification would be the angular subtense the display subtends to an observer divided by the imager FOV. Note that M depends on display height and observer viewing distance.

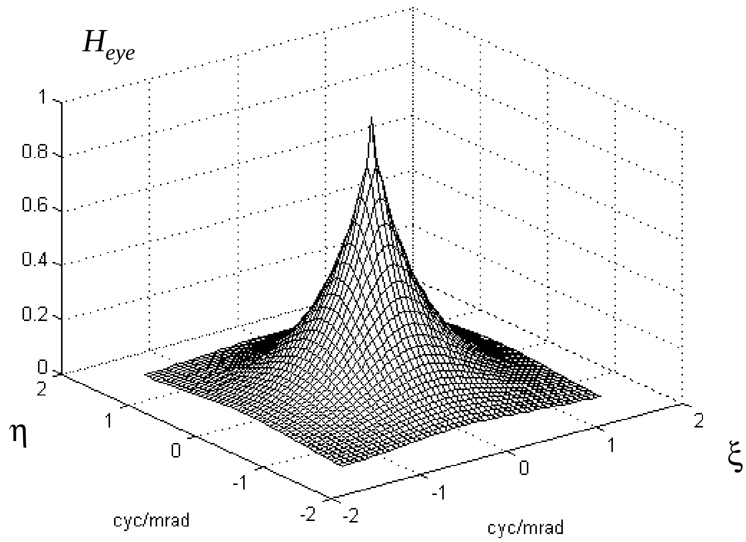

Figure 3-16 Eye Transfer Function.

The retina transfer function is:

$$H_{retina}(\rho) = \exp\{-0.375(\rho / M)^{1.21}\} \tag{3-64}$$

Finally, the transfer function of the eye due to tremor is:

$$H_{tremor}(\rho) = \exp\{-0.4441(\rho / M)^{2}\} \tag{3-65}$$

which completes the eye model.

As an example, let the magnification of the system equal 1. With a pupil diameter of 3.6 mm corresponding to a display brightness of 10 fL and viewing with one eye, the MTF of the eye is shown in Figure 2.14. The *io* and *fo* parameters were 0.742 and 27.2, respectively.

3.2.15. User Defined (Custom Post-Sample MTF)

See section 3.2.7 User Defined (Custom Pre-Sample MTF) on page 102

3.3. Noise

Noise calculations are straightforward for most sensor configurations except uncooled and PtSi sensors. The noise bandwidth is calculated and then σ_{tvh} is calculated for all sensors. For uncooled and PtSi, a Peak D* and relative detectivity is determined from the input parameters (See Uncooled and PtSi sections below).

3.3.1. Noise Bandwidth

For a staring imager, the noise bandwidth is

$$\Delta f_{noise} = \frac{1}{2(t_{\text{int}})} \tag{3-66}$$

where t_{int} is the integration time.

For a scanned sampled imager

$$\Delta f_{noise} = \int_0^\infty \left[sinc(t_{\text{int}} \nu) H_{Lowpass}(\nu) \right]^2 d\nu \tag{3-67}$$

where ν is the sensor temporal frequency.

For a scanned non-sampled imager

$$\Delta_{noise} = \int_0^\infty H^2_{Lowpass}(\nu) d\nu \tag{3-68}$$

3.3.2. Random Spatial-Temporal Noise

The random spatial temporal noise, σ_{tvh}, is calculated assuming an ambient temperature of 300 Kelvin. The σ_{tvh} is

$$\sigma_{tvh} = \frac{4Fnumber^2 \sqrt{\Delta f_{noise}}}{\Pi t_{optics} A_{\text{det}} \int_{\lambda_1}^{\lambda_2} D^*(\lambda) \frac{\partial L(\lambda)}{\partial T} d\lambda} \tag{3-69}$$

where A_{det} is the detector area, $D^*(\lambda)$ is $D^*_{peak} \bullet D_{normalized}(\sigma)$, and $\frac{\partial L(\lambda)}{\partial T}$ is the partial derivation of the ambient radiance with respect to temperature.

3.3.3. Uncooled

If an uncooled sensor is used, then both D^*_{peak} and Normalized DCλ are determined from the measured detector noise, the frame rate of operation, the measured Fnumber, and the optics transmission. The measured frame rate must match the NVTHERM system frame rate or NVTHERM will not run.

$$D^*_{peak} = \frac{4(Fnumber)^2 \bullet \sqrt{\frac{FrameRate}{2}}}{\sqrt{DectectorArea} \bullet t_{optics} \bullet \delta \bullet SystemNoise} \tag{3-70}$$

Where

- Fnumber is the F-number of the noise measurement optics
- t_{optics} is the optics transmission of the measurement optics
- System Noise (sometimes called NETD is uncooled systems) is the noise limited by the frame rate bandwidth in Kelvin.

Finally

$$S = \int_{\lambda 1}^{\lambda_2} \frac{37415}{\lambda^5} \bullet \frac{1}{\left[e^{\left(14387.9/\lambda T\right)} - 1\right]^2} \bullet \frac{14387.9}{\lambda T^2} \bullet e^{14387.9/\lambda T} \bullet d\lambda \qquad (3\text{-}71)$$

The normalized D(λ) is set to 1.0 with spectral increments of $\dfrac{CutoffWavelength - CutonWavelength}{9}$.

3.3.4. PtSi

If the detector is Platinum Silicide, then D^*_{peak} and Normalized D(λ) is calculated from the emission coefficient and the barrier height.

$$D^*_{peak} = \left[\frac{1.24 EmissionCoefficient\left(1 - \dfrac{CutonWavelength}{\lambda Cutoff}\right)^2}{1{,}000{,}000(6.63E-34)(3E8)\sqrt{2\delta}}\right] \qquad (3\text{-}72)$$

Where $\lambda_{Cutoff} = 1.24/BarrierHeight$

Cuton Wavelength is the sensor Cuton Wavelength

δ = Total number of photos

$$\delta = \int_{\lambda 1}^{\lambda 2} \left\{ \frac{\left[\dfrac{37418}{\lambda^5} \bullet \dfrac{1}{\left(e^{14388/\lambda T} - 1\right)}\right]}{\left(\dfrac{(1{,}000{,}000)(6.63E-34)(3E8)}{\lambda}\right)} \right\} \bullet \left[\frac{1.24 EmissionCoefficient\left(1 - \dfrac{\lambda}{\lambda_{cuktoff}}\right)^2}{\lambda}\right] d\lambda$$

(3-73)

The normalized D(λ) is

$$D(\lambda)=\frac{\dfrac{1}{D*_{peak}}\left[\dfrac{1.24 EmissionCoefficient\left(1-\dfrac{\lambda}{\lambda_{cutoff}}\right)^{2}}{\lambda}\right]}{\left(\dfrac{(1{,}000{,}000)(6.63E-34)(3E8)}{\lambda}\right)\sqrt{2\delta}} \tag{3-74}$$

Where λ varies in 10 increments of the range from the Cutoff Wavelength to the Cuton Wavelength.

3.4. System Transfer Spurious Response

3.4.1. Sampled Imager Response and the Spurious Response

The amount of spurious response in an image is dependent on the spatial frequencies that comprise the scene and on the pre-sample blur, sampling, and post-sample blur characteristics of the sensor. However, the spurious response *capacity* of an imager can be determined by characterizing the imager response to a point source. This characterization is identical to the MTF approach for continuous systems.

The response function for a sampled imager is found by examining the impulse response of the system. This procedure is identical to that used with non-sampled systems. The function being sampled is the point spread function of the pre-sampled image. Assume the following definitions: for simplicity, the equations and examples will use one dimension, but the concepts generalize to two dimensions.

$H(\omega)$ = Pre-sample MTF (optics and detector)

$P_{ix}(\omega)$ = Post-sample MTF (display and eye)

$R_{sp}(\omega)$ = Response function of imager

= Transfer response (baseband spectrum) plus spurious response

ω = spatial frequency (cycles per milliradian)

ν = sample frequency (samples per milliradian)

d = spatial offset of origin from a sample point

Then the response function $R_{sp}(\omega)$ is given by the following equation.

$$R_{sp} = \sum_{n=-\infty}^{n=\infty} H(\omega - n\nu) e^{-i(\omega - n\nu)d} \quad P_{ix}(\omega)$$

$$R_{sp} = H(\omega) e^{-i\omega d} \quad P_{ix}(\omega) + \sum_{n \neq 0} H(\omega - n \quad \nu) e^{-i(\omega - n\nu)d} \quad P_{ix}(\omega) \tag{3-75}$$

The response function has two parts, a transfer function and a spurious response function. See Figure 3-17 for a graphical illustration of the transfer and spurious response functions. The n=0 term in Equation 3-75 is the transfer response (or baseband response) of the imager. This term results from multiplying the pre-sample blur by the display and eye MTF. The transfer response does not depend on sample spacing, and it is the only term that remains in the limit as sample spacing goes to zero. A sampled imager has the same transfer response as a non-sampled (that is, a very well-sampled) imager.

However, a sampled imager always has the additional response terms (the n≠0 terms), which are referred to as *spurious response*. The spurious response terms in Equation 1 are caused by the sample-generated replicas of the pre-sample blur; these replicas reside at all multiples of the sample frequency. The spurious response of the imager results from multiplying the sample-generated replicas of the pre-sample blur MTF by the display/eye MTF. The position of the spurious response terms on the frequency axis depends on the sample spacing and the effectiveness of the display and eye in removing the higher frequency spurious signal. The phase relationship between the transfer response and the spurious response depends on the sample phase.

Performance of a sampled imaging system can be related to the ratio *SR* of integrated spurious response to baseband response. Three quantities have proven useful: total integrated spurious response as defined by Equation 3-76a, in-band spurious response as defined by Equation 3-76b, and out-of-band spurious response as defined by Equation 3-77c. If the various replicas of the pre-sample blur overlap, then the spurious signals in the overlapped region are root-sum-squared before integration.

$$SR = \frac{\int_{-\infty}^{\infty} (\text{Spurious response}) d\omega}{\int_{-\infty}^{\infty} (\text{Baseband signal}) d\omega}$$

$$SR_{in-band} = \frac{\int_{-\upsilon/2}^{\upsilon/2} (\text{Spurious response}) d\omega}{\int_{-\infty}^{\infty} (\text{Baseband signal}) d\omega}$$

$$SR_{out-of-band} = SR - SR_{in-band} \tag{3-76}$$

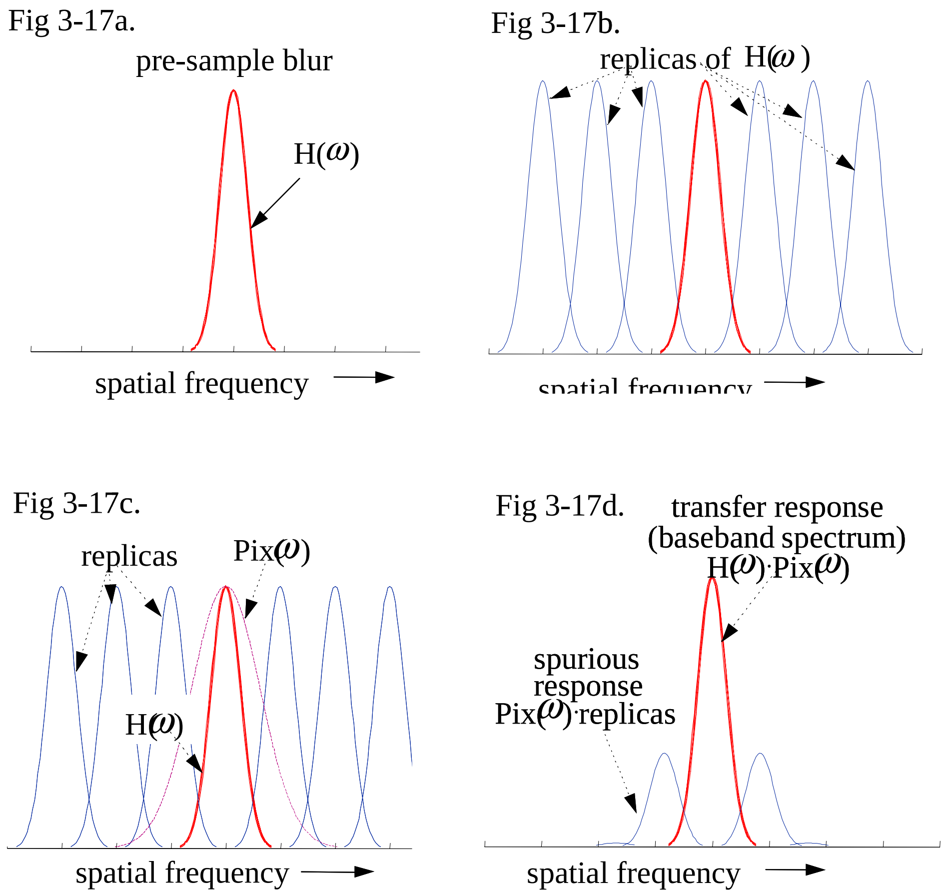

Figure 3-17. The pre-sample blur MTF, H(ω), is shown in Figure 3-17a. Sampling H(ω) replicates H(ω) at multiples of the sample frequency as shown in Figure 3-17b. The display and eye MTF, Pix(ω), is shown in Figure 3-17c, along with the pre-sample blur and the sample-generated replicas of the pre-sample blur. In Figure 3-17d, the transfer response (baseband spectrum) is created by Pix(ω) multiplying H(ω) (frequency by frequency), and the spurious response is created by Pix(ω) multiplying the sample-generated replicas of H(ω).

MTF Squeeze model

Experiments were conducted to determine the affect of under-sampling on tactical vehicle recognition and identification. A variety of pre-sample blurs, post-sample blurs, and sample spacings were used. Baseline data was collected for each pre-sample and post sample blur combination without any spurious response (that is, with a small sample spacing). The baseline data provided the probability of recognition and identification versus total blur when no spurious response was present.

For each spurious response case, we found the baseline case without spurious response which gave the same probability of recognition or identification. A curve fit was used to relate the actual blur (with spurious response) to the increased baseline blur (without spurious response) which gave the same recognition or identification probability.

The effect of sampling on performance was found to be a separable function of the spurious response in each dimension. For the cases where the sampling artifacts were applied in both the horizontal and vertical direction, the two dimensional relative blur increase (RI) for the recognition task is:

$$RI \quad = \quad \frac{1}{1-0.32SR} \tag{3-77}$$

where SR is the spurious response ratio defined by Equation 3-76. For cases where the sampling artifacts were applied in only the horizontal or vertical direction, the relative blur increase for recognition is:

$$RI \quad = \quad \frac{1}{\sqrt{1-0.32SR_{V\ or\ H}}}. \tag{3-78}$$

Note that, for both Equations 3-77 and 3-78, *the relative increase in blur is in two dimensions.* That is, even if the spurious response is in one direction, the relative increase shown in Equation 3-78 is applied to both directions.

By the Similarity Theorem, a proportional increase in the spatial domain is equivalent to a contraction in the frequency domain. This turns an equivalent blur increase into an MTF contraction, or *MTF squeeze,* and allows the equivalent blur technique to be easily applied to performance models. Instead of an increase in the effective size of the point spread function, the Modulation Transfer Function is contracted. The MTF squeeze for recognition is:

$$MTF_{squeeze} \quad = \quad \sqrt{1.0-0.32SR_H}\ \sqrt{1.0-0.32SR_V}\,. \tag{3-79}$$

Figure 1 illustrates the application of contraction, or *MTF squeeze*, to the system MTF. The spurious response given by Equation 3-76 is calculated independently in the horizontal and vertical directions, and the squeeze factor given by Equation 3-79 is calculated. At each point on the MTF curve, the frequency is scaled by the contraction factor. The contraction is applied separately to the horizontal and vertical MTFs. The MTF squeeze is not applied to the noise MTF.

$$f_1 = \sqrt{1.0-0.32SR_H}\ \sqrt{1.0-0.32SR_V}\ f_2$$

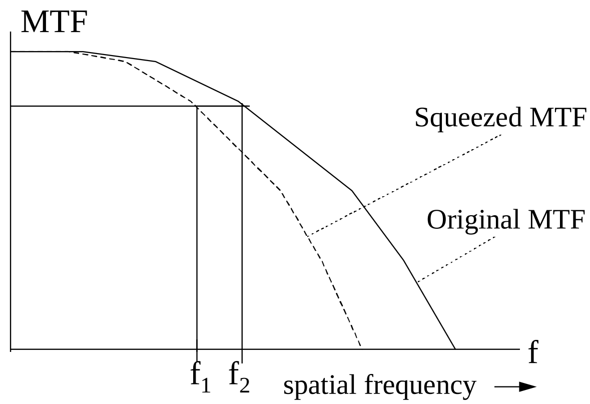

Figure 3-18. Application of the MTF Squeeze. Contraction is calculated based on total spurious response ratio in each direction. Contraction of frequency axis is applied to both horizontal and vertical MTF. Contraction is applied to signal MTF, not the noise MTF.

The results of the identification experiment using tracked vehicles suggest that target identification is strongly affected by out-of-band spurious response but is only weakly affected by in-band spurious response. The identification MTF squeeze factor is calculated using Equation 3-80. Again, the effect of sampling was found to be separable between the horizontal and vertical dimensions.

$$MTF_{squeeze} = \sqrt{1-SR_{H-out-of-band}}\ \sqrt{1-SR_{V-out-of-band}} \quad (3\text{-}80)$$

where $SR_{out\text{-}of\text{-}band}$ is calculated using Equation 3-76.

3.5. Range Predictions

3.5.1. Two-Dimensional MRT

A two-dimensional MRT is determined using the vertical and horizontal MRTs. Consider the horizontal and vertical MRTs shown in 3-19.

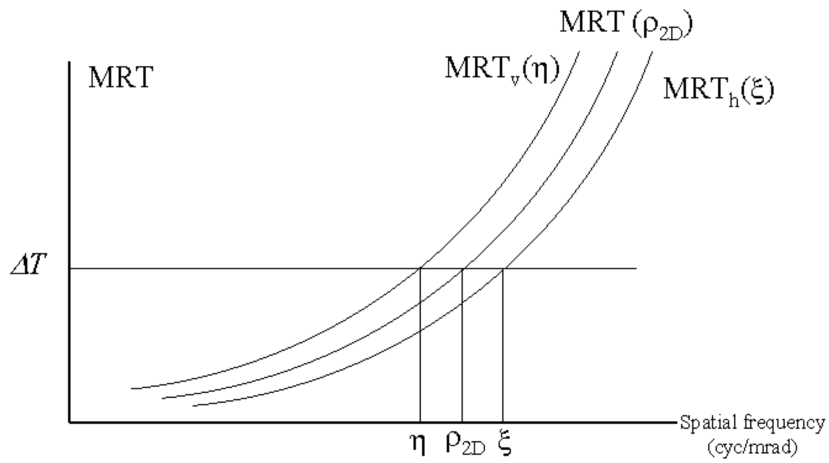

Figure 3-19

The spatial frequencies of the horizontal and vertical spatial frequencies gives the two-dimensional MRT spatial frequency

$$\rho_{2d} = \sqrt{\xi\eta} \tag{3-81}$$

The matching MRT is then plotted as a function of the two-dimensional spatial frequency. This new function is the two-dimensional MRT. Note that the conversion is a spatial frequency conversion and no manipulation is performed on the two-differential temperatures.

3.5.2. Probability as a Function of Range

The procedure for producing a probability of detection, recognition, or identification curve is quite simple. Consider the procedure flow as given in 3-20. There are four parameters needed to generate a static probability of discrimination curve as a function of range: The target contrast, the characteristic dimension, an atmospheric transmission estimate within the band of interest for a number of ranges around the ranges of interest, and the sensor two-dimensional MRT.

The atmospheric transmission is determined and an equivalent blackbody apparent temperature is calculated based on the atmospheric signal reduction.

Once an apparent differential temperature is obtained, the highest corresponding spatial frequency that can be resolved by the sensor is determined. This is accomplished by finding the spatial frequency (on the MRT curve) that matches the target apparent differential temperature. The target load line is the target contrast modified by the atmospheric transmission. The number of cycles across the critical target dimension that can actually be resolved by the sensor at a particular range then determines the probability of discriminating (detecting. recognizing, or identifying) the target at that range.

$$N = \rho \frac{d_c}{R} \tag{3-82}$$

where ρ is the maximum resolvable spatial frequency in cycles per milliradian, d_c is the characteristic target dimension in meters, and R is the range from the sensor to the target in kilometers.

The probability of discrimination is determined using the Target Transfer Probability Function (TTPF) given in section 1. The level of discrimination (detection, recognition, or identification) is selected and the corresponding fifty percent cycle criteria, N50 , is taken. The probability of detection, recognition, or identification is then determined with the TTPF for the number of cycles given by Equation 4. The probability of discrimination task is then assigned to the particular range. A typical probability of discrimination curve will have the probability plotted as a function of range. Therefore, the above procedure would be repeated for a number of different ranges.

While the following may be obvious, there are a number of characteristics that improve probability of detection, recognition, and identification in infrared systems. Improvements are seen with larger targets, larger target-to-background contrast, larger target emissivities, larger atmospheric transmission, smaller MRT values (as a function of spatial frequency), and usually smaller field-of-views (if the target does not have an extremely small differential temperature).

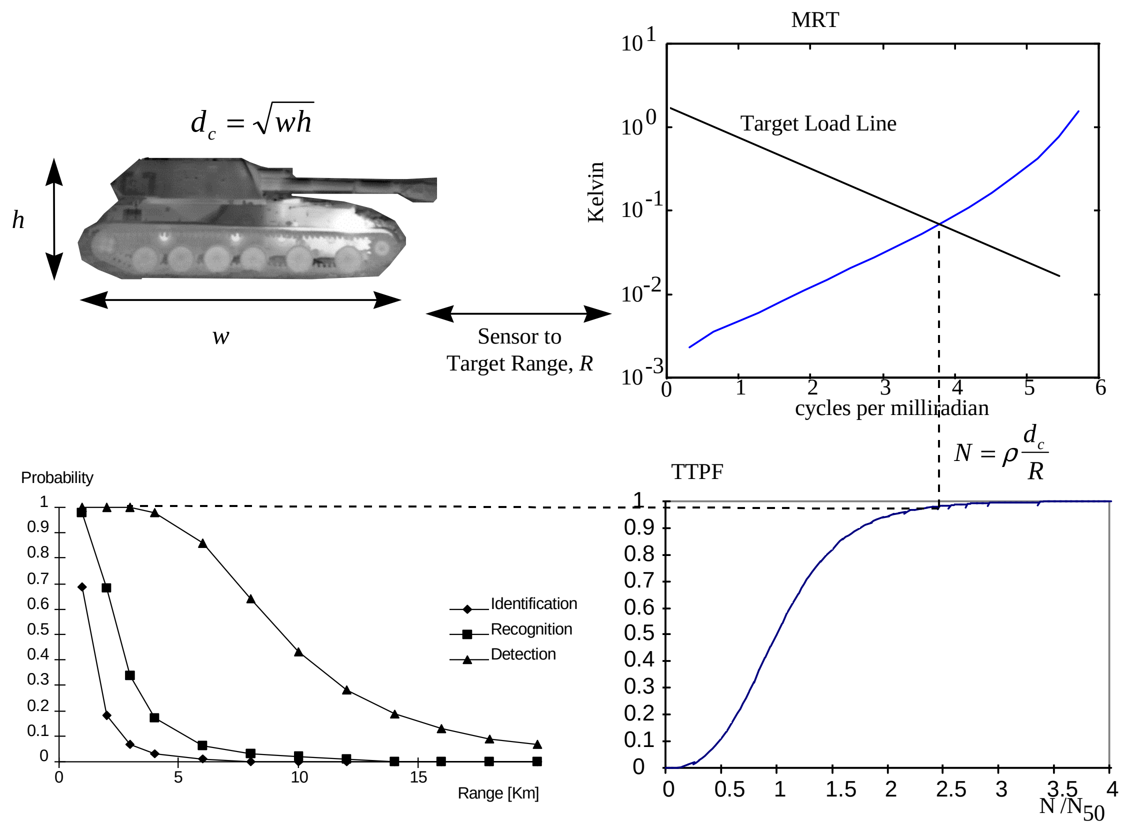

Figure 3-20. Tactical Acquisition Process.

3.5.3. Range as a Function of Probability

Probabilities of 0, 0.1…. 0.9, and 1 are used to interpolate ranges from the "Probabilities as a Function of Range" vectors. As a result, ranges are determined for these probabilities.

4. Bibliography

1. J.A. Ratches, et.al., "Night Vision Laboratory Static Performance Model for Thermal Viewing Systems," Research and Development Technical Report ECOM-7043, US Army Electronics Command, Fort Monmouth, N.J. 1975.
2. 2. J.D. Howe, “Electro-Optical Imaging System Performance Prediction,” In *Electro-Optical Systems Design, Analysis, and Testing,* (Dudzik Ed.), *The IR & EO Systems Handbook, Vol 4,* Ch. 2, ERIM IIAC, Ann Arbor, MI and SPIE, Bellingham, WA, 1993.
3. 3. W.R. Lawson, “Electrooptical System Evaluation,” In *Photoelectronic Imaging Devices*, Vol. 1, p. 375. L.M. Biberman and S. Nudelman, eds. Plemun, New York , 1971.
4. J. M. Lloyd, *Thermal Imaging Systems*, Plenum Press, New York, 1975, pp 184
5. R. Vollmerhausen and R. Driggers, *Analysis of Sampled Imaging Systems*, SPIE Press, Bellingham Washington, 2000.
6. G. Holst, “Effects of Phasing on MRT Target Visibility,” *SPIE Vol 1488, Infrared Imaging Systems: Design, Analysis, Modeling, and Testing II*, March, pg 90, 1991.
7. C. M. Webb, “Results of Laboratory Evaluation of Staring Arrays,” *SPIE Vol 1309, Infrared Imaging Systems: Design, Analysis, Modeling, and Testing*, pg. 271, 1990.
8. C. M. Webb, “Dynamic Minimum Resolvable Temperature Difference for Staring Focal Plane Arrays,” *Proceedings of the IRIS Specialty Group on Passive Sensors,* Infrared Information Analysis Center, ERIM, Ann Arbor, MI, 1993.
9. R. Vollmerhausen, R. Driggers, C. Webb and T. Edwards, "Staring Imager Minimum Resolvable Temperature (MRT) Measurements Beyond The Sensor Half Sample Rate," accepted by *Optical Engineering*, Jan, 1998.
10. W. Wittenstein, W. Fick, and U. Raidt, "Range Performance of Two Staring Imagers - Presentation of the Field Trial and Data Analysis," *SPIE Vol 2743*, Page 132.
11. S. Park and R. Hazra, "Aliasing as Noise: A Quantitative and Qualitative Assessment," *SPIE Vol 1969*, Pg 54.
12. T. Meitzler and G. Gerhart, "Spatial Aliasing Effects in Ground Vehicle IR Imagery," *SPIE Vol 1689*, Pg 226.
13. P. Owen and J. Dawson, "Resolving The Differences In Oversampled and Undersampled Imaging Sensors: Updated Target Acquisition Modeling Strategies for Staring and Scanning FLIR Systems," *SPIE Vol 1689*, 1992, pg 251.
14. F. Huck, S. Park, D. Speray, and N. Halyo, "Information Density and Efficiency of Two-Dimensional Sampled Imagery, *SPIE Vol 310,* 1981, Pg 36.
15. J. Kruthers, T. Williams, G. O'Brien, K. Le, and J. Howe, "A Study of the Effects of Focal Plane Array Design Parameters on ATR Performance," *SPIE Vol 1957,* pg 165.
16. L.E. Tannas, *Flat-Panel Displays and CRTs*, pp.19 & 39, Van Nostrand Reinhold Co., New York, 1985.
17. O.H. Shade, “Image Reproduction by a Line Raster Process,” In *Perception of Displayed Information*, (L. Biberman, Ed.), pp.233-277, Plenum, New York, 1973.
18. R. Legault, “The Aliasing Problems in Two-dimensional Sampled Imagery,” In *Perception of Displayed Information,* (L. Biberman, Ed.), pp.279-312, Plenum, New York, 1973.
19. C.H. Sequin, IEEE Transactions, Vol. 20, pg. 535, 1973.
20. D.F. Barbe and S.B. Campana, “Imaging Arrays Using the Charge Coupled Concept,” In *Advances in Image Pickup and Display* (B. Kazan, Ed.), Vol. 3, pp. 171-296, 1977.
21. J. D'Agostino, M. Friedman, R. LaFollette, and M. Crenshaw, "An Experimental Study of the Effects of Sampling on FLIR Performance," *Proceedings of the IRIS Specialty Group on Passive Sensors,* Infrared Information Analysis Center, ERIM, Ann Arbor, MI, 1990.
22. J. Howe, L. Scott, S. Pletz, J. Horger, and J. Mark, "Thermal Model Improvement Through Perception Testing," *Proceedings of the IRIS Specialty Group on Passive Sensors,* Infrared Information Analysis Center, ERIM, Ann Arbor, MI, 1989.
23. S. Park and R. Schowengerdt, "Image Sampling, Reconstruction, and the Effect of Sample-Scene Phasing," *Applied Optics*, Vol 21, No 17, pg 3142.
24. W. Wittenstein, J. Fontanella, A. Newberry, and J. Baars, "The Definition and the OTF and the Measurement of Aliasing for Sampled Imaging Systems," *Optica Acta*, Vol 29, No 1, pg 50.

25. R. Vollmerhausen, “Impact of display modulation transfer function on the quality of sampled imagery,” *Aerospace/Defense Sensing and Controls.* Society of Photo-Optic and Instrumentation Engineers, paper 2743-09, 1996.
26. R. Vollmerhausen, “Display of Sampled Imagery,” *IRIA-IRIS Proceedings: Meeting of the IRIS Specialty Group on Passive Sensors,* Vol. 1, pp 175-192, 1990.
27. *Instructions for the Use of the RIT Alphanumeric Resolution Test Object,* Graphic Arts Research Center, Institute of Technology, Rochester, New York.
28. J.D. Howe, “Electro-Optical Imaging System Performance Prediction,” In *Electro-Optical Systems Design, Analysis, and Testing,* (Dudzik Ed.), *The IR & EO systems Handbook, Vol 4,* pg. 92, ERIM IIAC, Ann Arbor, MI and SPIE, Bellingham, WA, 1993.
29. Flynn, D. and Sieglinger, B., "Formalism for Analyzing Spatial, Spectral, and Temporal Effects in a Hardware-in-the-Loop System Involving a Pixelized Projector and a Passive Imaging Sensor," *Proceedings of the Society of Photo-Instrumentation Engineers,* Vol 2741, pg 46, 1996.

5. Example Sensors

There are 13 example sensors that are provided with NVTherm. They are listed below with a short description.

Default	Staring Midwave
Sensor1	First Gen Longwave, Narrow FOV, 120x1 Detectors
Sensor2	First Gen Longwave, Medium FOV, 120x1 Detectors, EO Mux
Sensor3	First Gen Longwave, Narrow FOV, 120x1 Detectors, EO Mux
Sensor4	Second Gen, Longwave, Narrow FOV, 480x4 Detectors
Sensor5	Second Gen, Longwave, Narrow FOV, 480x4 Detectors
Sensor6	Second Gen, Meas Optics MTF, Wide FOV, 480x4 Det
Sensor7	Staring Midwave, PtSi, Wide FOV
Sensor8	Staring Midwave, Meas Optics, UltraNarrow FOV
Sensor9	Staring Longwave, Uncooled, Medium FOV
Sensor10	Staring Longwave, 1024 by 1024
Sensor11	Gimbal Scan Longwave, 120deg by 1.8deg, Second Gen
Sensor12	Line Scanner, Longwave, 8 by 8 detectors
Sensor13	Serial Scan Longwave Narrow FOV